

REVIEW

# Micro gas turbine: Developments, applications, and key technologies on components



Jingqi Li, Yulong Li\*

National Key Laboratory of Science and Technology on Aero Engines Aero-thermodynamics & Collaborative Innovation Center for Advanced Aero-Engine, School of Energy and Power Engineering, Beihang University, Beijing 100191, China

Received 7 March 2022; accepted 10 November 2022

Available online 4 March 2023

## KEYWORDS

Distributed generation;  
Micro gas turbines  
(MGTs);  
Compressor;  
Turbine;  
Optimization

**Abstract** Owing to their precedent characteristics, micro gas turbines (MGTs) have been favored as popular power machinery in plenty of energy systems such as distributed energy systems, range extenders, solar power generations, fuel cell systems and individual power supplies. Their specific features essentially include but are not limited to strong fuel adaptability, low emissions, flexible structure, and easy maintenance. Over the past 20 years, various types of MGTs have been developed. Classical and forward-looking technologies have been employed in the design and production of MGTs and their components. Among them, fully radial flow structures, gas lubricated bearings and efficient recuperators are typical approaches to enhance the overall performance and compactness, however, the exploitation of ceramic based materials and intelligent algorithms in component design can also assist in improving the performance. The applications of MGTs have been expanded to many fields, and the research on related components has also made new progress. Due to the time frame, there is no systematic summary of the latest relevant research, so it is essential to have a comprehensive understanding of the applications of MGTs and their pertinent components. This paper aims to present a comprehensive review on MGTs, covering the development status, applications, factors of performance and representative explorations of their components. Some investigations regarding the characteristics of commercial MGTs are also conducted. Applications in distributed energy, range extenders, solar generations, and fuel cell systems are distinctly introduced. Recent research work

\*Corresponding author.

E-mail address: [liyulong1897@163.com](mailto:liyulong1897@163.com) (Yulong Li).

Peer review under responsibility of Propulsion and Power Research.



Production and Hosting by Elsevier on behalf of KeAi

on compressors, turbines, combustors, recuperators, and rotor systems are reviewed and analyzed. The technologies and methods associated with materials, manufacturing, and cycles beneficial to the future development of MGTs are also explained and discussed in some detail.

© 2023 The Authors. Publishing services by Elsevier B.V. on behalf of KeAi Communications Co. Ltd.

This is an open access article under the CC BY-NC-ND license (<http://creativecommons.org/licenses/by-nc-nd/4.0/>).

## Nomenclature

$m$	mass flow (unit: kg/s)
$n$	rotating speed (unit: rpm)
$P$	pressure (unit: Pa)
$T$	thermodynamic temperature (unit: K)
$R$	gas constant (unit: J/(mol·K))

### Greek letters

$\beta$	pressure/expansion ratio
$\eta$	efficiency
$\varepsilon$	recuperator effectiveness

### Abbreviations

AM	additive manufacturing
ACCT	active control casing treatment
CFD	computational fluid dynamics
CHP	combined heat and power
CMC	ceramic-matrix composite
CSP	concentrated solar power
DED	directed energy deposition
DES	distributed energy system
DIFF	diffusion combustion flameless combustion
EV	electric vehicle
FC	fuel cell

FEA	finite element analysis
FLOX	flameless oxidation
FPBO	fast pyrolysis bio-oil
ICE	internal combustion engine
ICR-GT	intercooling regenerative gas turbine
LDI	lean direct inject combustion
LHV	low heat value
LP	lean premix combustion
LW	liquefied wood
MCFC	molten carbonate fuel cell
MGT	micro gas turbine
NAVD	non-axisymmetric vane diffuser
NSGA	non-dominated sorting genetic algorithm
ORC	organic Rankine cycle
RANS	Reynolds-averaged Navier-Stokes
RE	range extender
RQL	rich-quench-lean combustion
R-GT	regenerative gas turbine
SE	Stirling engine
SOFC	solid oxide fuel cell
SVO	straight vegetable oil
TBC	thermal barrier coating
TIT	turbine inlet temperature
ULSD	ultra-low-sulfur diesel
VOC	volatile organic compounds

## 1. Introduction

The growing diversification of energy and resources to sustain anthropogenic activity has attracted an increasing concern worldwide, in the context of the development of the modern social and economic structure. The widespread exploitation of natural fossil fuels exposes the unsustainability of energy and leads to an impact on the environment. A reduction in unnecessary consumption in the energy system will contribute to more sustainable development. The traditional energy structure has apparent characteristics of centralized supply, which brings unnecessary loss and economic waste in energy transfer. Therefore, small-scale energy systems with clean emissions are generally encouraged as complementary optimization approaches, and new demands on distributed energy systems are produced.

The distributed energy system (DES), which provides the on-demand supply and gradient utilization of energy, has been developed rapidly worldwide since when proposed at the end of the 20th century [1,2]. Conventional power

device, like internal combustion engine (ICE), was unable to meet the demand for fuel forms and emission standards required by DES, therefore, the micro gas turbine (MGT) with an appropriate power range can be considered one of the alternatives. Based on the Brayton cycle's combustion characteristics in the presence of high pressure, MGTs have good adaptability to various properties of fuels. Both low and high heating values of gaseous or liquid fuels can provide appropriate combustion performance. With advanced combustion technology, the emission of MGTs can also reach a low level [3,4]. Additionally, MGTs also have remarkable development potentials for standby power sources, mobile power sources, new energy power generations, mechanical drives, and range extenders for transportation [5,6]. By this view, the performance and development of MGT have received extensive attention in recent years.

MGTs represent a kind of gas turbine with power levels up to 500 kW [7]. A typical MGT consists of a compressor, a combustion chamber, and a turbine. Also, modern high-

efficient MGTs are commonly equipped with recuperators to recover the waste heat. [Figure 1\(a\)](#) [6] illustrates a typical MGT generator set. The airflow passes through the inlet, the compressor impeller, the cold passage of the recuperator, the combustion chamber, the turbine impeller, the hot passage of the recuperator and then exits. Based on this process, [Figure 1\(b\)](#) shows a schematic representation of the MGT cycle. The ambient air is compressed into high-pressure air in the compressor and heated in the recuperator, where the waste heat of the exhaust gas is recovered. The air then enters the combustion chamber and burns, forming high-pressure gas at high temperatures. The gas impacts the turbine and drives the compressor and generator. Reale et al. [8] have provided a brief review of MGTs and related systems, enumerating some layouts of combined systems, and analyzing the role of computational fluid dynamics (CFD) in combustion chamber research. Al-attab et al. [9] summarized the typical research and application of external combustion gas turbines, involving a certain range of MGT applications. Ward et al. [10] reviewed the effect of humidification on the improvement of cycle efficiency and flexibility of MGTs and their components, by introducing the relevant structural layout. Additionally, the application of specific technologies to MGTs and the review studies on the components of MGTs, such as fuel nozzles [11] and recuperators [5], were examined.

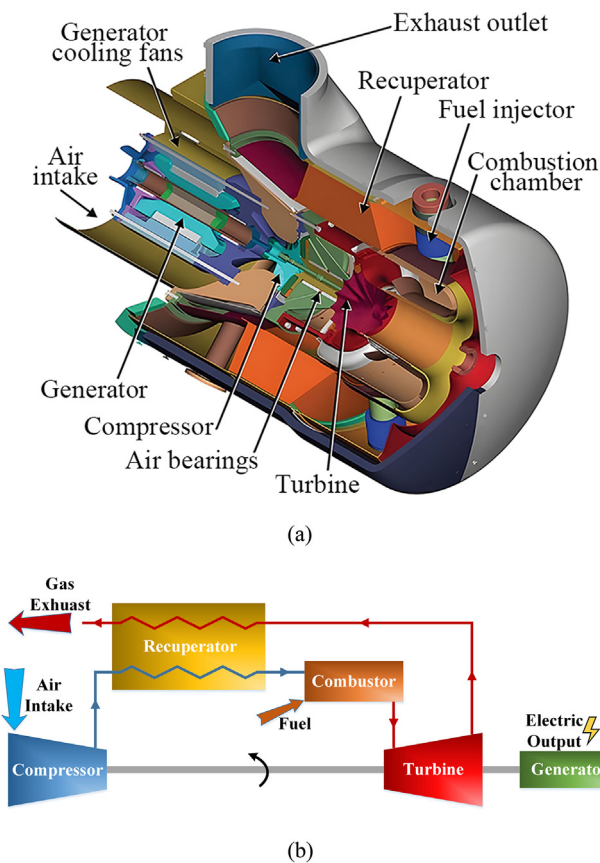


**Figure 1** Schematic representations of: (a) an MGT generator set from Capstone [6], (b) a typical cycle of the MGT.

In contrast to previous works, this study fully covers the developments of MGTs technologies from the perspectives of applications, performances and beneficial representative explorations on components in the global framework. The comprehensiveness and the latest time of the review represent other distinctive features of the present work. The technology of components is further evaluated from the perspective of serving the overall performance of MGTs. This review paper is aimed to provide a direction for future development, which includes challenges and opportunities.

Current development directions of MGTs aim to improve efficiency and simplify their structure. Increasing the turbine inlet temperature and reducing component loss are effective ways to enhance efficiency. Simplifying structure and employing lightweight materials can also magnify the compactness of MGTs and make them more flexible for a diverse range of applications. This paper attempts to provide a relatively comprehensive review based on previously published literature, covering the development and current status of MGTs, applied research, definition and influencing factors on performances, and related studies on components. Section 2 outlines the current development process of MGTs and the mainstream performance of the MGTs. Section 3 explains various applications of MGTs and then the conflicts of MGTs in these applications are discussed. Section 4 summarizes the influential factors of MGTs performances from static, dynamic and thermo-economic points of view. Section 5 displays the key technologies of MGTs components and the current status of related research. Finally, Section 6 summarizes the key points of MGTs reviewed in this paper, and prospects the future research direction of MGT-related-technologies from six perspectives.

## 2. Development and current status

The structure and performance of MGTs have been increasingly improved for decades after their first appearance. So far, several companies have released relevant products. The development process and the mainstream performance of MGTs are inclusively explained in this section.

### 2.1. The development of MGTs

Gas turbine technology has become attractive since Holz developed the first 370 kW gas turbine in the 1920s [12]. The initial research was performed with the aim of increasing the power level. Small and micro-scale gas turbines designed for low-power applications first appeared in the 1950s. Initially, MGTs were designed as automotive engines and auxiliary power supply devices for military products [13–15]. The former failed due to variable operating conditions under the vehicle circumstances and the latter was demonstrated in Allison's power supply for Patriot air defense systems in 1978. In the 1990s, with the introduction and application of distributed generation, the

demand for MGTs surged in the business market intensified [16]. A group of pioneering MGTs represented by Capstone, AlliedSignal and Elliott products, came to market around 2000.

With the development of material technology and machining technology, the structure and performance of MGTs have also been improved [17]. Early MGTs, in the 1960s, had a similar configuration to large scale gas turbines. The generator was separated from the gas turbine shaft and connected by a gearbox and coupling. The connection brought some efficiency loss, but allowed the generator to operate at lower rotation speeds, as the gas turbine was running at tens of thousands of rpm. It was considered as a stopgap measure when the high-speed generators were not mature. The centrifugal compressor was chosen because of the appropriate pressure ratio of MGTs, and its extensive exploitation. Limited by the material progress at the time, the turbine inlet temperature (TIT) of MGTs was limited to 800–900 K, and the efficiency was about 20%.

The application of high-speed generators enables gas turbines to directly drive the generators. The coupling and gearbox are removed to simplify the MGT system and thereby improve efficiency. Since high-speed generators are typically designed in coupling with gas turbine structures, great improvements in compactness are achieved, resulting in a reduction of the overall size and weight.

The application of recuperators in MGTs is also of great significance. By recovering the waste heat, the overall thermal efficiency of MGTs is substantially enhanced by about 5%–10%. A compact recuperator allows the airflow to experience less distance and pressure loss before entering the recuperator, reducing the flow losses, however an externally placed recuperator may have better potential in heat transfer performance, because its size is unconstrained.

Gas/liquid lubricated bearings are another crucial technique employed in MGT systems. The lubricated bearings break the limitation on the maximum rotating speed subjected to the performance of the rolling bearing. Therefore the rotor impeller with a small flow and large load can gain superior designability at high rotating speed, and thus the overall efficiency is enhanced. MGTs using gas/liquid lubricated bearings tend to have longer life spans as well as

lower frequency maintenance, assisting in the reduction of running costs.

The latest mainstream MGTs, benefiting from the progress of high-temperature materials, raised a TIT to 900–1200 K. The thermal efficiency is considerably enhanced, to about 25%–35%. The radial flow compressors and turbines with the back-to-back arrangement are common structures, and annular combustors are set to increase compactness.

## 2.2. MGTs for business use

In the past 20 years, new products of MGTs have been released to a greater extent. The products from Capstone, AlliedSignal, Elliott and Turbec have taken a large share of the commercial MGTs market, while some other brands' products have also been proposed. Figures 2–4 illustrate the physical or schematic pictures of these MGTs.

Most of the commercial MGTs have equipped with the technologies mentioned above. C-series from Capstone (see Figure 2(a) [18]), equipped with fully radial flow impellers, air bearings and compact annular recuperator, are the benchmarking products. Capstone MGT program has launched C30, C65, C200 and other products since 1995, among which the 30 kW business model was expected to have a fixed cost of about 500 \$/kW and a generation cost of 45–50 \$/MWh [14]. However, similar to the C-series products in the rotor structure, AlliedSignal AS75 [19] has a single cylinder combustor and an independent recuperator (see Figure 2(b) [19]). The TIT at about 900 °C helps AS75 to achieve higher efficiency. Honeywell Parallon75 [20] is launched on the basis of AS75 and is applied in the 70 kW solar power generation project in Nanjing, China. TG80CG represents an 80 kW class MGT from Bowmen (see Figure 2(c) [21]), based on the air bearings. It can provide 80 kW of power, at an efficiency between 25% and 28%, and an additional 150 kW of heat at the same time [22].

One of the major features of the products mentioned above is the exploitation of air bearing. However, limited by technical maturity, some other products utilize oil-lubricated bearings. Elliott's TA series MGTs meet the power requirements of 45 kW, 60 kW, 80 kW, and 200 kW (see Figure 3(a) [4]). Figure 3(b) [23] presents the TA45 rotor

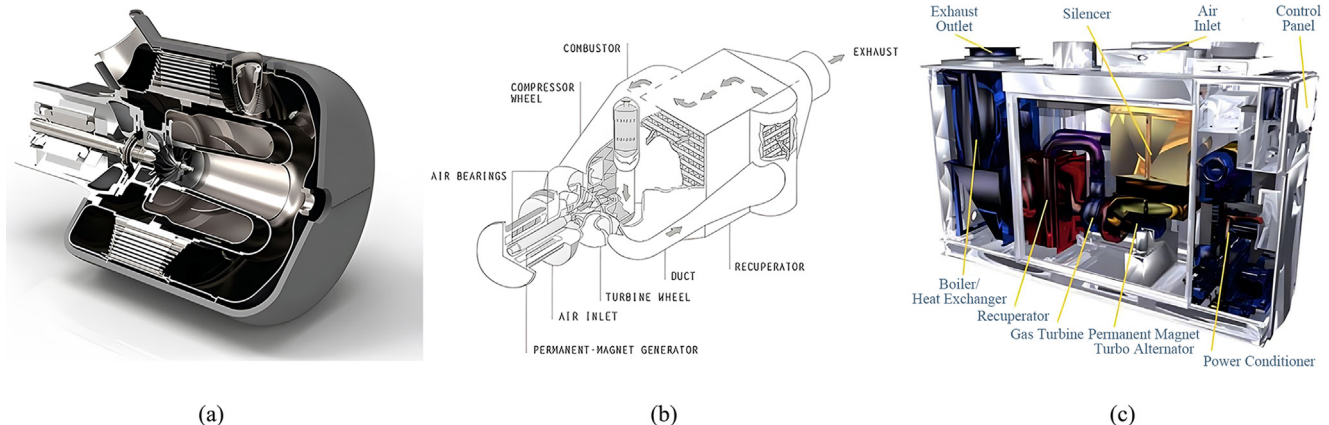


**Figure 2** Photos of various MGTs: (a) Capstone C30 [18], (b) AlliedSignal AS75 [19], (c) Bowmen TG80CG [21].

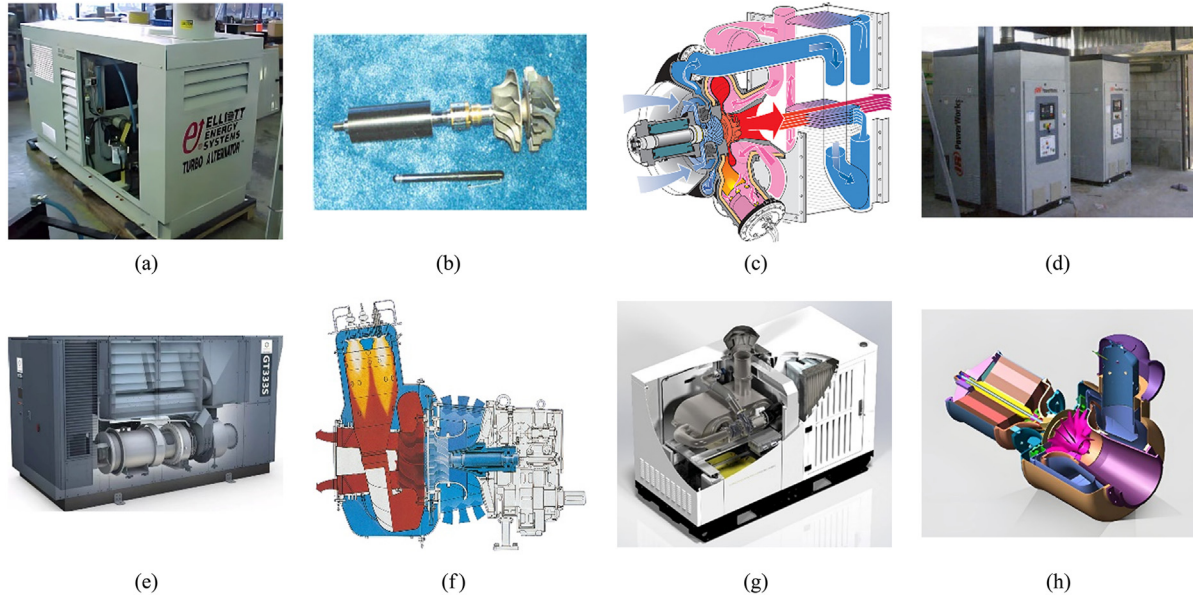


**Figure 3** Photos of various MGTs: (a) Elliott TA45 [4], (b) rotor system of TA45 [23], (c) Turbec T100 [25], (d) PowerWorks PW70 [4], (e) FlexTurbine GT33s [27], (f) reference model of GT33s (KG2) [28], (g) Bladon [29], (h) ET group [30].

system where the compressor pressure ratio reaches 4.3 at the rated speed of 116,000 rpm and the overall efficiency reaches 30% [23]. Released by Turbec (have been acquired by Ansaldo) in 1999, the T100 MGT has been applied to more than 500 facilities worldwide [24]. The structure and workflow of the T100 have been presented in Figure 3(c) [25]. The T100 has the highest TIT of around 950 °C, and

the NO<sub>x</sub> emission is reduced to less than 15 ppm via advanced combustion technology [26]. The electrical efficiency is about 30%, slightly higher than previously introduced MGTs, which may mostly benefit from its higher TIT. However, compared with the advantages brought by the higher TIT and power size, the efficiency gains of T100 are limited. This issue suggests that the component may be

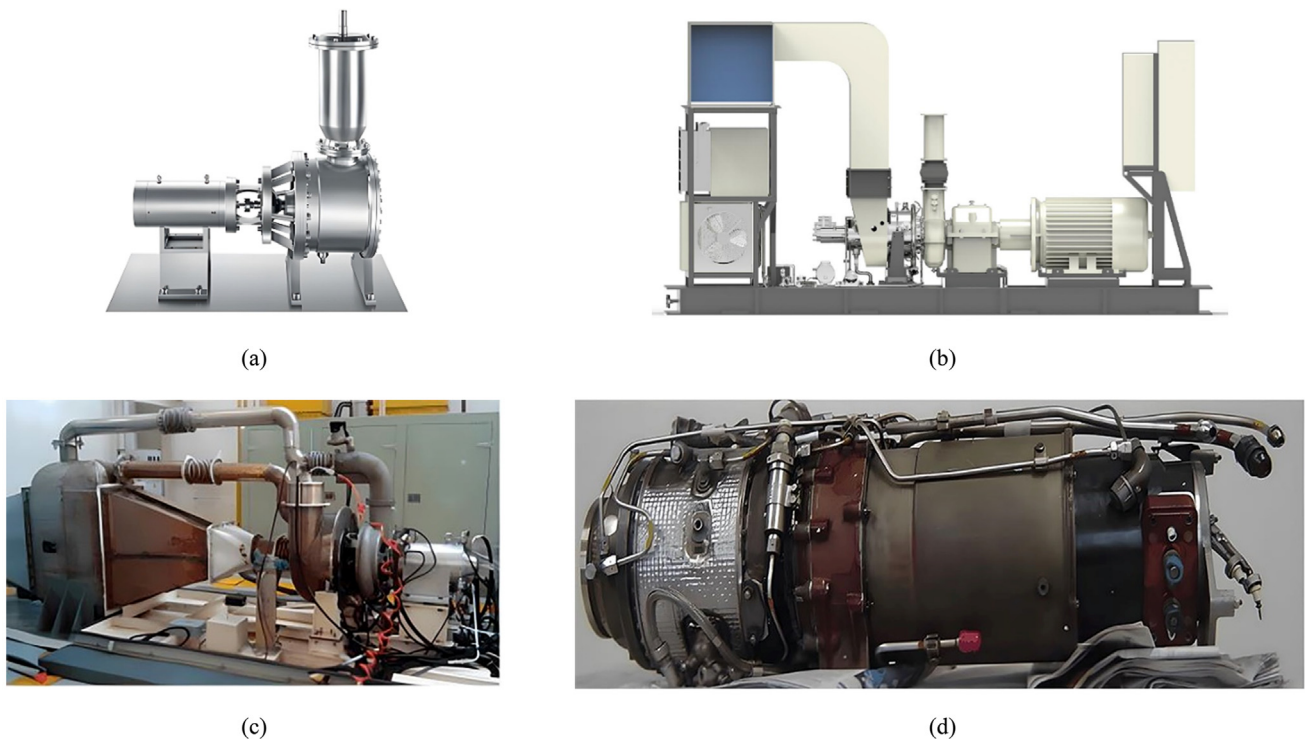


**Figure 4** MGTs of local companies in China: (a) ENN E100 [31], (b) Wisdomturbine [32], (c) AVIC Dong'an 100 kW MGT [33], (d) AVIC WD18 [33].

designed conservatively, perhaps to consider service life or stability.

In corporation with some technology from ordinary turbine engines, a number of products have also shown good performance. The 70 kW-class MGT from PowerWorks (Ingersoll Rand), illustrated in Figure 3(d) [4], contains a double-shaft structure. Actually, double-stage turbines are separated by two shafts to drive the compressor and generator. Although this design is believed to increase the complexity of turbine structure and losses, PW70 achieves the tied-highest efficiency among the current products, indebted to its proper overall design. Another product with the highest efficiencies is produced by Flex Turbine (see Figure 3(e) [27]). Drawing on another Ingersoll Rand product, KG2 (see Figure 3(f) [28]), Flex Turbine redesigned a 333 kW MGT in the early 2000s, the so called GT333s [27]. Equipped with couplings and gearboxes, GT333s reach maximum efficiency of 33%, and all the emissions of CO, NO<sub>x</sub>, and VOC are less than 5 ppm.

In addition, Bladon [29] and ET group [30] have also introduced their MGT products. The disclosed information reveals that Bladon's 12 kW MGT (see Figure 3(g) [29]) has a rotating speed of 134,000 rpm, which supports the speculation of using air bearings. The 45 kW-class MGT of the ET group has been demonstrated in Figure 3(h) [30]. With a uniquely biased recuperator, it can reach a power generation efficiency of 28% at a rated speed of 60,000 rpm.

Local companies in China have recently launched MGTs based on mature technologies. For instance, ENN Energy has introduced the 100 kW-class MGT, the so called E100, as illustrated in Figure 4(a) [31]. The turbine shaft is supported by oil-lubricated bearings and connected to the generator through a coupling. This company also plans to conduct subsequent research on MGTs using air bearings and integrated shafts. The 240 kW-class, two-shaft MGT from Wisdomturbine (see Figure 4(b) [32]) has a TIT of 1200 K, thus growing the efficiency up to 22.9% for a simple cycle [32]. In Figure 4(c) [33] and Figure 4(d) [33], AVIC Dong'an also presents a 100 kW-class MGT and an 18 kW auxiliary power unit, respectively.

The main parameters of current commercial MGTs have been summarized in Table 1. Currently, the compressor

pressure ratio of MGTs is generally in the range of 3–5 according to different power levels, and the rotating speed is generally above 50,000 rpm, with a maximum value of 134,000 rpm. A lower power level demands a higher rotating speed in order to obtain better impeller performance. The TIT is limited to less than 950 °C with an overall efficiency of 25%–33%. Additionally, it can be concluded that it is easier for MGTs at a high power level to achieve higher efficiency, while a lower-powered MGT has advantages in terms of operational flexibility.

### 3. Applications

MGTs were initially designed for vehicles but developed rapidly after the appearance of the DES concept. Thanks to the appropriate size and power level, MGTs have been further utilized in solar power generation and gas turbine-fuel cell systems and they play a pivotal role in the performance of complex systems. This section aims to introduce several typical applications of and corresponding research on MGTs.

#### 3.1. Distributed energy system

The distributed energy system is a kind of energy system based on distributed power generation technology and the concept of energy cascade utilization. For directly facing users, DES provides on-demand supply and meets various requirements. The DES represents a concept of power production and management, but is often associated with distributed generation in practical technology research [34–36]. In order to further match demand as well as reduce distribution losses, small and micro generation devices of kW-level are the main development trends of miniaturization of distributed generation systems. Combined heat and power (CHP) systems are mostly employed in distributed generation. With the advantage of proximity to users, the heat by-products are utilized for heating in a CHP system [37].

Figure 5 presents a basic system diagram of the MGT-CHP system, composed of an MGT, a generator, and

**Table 1** The main characteristics of the commercial MGTs.

Model	Manufacturer	Power (kW)	Pressure ratio	TIT (°C)	Rotate speed (rpm)	Recuperator	Efficiency (%)
C30 [18]	Capstone	30	3.2	840	96,000	Y	26
AS75 [19]	AlliedSignal	75	3.7	900	72,000	Y	28.5
TA45 [23]	Elliott	45	4.3	870	116,000	Y	30
T100 [24,26]	Turbec (Ansaldo)	100	4.5	950	70,000	Y	30
PW70 [4]	PowerWorks	70	3.3	870	60,000	Y	33
TG80CG [22]	Bowmen	80	4.3	680	68,000	Y	25–28
Bladon12 [29]	Bladon	12	—	—	134,000	Y	25
ET45 [30]	ETgroup	45	—	—	60,000	Y	28
GT333s [27]	FlexTurbine	333	—	—	—	Y	33
E100 [31]	ENN	100	4.2	—	51,000	Y	26
T2-200 [32]	Wisdomturbine	240	7.5	927	54,000/44,000	N	22.9

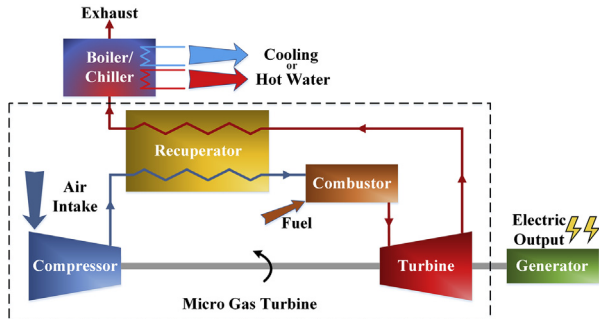


**Figure 5** Basic schematic representation of the MGT-CHP system.

refrigeration or heating devices. A complex system also includes controllers, thermal storage units, and auxiliary boilers to meet peak heat demand [38].

Numerous studies have been conducted on the application of MGTs in distributed energy systems. In 2000, Pilavachi et al. [39] introduced MGTs and cogeneration systems, pointing out that the EU requires the overall efficiency of cogeneration systems to reach above 60%. In fact, the MGT-CHP-based systems could achieve 90% of the overall efficiency [38]. Murugan et al. [40] summarized the micro-CHP systems for residential exploitation. By comparing the characteristics of different energy conversion devices, they pointed out that MGTs are promising techniques suitable for residential, commercial and educational buildings. Caresana [41] and Gimelli [42] also believed that MGT-CHP-based systems have excellent applicability for small and medium-sized power consumers, such as shopping centers and remote areas.

The characteristics of several prime movers for mCHP have been presented in Table 2 [40]. Compared with internal combustion engines, MGTs have fewer moving parts, better fuel adaptability, and lower emissions [41,42]. MGTs are also easy to maintain and could meet high environmental standards. Compare with fuel cells (FC), organic Rankine cycle (ORC) system and Stirling engine (SE), MGTs generally have higher power density and higher exhaust gas

temperature, which are good driving heat sources to achieve efficient cogeneration [43].

Based on these advantages, many distributed energy systems with MGT have been exploited since commercial MGTs entered the market in the late 1990s. Take Capstone as an example [18]: the C30 provides electricity and hot water for the MTS Argonon dual-fuel vessels and California's Tahoe Center, at an altitude of 6300 feet. Two 65 kW products are utilized in the ONE NK Leisure Centre, supplying 75 kWh of electricity and 130 kWh of heat annually. Lotte New York Palace Hotel has been equipped with twelve C65, achieving 780 kW power generation, and 3.45 MMBtu/h hot water at 93 °C. It can also be exploited for building refrigeration with an absorption chiller. Additionally, Capstone's products are employed in more than 30 distributed generation facilities worldwide.

In order to enhance the performance of cogeneration, researchers have proposed methods for evaluating the performance of CHP systems and examining the influencing factors. The methods based on the first law (relate with energy) and the second law (relate with exergy) of thermodynamics have been employed to examine the influencing factors and predict the performance of CHP systems [44–46]. To this end, Balli et al. [47] evaluated the performance of MGT-CHP systems by scrutinizing the energy and exergy. The working conditions of T100 were taken as the template. The energy rate, exergy rate, and other properties at various system locations were obtained to evaluate the energy loss/exergy consumption of each component. The energy/exergy discrepancy between the inlet and outlet of the system represents the sum of energy losses/exergy consumption in components. The performed study revealed that the exhaust gas could cause a maximum energy loss of 44.03 kW (about 13.14%) since the waste heat was not exploited. In general, exergy is defined as the representation of the quantity and quality of energy. With 345.27 kW of fuel exergy input, 99.15 kW electrical exergy and 24.46 kW heat exergy growth were produced. The total exergy consumption was 221.66 kW, which is mainly due to the exergy destruction of the irreversible process. The irreversible

**Table 2** The characteristics of prime movers for mCHP [40].

	MGT	ICE	FC	ORC	SE
Recoverable heat	45%–55%	15%–20%	25%–35%	45%–65%	—
Moving parts	Shaft & Impeller	Crankshaft & multiple pistons	—	Shaft & Impeller	Pistons
Energy source	HC fuels of high/low heat value, Biofuel, H <sub>2</sub> , NH <sub>3</sub> , waste heat	HC fuels like Petrol and diesel, H <sub>2</sub>	HC fuels, H <sub>2</sub>	Indirect heating: low quality heat source from heat exchange	Indirect heating
NO <sub>x</sub> emission	<10 ppm	<100 ppm	<10,000 ppm	—	—
Generation efficiency	25%–33%	20%–40%	30%–40%	<10%	10%–20%
Co-generation efficiency	60%–90%	60%–80%	60%–90%	65%–80%	65%–90%
Maintenance	>8000 h	<1000 h	—	150–250 h/year	—
State	Uncommon	widespread	Proven technology	Development, early market	Development, early market

reaction of high-quality chemical energy to low-quality process heat in the combustion chamber caused a maximum exergy loss of 129.61 kW (about 37.54%). Thu et al. [45] believed that 70% of exergy loss occurs in the combustion chamber, where the excess air coefficient increases from 550% to 720% when the magnitude of exerted load changes from 100% to 25%. Together with the poor heat transfer in the recuperator at low flow rates, the MGT-CHP system has a larger loss under the evaluation of the second law. Feng et al. [48] pointed out that the performance would decrease at part-load conditions and could be restored by adding energy storage systems, which made it suitable for full conditions. Other explorations have revealed that Humidified cycle is helpful to the flexibility of distributed generation systems [49,50].

### 3.2. Range extender

Electric vehicles (EVs) have received great attention in the context of environmental protection, but still confront challenges like heavy weight, high price, low energy density, and short mileage due to the battery limitations [51,52]. The range extender (RE) is an effective approach to unlock the mileage problem by providing additional power sources [53]. While the current RE is generally modified from the ICE, the MGTs are considered to be a promising development direction for REs. Compared with ICE, MGTs possess outstanding advantages in power density, fuel adaptability and emission performance, hence leading to the reduction of CO emissions by 30% and NO<sub>x</sub> emissions by 50% [54–56].

Generally, an MGT-RE powertrain consists of ranger extender (MGT), generator, power converter, battery pack and electric motor, as illustrated in Figure 6 [57]. In this

**Table 3** MGT range extender vehicles.

Year	Brand	Power (kW)
2005	Volvo [58]	300
2009	Capstone [59]	30
2010	Jaguar [60]	70
2016	Techrules [62,63]	15–30
2017	Wrightspeed [67]	80
2019	Mitsubishi [64]	60

system, MGT provides a power source and generates electricity as an RE. Further, the source motor output and the wheel load input are isolated by the electrical connection, which solves a series of problems caused by the old direct drive strategy. This fact implies that the RE is a practical scheme for MGTs applied to vehicles.

Table 3 presents some vehicles equipped with Res of MGT. Volvo tested the VT300 gas turbine drive on heavy trucks in 2005 and made positive progress [58]. The Capstone CMT-380 concept car [59] was equipped with a 30-kW gas turbine and gained a total mileage of 800 km with a battery pack. The Jaguar C-X75 released in 2010 had four electric motors driven by two 70 kW MGT generators from Bladon Jets [60]. Single MGT had a power-to-weight ratio of 2 kW/kg [61], which is higher than that of the usual ICE powertrain. MGT range extender vehicles produced by Techrules [62,63], Mitsubishi [64], Hybrid Kinetic [65] and Delta Motorsport [66] have also been reported in the literature. Wrightspeed exploited recuperated 80-kW MGT as the power unit of electric trucks [67]. The RE of Wrightspeed, as presented in Figure 7 [67] has achieved good economic benefits.

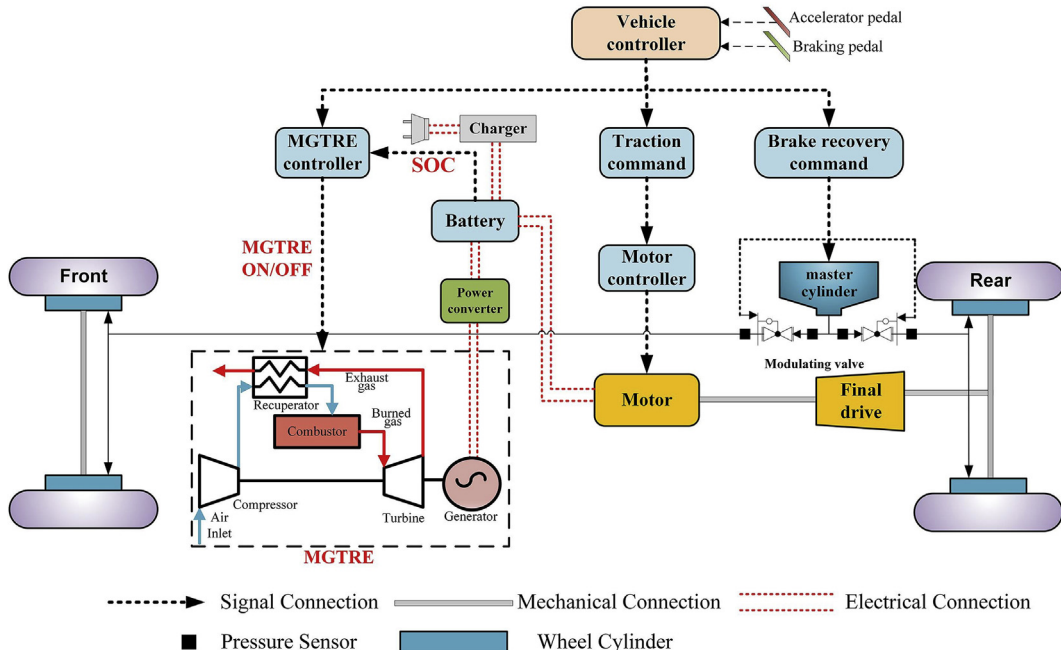


**Figure 6** Overall schematic representation of an MGT-REEV system [57].

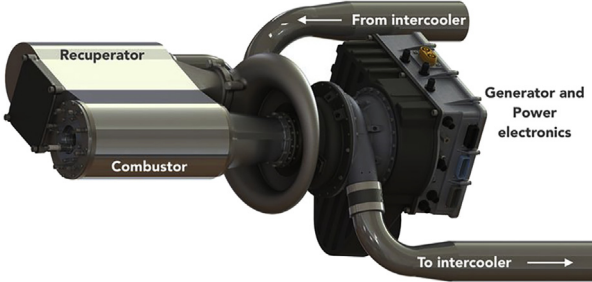


**Figure 7** Wrightspeed range extender [67].

Concerning the MGT range extenders, researchers have focused on the overall performance and studied the factors that affect the emissions, fuel consumption and power performance of MGT-REEV. Karvountzis-Kontakiotis et al. [68] established a vehicle model based on the Power demand and NEDC standard in MATLAB. Simulations were performed on the ICE, ICE range extender and MGT range extender in the presence of various circumstances. These investigators exploited a thermo-kinetic-based model to estimate CO and NO emissions, and discovered that using MGT as range extender can remarkably enhance emissions. The obtained results indicate the reduction of NO and CO emissions in order by about 79.6% and 92% through consuming more fuel. Tan et al. [69] also developed a model to simulate MGT-REEV and emphasized that MGT-REEV had comparable mileage to ICE. The 10 kW power output could meet the operation demand of their battery pack. The authors also modified a turbocharger into MGT based on the simulation results and conducted performance tests, which showed a peak power of 9.5 kW. Arefin et al. [70] examined an electric truck with a range extender, focusing on the performance of noise, emission, and output power. The produced noise by the MGT was low at low speeds, while the high-frequency noise from generators was apparent and covered all the operating conditions. The results also revealed that the best ambient temperature (i.e., those placed in the range of 20–22 °C) would affect the output power. Furthermore, air filters would increase the power output by 3% and lessen emissions at high speeds. Sim et al. [71] developed an MGT for range extenders, which increased the mass/volume power density by 400%/500% compared to diesel engines.

Since MGTs represent scaled-down versions of gas turbines, their characteristics are commonly affected by their power level. In order to gain higher thermal efficiency, MGTs usually work in the presence of high speed shafts, resulting in larger generators and inverters, which is detrimental to vehicle-board applications [72]. The low powers can also lead to scale effect problems in component performance. By affecting component efficiency, it has a substantial influence on the overall performance of the REEV, such as battery pack size and charging time, according to Javed et al. [73]. The slow response also restricts MGTs for vehicle use. The MGT-RE dynamic model established by

Shah et al. [74] showed that the dynamic response of the MGT to several power demand strategies under NEDC working conditions exhibited a large delay, requiring an energy buffer to allow operation in a vehicle.

Current explorations support the application of MGTs in REs and they have formed relevant industrialization. The advantages of MGTs are emission and fuel adaptability. While longer life, lower vibration and more compact size are potential drivers for further commercial exploitation. Higher cost, and non-maximum efficiency at the same power level are among the major problems that limit their application. By this view, the slow start-up speed still needs further research and solution to meet flexible requirements for vehicle use.

### 3.3. Concentrated solar power system

Solar thermal power systems have attracted more attention due to their high efficiency and cheap heat storage [75]. In the 1980s, solar thermal power systems using gas turbines as power conversion machinery were designed in the United States and widely tested [76]. In a gas turbine-concentrated solar power (GT-CSP) system, the pressurized air is heated by the collected and stored solar heat, to increase the inlet temperature of the combustion chamber and reduce fuel consumption. Although some earlier studies have pointed out that heavy gas turbines are attractive alternatives to solar thermal power generation [77,78], due to their maturity, current megawatt-scale gas turbines with solar power generation systems were rarely reported [79]. Kilowatt-scale MGTs are suitable for concentrated solar power (CSP) systems. A small power makes the system scale manageable. The heliostat will not occupy too much area, making the system less constrained by the size of the site.

Figure 8 shows a typical MGT-CSP system. Sunlight is concentrated through the heliostats into the receiver, and the concentration ratio can be high. As the MGTs adapt to high TIT, the allowable highest temperature of solar receiver can be much higher, as demonstrated in Figure 9 [80]. A supplementary combustor is often equipped to manage the energy input to stabilize working condition of MGT. In addition to the tower collectors that have been demonstrated, the form of energy collection also includes dish collector systems, which is often with smaller individual

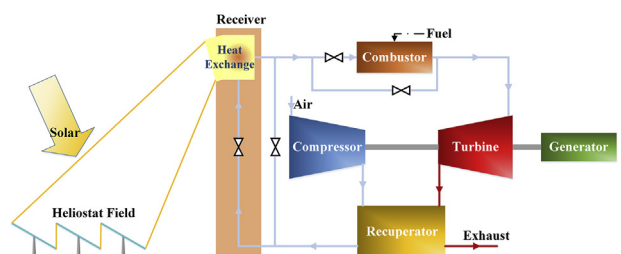


**Figure 8** Schematic representation of a tower MGT-CSP system.

power. Common turbochargers can be retrofitted and integrated [81]. Due to the small size and weight, MGTs have the advantage to be easily integrated next to the heat collector, which is also favored by space CSP systems [82]. Some current MGT-CSP facilities have been also illustrated in Table 4.

The project code, named Solgate [83,84] and Solhyco [85,86], has been carried out in the PSA platform, Spain, establishing MGT-CSP systems with the full power of 250 kW and 75 kW, respectively. The power system of Solgate has been modified from Turboshaft OST3. On the

other hand, Solhyco implements a commercial gas turbine, named T100. Both systems have a tower collector, receiver cavity boxes are applied to collect the heat, and the absorber tubes are arranged in the box to transfer the heat to the compressed air flowing inside. The Solgate system is also equipped with a two-stage concentrator to increase the temperature, which is considered an effective solution to reduce high temperature surfaces and heat loss [87]. The facility with a tower scheme also includes Tulip™ built by AORA Solar in Israel [88] and the 75 kW solar-thermal project built in Nanjing, China [20].

The US. South West Solar corporation and Brayton Energy jointly launched the 80 kW Solar CAT project using Brayton 80 kW MGT as the power core, having a 23 - meter diameter dish collector [89,90]. The MGT is usually recommended to be installed near the dish focal point to avoid heat loss caused by long pipelines. Casaccia has provided an MGT-CSP system with a low power level of 3–10 kW, showing well integration [91,92].

In addition to these practical MGT-CSP systems, some explorations have also proposed related designs. Giostri et al. [93] evaluated the thermodynamic performance of a dish receiver system with a design power of 31.5 kW and a TIT of 850 °C, which was fully provided by solar energy. Poživil et al. [94] developed a solar receiver for MGT, and it was revealed that pressurized pressured air could obtain 47 kW of energy in the heat exchange with the cylindrical SIC cavity surrounded by the mesh porous ceramics and gain a pressure loss of 2.7%. Ragnolo et al. [95] designed an MGT system for dish collectors such that the receiver was

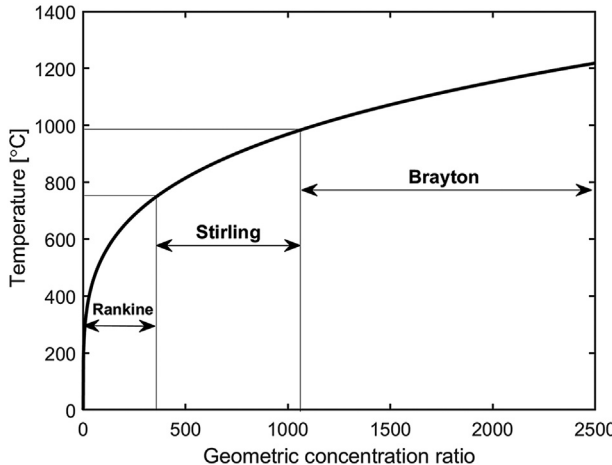


**Figure 9** The applicable temperature range of the thermal cycle as a function of the concentration ratio [80].

**Table 4** MGT-CSP facilities.

Location/Project/ Company	Code name	MGT models	Power	Receiver & Method	Time/Reference
Spain PSA	CESA-1	OST3 (modified from a turboshaft)	250 kW in design; 230 kW in experiment due to damage	Tower	1999/[83]
	Solgate			Triple receiver model, each one includes a sec- ondary concentrator and a receiver vessel make up with absorber tubes Solar hybrid co- generation	2006/[84]
Israel AORA Solar	Tulip™	Turbec T100	600 °C–800 °C; Receiver could provide maximum 181.9 kW; Operating at 75 kW under full solar input	Tube collector	2008/[85]
				Solar hybrid co- generation	2010/[86]
US. South West Solar/Brayton Energy	Solar CAT	Brayton Energy 80 kW	100 kW electric 170 kW heat	Dish collector with a diameter of 23 m	2011/[89] 2016/[90]
EU. ENEA Casaccia	OMSoP	Provided by Compower and modified by CITY University	3–10 kW full solar input	Dish, MGT installed at the focal point	2015/[91] 2017/[92]
Nanjing, China	—	Parallon75	75 kW	Tower, pressure cavity receiver	2007/[20]

placed in front of the combustion chamber and could provide 25 kW of preheating energy in the presence of nominal solar input.

As mentioned above, the MGT in the CSP system is not completely heated externally in general, but retains the combustion chamber. The fuel consumption usually varies inversely with the sun intensity to maintain a steady power generation. The uneven distribution of solar radiation during days and seasons makes dynamic change in the fuel consumption. Therefore, the operating cost of CSP systems often considers fuel consumption and relates to the operation strategies, requiring considerations from multiple perspectives. According to M.C. Cameretti's research [96], the total cost of the MGT-CSP system is due to the area of the heliostats, as shown in Figure 10. An excessively large mirror surface can lead to an increase in maintenance costs. The optimized total cost is 35,655 euros per year, and the fuel cost accounts for more than 87% of the total costs. The system can generate electricity of around 615 MWh. In the solar power generation and desalination system described by Coppitters [97], solar energy enhances the generation efficiency by about 3.2%. The proposed designs achieve a levelized cost of water between \$ 1.78/(m<sup>3</sup>/d) and \$ 1.92/(m<sup>3</sup>/d), which is comparable with conventional solar-powered desalination plants. Exergoeconomix can be employed to evaluate the cost of electricity generation. Babaelahi [98] conducted multi-objective optimization on thermal efficiency, exergetic efficiency and the cost of electricity generation, and then the trade-off between electricity generation cost and efficiency is presented. Giostri [87] also modeled and analyzed a small-scale MGT-CSP system. By optimizing the optics, the system obtained a levelized cost of energy of 175 €/MWh, which was relatively cheaper than large-towers solar systems.

MGTs are ideal power machines for CSP systems. The compression and circulation method allow complex flow piping to meet the integration needs of CSPs. Extensive fuel adaptability enables it to be combined with biofuels and other technical means, thereby further reducing fuel costs [99]. Current commercial and experimental setups have

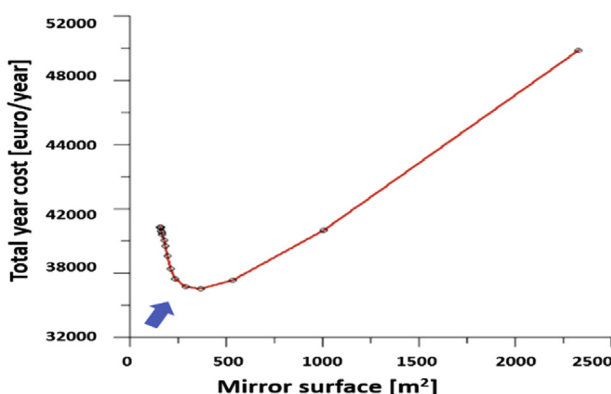


Figure 10 Plot of the total annual cost in terms of the mirror surface area [96].

indicated the maturing of this technology. Further investigations are still required on control methods suitable for various insulation conditions [100], as well as design methods appropriate for complex coupled systems. In particular, the performance of receivers and heat exchangers will also have a crucial impact on the application of MGTs in CSP systems.

### 3.4. Micro gas turbine - fuel cell system

High-temperature fuel cell systems have been extensively employed in distributed energy systems since combining fuel cells with MGTs can improve efficiency [101]. There are usually two types of fuel cells combined with MGTs: molten carbonate fuel cell (MCFC) and solid oxide fuel cell (SOFC). The mixed cycle can also be divided into two types: the top-level cycle and the bottom-level cycle. A top-level cycle is defined as a high-pressure cycle, which usually contains a pressurized tubular fuel cell [102]. The oxidant end of the fuel cell is fed with high-pressure gas after the compressor. While the bottom-level cycle works under the action of normal pressure. The oxidizer enters the fuel cell before or after going through the MGT. Figure 11 presents a schematic representation of the top cycle. The operation of the fuel cell in a high-pressure air environment after the compressor is bound to increase the efficiency and power density of the fuel cell. The high-temperature exhaust gas is utilized as a heat supplement or directly expands in the turbine. The SOFCs are generally considered to be suitable for top cycles to achieve high efficiency [103,104]. Figure 12 illustrates a schematic representation of the bottom cycle. The ambient air is compressed first and then preheated in the heat recovery unit. A high-temperature heat exchanger is exploited to exchange heat between burned gas and compressed air, and the heated air directly drives the turbine. The turbine exit air is burned with the unreacted fuel components from the anode of the fuel cell, and the gas enters the cathode of the fuel cell as a reactant. In the cycle, both reactants in the anode and cathode are at normal pressure, which is consistent with the characteristics of the bottom-level cycle. Usually, the repeated transportation of CO<sub>2</sub> between anode and cathode makes MCFCs suitable for the bottom cycle [105].

A lot of research on MGT-FC cogeneration has been conducted. Komatsu et al. [106] believed that the decrease in system efficiency in the presence of partially applied loads was mainly due to the decrease in the operating temperature of the SOFC module. The results indicated that the SOFC-MGT system could reach a generation efficiency of 60% (LHV) at the design point while the efficiency remained above 50% (LHV) at a load level of 60%. These results display that the MGT with a flexible airflow should maintain the operating temperature. Jia et al. [107] proposed a co-gasification system of woody biomass and animal manure with MGT-SOFC. The results show that the thermal efficiency could reach 55%, which was close to the

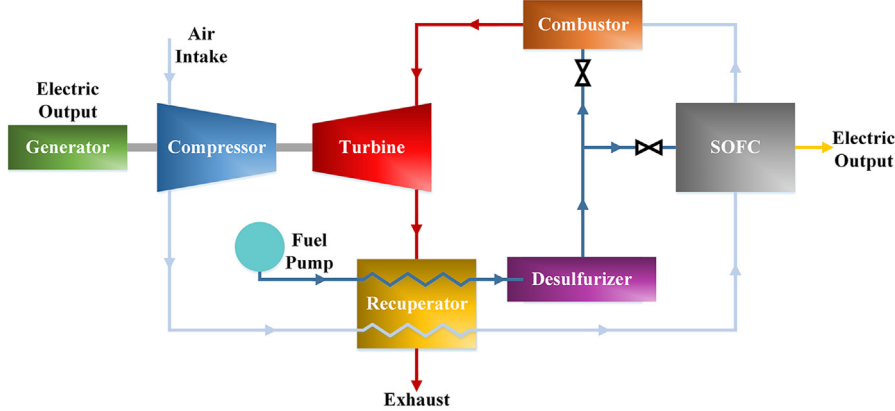


**Figure 11** Schematic representation of a top cycle MGT-SOFC system.

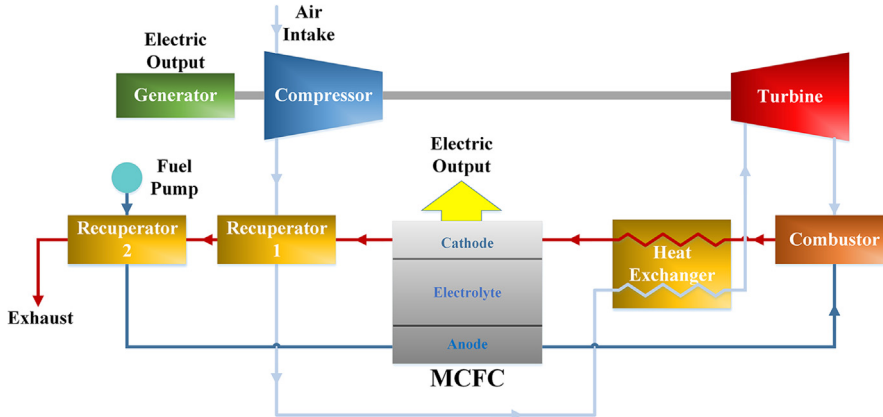


**Figure 12** Schematic representation of a bottom cycle MGT-MCFC system.

efficiency of MGT systems burning waste gas on the basis of the SOFC (about 42%–58%). Further the system gained considerable investment returns.

Ebrahimi et al. [108] combined a cycle of SOFC, MGT, and ORC. The high-enthalpy exhaust gas from the fuel cell was utilized in the MGT and the exhaust gas from MGT was then exploited in a heat recovery steam generator in the Rankine cycle. Sensitivity analysis of the system had been conducted, giving out a maximum total efficiency of 65%. For further research, biomass fuel was utilized in a similar system for cogeneration [109].

Liu [110] explored the performance of a pressurized MCFC-MGT system based on a commercially available MGT. The understudied system was less efficient than SOFC and traditional MCFC systems. Several control approaches for the case of partially exerted load were developed and explained. The alternative speed method of gas turbine provided better performance, but was confronted with a risk of the surge. Ahn et al. [111] designed an MCFC-MGT system with a carbon capture device, which achieved

almost 100% CO<sub>2</sub> capture. Compared with other normal MCFC systems, the system with carbon capture had a higher output power. In later research, off-gas recirculation was assessed to substantially enhance the thermal efficiency of the global system, by over 57% [112].

The integration of the MGT and FC system remarkably improves the system efficiency, where FC can be very beneficial to MGT to bypass the efficiency limitation of the Carnot cycle. Such a system is considered to be a promising application direction. Further, some models have been put into commercial operation [113]. However, compared to other MGT systems, the application of the FC system requires more cost in the cogeneration system, and the return on investment should be further paid attention to.

### 3.5. Other applications

In addition to the above-mentioned applications, mobile/emergency power sources also represent foreseeable applications of MGTs. With respect to small size, lightweight,

good fuel adaptability, and equivalent running cost to an internal combustion engine, MGTs have inherent advantages in the field of kilowatt level mobile power and are appropriate choices for emergency rescue, disaster relief power supply and applications requiring high power generation quality.

With the advent of ultra-MGTs of smaller scales and power levels, it became possible for MGTs to be exploited in single-soldier power systems [114–116]. High energy density, low vibration, smooth operation, and low noise are among the outstanding advantages. Although the energy conversion is improvable, MGTs still have a larger power density than lithium batteries.

#### 4. Multidimensional performances of MGTs

The performance of MGTs has been always the focus of attention of investigators and engineers. A reasonable overall design and higher components performances can enhance the overall performances of MGTs, to be favored by more applications, as the capability of MGTs has a great impact on integrated systems [117,118]. This section has been mainly organized based on the following three perspectives.

##### 4.1. Steady-state performance

Steady-state thermal analysis should be carefully examined to obtain the performances at the design point of MGTs. Such an effect on the performance of the MGT of typical operating parameters as well as the key component performance, such as pressure ratio, TIT, impeller efficiency, and recuperator effectiveness can be obtained. This analysis is general to all scales of gas turbines, and has been disclosed in publications and textbooks [119,120].

The steady-state analysis is generally based on commercial software/packages (GSP, WTEMP, and GT-Power) or private codes [121]. The component equations are established one by one according to the cycle structure. In addition, the states are solved by recursion or iteration process according to the input boundaries and mass/energy conservation. Compared with the predicted results by a theoretical formula based on the ideal gas model, the solution results by a program package or specific software code in accordance with the real physical properties lead to more reliable accuracy estimation.

The thermodynamic sensitivity analysis conducted by Galanti and Massardo [122] was employed to display the influence of the law of component parameters such as turbomachinery efficiency, TIT and recuperator effectiveness. Figure 13 [122] illustrates the classical “efficiency vs. specific work” graph for both cycles under investigation. As it is seen, the R-GT exhibits a simple regenerative cycle, while the ICR-GT exhibits an intercooling regenerative cycle. From the efficiency standpoint, there is an optimal pressure ratio, which is limited by the TIT. An increase of

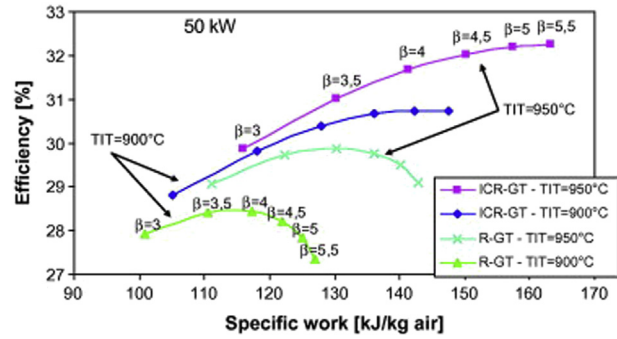


**Figure 13** R-GT and ICR-GT cycle efficiency in terms of the specific work varying pressure ratio and TIT [122].

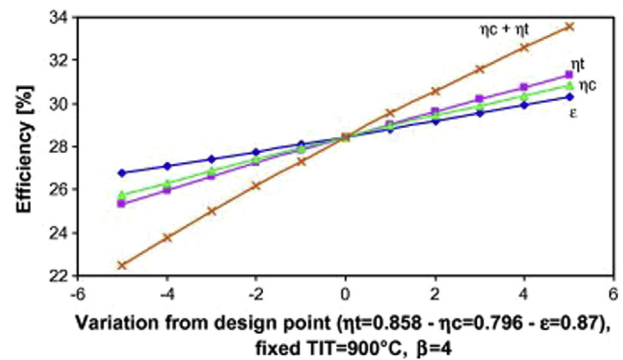


**Figure 14** The R-GT cycle efficiency in terms of the components' efficiency/effectiveness [122].

the TIT from 900 K to 950 K leads to a 2% increase in maximum efficiency. The specific work presents a monotonic trend as a function of the pressure ratio, which implies that a higher pressure corresponds to a lower mass flow rate. It is beneficial to reduce the impeller size, but an excessively low mass flow with high specific work on the compressor/turbine will lead to difficulties in the design of the impeller.

The sensitivity analysis of the global efficiency of the R-GT cycle in terms of the impeller efficiency and recuperator effectiveness has been demonstrated in Figure 14 [122]. In the plotted results, the base points are chosen as recuperator effectiveness of 87%, compressor isentropic efficiency of 79.6%, turbine isentropic efficiency of 85.8% with a variable range of  $\pm 5\%$ . The isentropic efficiency of the turbine has the greatest impact on global efficiency, followed by that of the compressor. The plotted results reveal that the effect of recuperator effectiveness is relatively small such that a gain of 5% on the effectiveness leads to a 2% increase in global efficiency.

##### 4.2. Off-design performance and transient performance

The off-design performance and transient performance are taken as crucial representative features, since the flexible energy demand makes the MGTs operate between partial

load conditions, and the performance of MGTs is still of concern at the time. Further, response delay restricts the application of MGTs.

Simple partial load conditions can be analyzed by quasi-static methods and the key is to obtain the working characteristics of the impellers in the presence of partial load condition with variational rotating speed and mass flow. The transient performance analysis requires dynamic analysis models, generally based on the working curves of impellers, energy conservation equation, torque inertia equation, and the volume effect of the original volume. A co-working equation was also established for the analysis [121].

Commonly, two types of methodologies are utilized to obtain the working characteristics of impellers. For the actual impeller, the turbo component module relies on the compressor or turbine maps to evaluate the mass flow and temperature change of the gas with a quasi-steady-state approach, as presented in Figure 15 [123]. The mapping relationships among normalized mass flow, normalized rotated speed, pressure ratio and isentropic efficiency have been illustrated in the map, and a guideline can be helpful in positioning. For the simulated impeller, the module can be evaluated by the established formula [124,125].

Both methods require normalization of the mass flow and rotating speed. The common normalization approach is introduced as follows [121]: normalized mass flow:  $m\sqrt{T_i}/P_i$ , and normalized shaft speed:  $n/\sqrt{T_i}$ , where  $T$  represents the qualitative temperature at the impeller inlet,  $P$  represents the inlet pressure, and subscript  $i$  can be taken as ‘ $c$ ’ or ‘ $t$ ’ to signify the compressor and turbine respectively.

The dynamic performance of MGTs has typical characteristics of non-linear and large time-delay, which are essentially caused by the synthetical effect of rotational inertia of the shaft, thermal inertia of the recuperator, and

co-working of the impeller [126]. Since the rotational inertia of the MGTs is smaller than that of the large gas turbines, the influence of the thermal inertia of the recuperators on the system can be readily amplified. The control and monitoring of the turbine outlet temperature are important in transient conditions. In general, surge boundary brings limitations on the dynamic control, because the system failure is difficult to recover once the surge occurs. The high requirements are put forward for the control system, making it problematic for a simple PID controller to deal with complex coupling [127], and resulting in problems like overspeed or over-temperature. Therefore, the low-value comparator based on the temperature and speed limitations is extensively utilized in the regulation of MGTs. Furthermore, advanced fuzzy PID algorithms or expert control were also examined and applied [128,129].

With the increase of MGT applications, more complex systems have been proposed, including CSP, FC, grid-connected, and grid-independent generation. The regulation under multi-factor operating conditions of MGTs will be a common question. There are great discrepancies in energy injection between various systems, but the working model of cooperation impellers has specific versatility. The recuperator can also be described by a general heat exchanger model. In order to establish a generalized system model and relevant regulation mechanism based on the black box of energy supply will be beneficial for the adaptation of MGTs to different systems.

#### 4.3. Thermoconomic

As the promotion deployment is constrained by investment cost, the thermal economy of MGTs is also crucial factor affecting its design and optimization. The cost

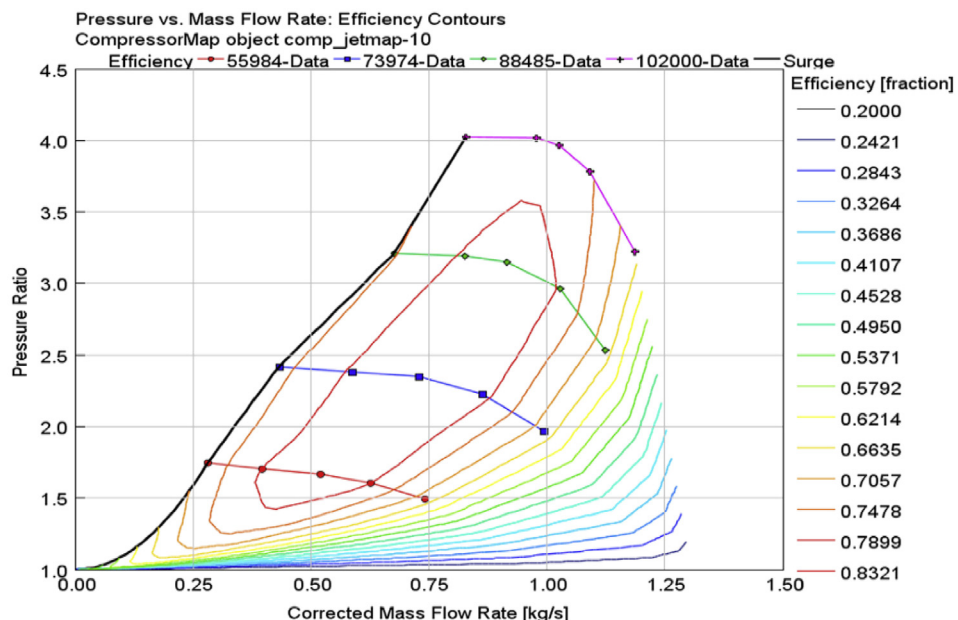


Figure 15 The working map of a compressor [123].

variation is related to efficiency improvement, so an examination of the role of harmony optimization in both thermal efficiency and thermal economy is required.

The capital cost evaluation of the components of MGTs has been introduced in previous works [121,130]. The equipment cost is usually dependent upon capacity with a 0.6 exponent, leading to a higher cost on small size components in MGTs [131]. Based on the established cost functions, the capital cost of compressors, turbines and recuperators can be obtained. According to Galanti and Massardo, the cost functions of components in MGTs are given in Table 5 [122]. The costs of impellers are commonly expressed in terms of flow, efficiency and pressure ratio. The coefficient  $f$  is introduced in the cost calculation of the recuperator to evaluate the material prices for various working temperatures. In the case of using superalloys, the factor  $f$  can be 1.5 to 9 times higher than the case of using stainless steel [132].

The investment in impellers increases along with the pressure ratio, while the investment in recuperators decreases, which is understandable that the temperature limitation of TIT reduces the heat transfer rate. Galanti and Massardo [122] stated that over 2% increase in turbine isentropic efficiency over design point resulting in a sudden rise in investment cost, as demonstrated in Figure 16 [122]. The turbine efficiency is the major factor among those of impellers.

The effectiveness of recuperator noticeably affects the cost such that with 5% additional effectiveness, the investment in recuperators increases by approximately 80%. Therefore, although high recuperator effectiveness can reduce waste heat and enhance system global efficiency, it is usually not particularly high due to cost constraints [57]. In the meantime, since the working temperature of the recuperator is related to the TIT, the material cost of recuperator is stepped determined by the TIT.

Further, for a simple regenerative MGT, the operating parameters pertinent the best global efficiency and the best thermal economy can be different. The trade-offs are usually observed between the capital investment and the overall performance.

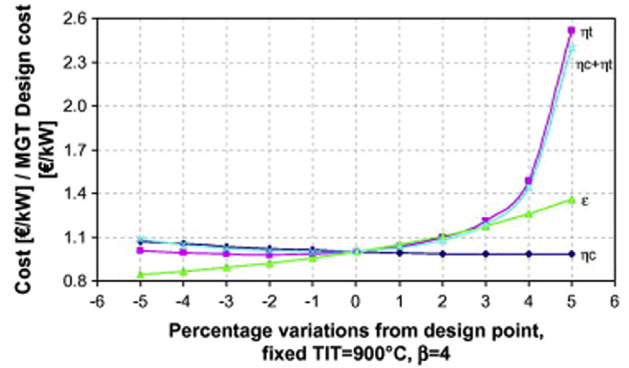


**Figure 16** The investment cost of the recuperative gas turbine in terms of the efficiency of the varying components [122].

## 5. Status of the component technology and research

As explained above, the researchers have innovated overall cycles to expand the application range of MGTs, and research works on the overall parameters is also introduced and discussed. The improved component performance is proven to have a positive impact. This section is aimed to focus on the key technologies of MGTs components and the latest research on compressors, turbines, combustion chambers, recuperators, and rotor systems.

### 5.1. Compressor

As a key component, the compressor's margin directly determines the operation adaptability of the MGT. The compressor system of MGTs is usually composed of an impeller, casing, and diffuser. The inlet guide vanes are common in medium and large gas turbines, but are rarely utilized in MGTs. The design of impeller machinery such as compressors has become mature since Wu [133] proposed the theory of three-dimensional flow in 1953. After the advent of CFD technology, numerical simulations have also provided great convenience for compressor design and theoretical research.

**Table 5** Cost functions of components in MGTs [122].

Components	Cost functions	Coefficients
Compressor	$\Xi_{compressor} = \sqrt{R_g/R_{ref}} \cdot c_1 \cdot \frac{\dot{m}_a}{c_2 - \eta_{pol\_c}} \cdot \ln \beta_c$	$c_1 = 55.8, c_2 = 0.942$
Turbine	$\Xi_{turbine} = \frac{t_1 \dot{m}_g \sqrt{R_g/R_{ref}} \ln \beta_t}{t_2 - \eta_{pol\_t}}$	$t_1 = 376.1, t_2 = 0.903$
Combustor	$\Xi_{combustor} = \frac{cc_1 \dot{m}_s}{cc_2 - P_{in}/P_{out}}$	$cc_1 = 36.1, cc_2 = 0.995$
Recuperator	$\Xi_{recuperator} = 1.5 \left( r_1 \cdot \dot{m}_{in}^{cold} \cdot (P_{in}^{cold})^{-0.5} \cdot (\Delta P^{-0.5}) \cdot \frac{\epsilon}{1-\epsilon} \right) \cdot f$	$r_1 = 625.1$
Generator	$\Xi_{generator} = g_1 (P_{el})^{g_2}$	$g_1 = 18.7, g_2 = 0.95$

Current research on compressors is primarily focused on performance loss and instability to guide the design and optimization of compressor systems. The main purpose of this subsection is to introduce the research on centrifugal compressors designed for MGTs, including methods of stability expansion, efficiency enhancement and optimization.

### 5.1.1. Stability expansion

The principle of compressor instability and stability expansion has always been a prominent research direction in the mechanical analysis of compressors. For the compressors on MGTs, small-scale and radial flow are the main differences between large GTs. The wall friction near the blade tip and root alters the vortex structure and affects the free flow. Particularly, the enlarged assembly error between compressor and shell due to the scale effect can enhance the influence of the tip leakage flow [134]. Xiang et al. [135] examined the influences of tip clearance variation and impeller miniaturization by distinctly fixing the Reynolds number and tip clearance. The obtained results revealed that the compressor performance can be deteriorated when the Reynolds number decreases subjected to fixed tip clearance, indicating that the miniaturization can deteriorate the performance as the leakage flow disturbs more flow area.

Therefore, a series of stabilization measures have been investigated [136]. Thanks to the good process feasibility, the treatments of the wall treatment and self-circulating casing, as passive means have been examined and applied in centrifugal impellers. Xue et al. [137] explored the stability expansion of self-circulation casing treatment by implementing coupled optimization methods (i.e., optimal Latin hypercube sampling, polynomial surrogate model, Fourier amplitude sensitivity test and gradient mutation hybrid optimization algorithm). The isentropic efficiency at the design point or near-stall point was improved, and the stable working range was expanded by about 9.59%. Further, low-energy-fluid extraction and separation inhibition were considered as two main ameliorative mechanisms.

The mechanisms of instability caused by accessory systems such as volutes, diffusers, and intake pipes have been also of grave concern. For this purpose, Hellstrom et al. [138] carried out a numerical simulation on a centrifugal compressor with volute by adopting the large-eddy simulation method to capture large-scale unstable flows. The results indicated that a reverse flow can occur in the impeller inlet and diffuser due to the appearance of the radial pressure gradient, leading to a highly unstable flow near the surge point. Olivero et al. [139] scrutinized the flow of a single-stage centrifugal compressor with splitter blades based on a steady-state model. To this end, software CFX was exploited to solve the internal flow and the results showed that the excessive Mach number at the leading edge would cause the gradual reduction of the pressure, forming a low speed zone on the suction surface. Another low speed zone near the casing spread along the blade and spread into the diffuser. The results indicated that the blade inlet angle

should be appropriately optimized in order to eliminate excessive Mach numbers. Yang et al. [140] proposed an active control casing treatment (ACCT), in which injection holes were circumferentially drilled in the shroud at a position where a recirculation zone may be formed. Through conducting experiments, the obtained results revealed that the ACCT system could substantially extend the threshold of the flow. A better effect was also observed at low speeds, achieving the maximum improvement rate of 32.73%. Sun et al. [141] experimentally examined the instability mechanism in the entire working section of the centrifugal compressor. The gained results showed that the unstable flow at the inlet of the impeller caused stall surge at low speeds, while the unstable flow at the inlet of the diffuser produced deep surge at high speeds. In order to extend the stable flow range, Sun et al. [142] further designed a non-axisymmetric vaned diffuser (NAVD) by modifying the local passage angle and the local vane stagger based on a normal vaned diffuser. The comparative experimental results indicated that the NAVD delayed the surge at high levels of speed by suppressing the instability flow at the inlet of the diffuser, but the suppression was not apparent at low speed. Zhang et al. [143] carried out experimental research on centrifugal compressors with uniform inlet pipe and two types of inlet bent torsional pipe to explore the effects of various intake conditions on the performance and stable operating range. The results revealed that the interference of the high-pressure area induced by the pipe and the volute would lead to a reduction of about 22% in the stable operating range, while the rational arrangement of the pipe could weaken the pressure peak strip at the inlet region leading to an increase of around 6.4% at the near-stall point.

Moreover, acoustics have been reported in the study on the surge of centrifugal compressors. In this regard, Kabral et al. [144] proposed a method based on the full acoustic 2-port model [145] and experimentally studied the joint effect of the sound and flow fields on the centrifugal compressor stall and surge inception. The gained results displayed that the centrifugal compressor's unstable flow below the critical frequency can amplify the sound waves and cause surge or self-excited oscillation.

### 5.1.2. Loss mechanism

The efficiency of the compressor is directly related to the loss of flow in the compressor. Studying the loss mechanism and loss correlation in compressor systems will be of great benefit for designing of highly efficient compressors.

Zhang et al. [146] reviewed the research on loss mechanisms and loss correlations of centrifugal compressors, pointing out that preceding explorations were not accurate enough in compressors with high loads (pressure ratios) or at off-design points. The authors presented an approach to select the loss correlations based on the inlet Mach number and specific speed of the compressor. Three sets were demonstrated and performances of eight open-public centrifugal compressors were assessed. The results showed that

the deviations were less than 1.20% on the isentropic efficiency under the design condition while a maximum deviation on the total pressure ratio at about 7.67% occurred under the off-design condition. Li et al. [147] established a new set of loss correlations, including loss correlations of impellers, vaneless diffusers and vaned diffusers. An optimization methodology based on one-dimensional calculations using Insight platform was also proposed and good results were achieved, with an increase of the pressure ratio and efficiency, by about 4% and 2%, respectively.

The effect of the Reynolds number on the compressor flow is nontrivial at all [148]. The research on the loss of centrifugal compressors for low levels of the Reynolds number essentially focuses on the impeller. To evaluate the effect of the Reynolds number, Casey et al. [149] examined the friction loss in the centrifugal compressor and then suggested a correction formula for the correlation between surface roughness and compressor parameters. Dietmann et al. [150] proposed an approach for analysis of the Reynolds number and roughness on the compressor performance, and developed three methods to determine the influence of the Reynolds number. Zheng et al. [151] pointed out that an increase in the low Reynolds number causes development in the boundary layer thickness, which resulted in a smaller throat area. In addition, the obtained results reveal that the separation of the boundary layer near the outlet can also lead to a higher loss.

Although the impeller loss is considered to be the main factor, Tiainen et al. [152] proved that the loss of a vaneless diffuser cannot be ignored at low Reynolds numbers. Using the  $k-\omega$  SST mode, the authors performed numerical simulations on two compressors with and without splitter blades at design points, near surge, and near throttling conditions. The obtained results indicated that the thickness of the blade boundary layer and wall boundary layer in order exhibited an increase of about 20% and 37.8%, which caused the loss of the total pressure recovery coefficient at low Reynolds numbers. The effect of the diffuser on losses became highlighted as the Reynolds number lessened, which accounted for 50% of the total efficiency loss. The achieved results also proved the theory of boundary layer thickness of centrifugal compressors could be effectively exploited to study losses in more complex impellers.

### 5.1.3. Performance optimization

Another research direction of centrifugal compressors has been focused on the multi-point and multidisciplinary optimization of centrifugal compressors in efficiency, margin, strength stress and other parameters. Although the research introduced in this subsection is concerned with margin and efficiency, the optimization results are also of primary attention, and the mechanism should be only considered as a partial guide.

Meroni et al. [153] carried out optimization research on centrifugal compressors utilized in high-temperature

heat pump systems and developed a steady state mean-line model of centrifugal compressors which can be employed for various working fluids. The governing equations were solved with the latest state equation to estimate the thermodynamic and transport characteristics of fluids, and multi-objective optimization was also performed for the sake of power and cycle efficiency. Pakle et al. [154] pointed out that the optimal design of the compressor requires a trade-off between the pressure ratio, margin and blade back sweep angle. The compressor was effectively optimized by adjusting the contour of the meridian channel and changing the pre-rotation angle of the blades. The numerical simulations revealed an average of 16% increase in surge margin compared to the standard diffuser stage without altering choke flow and stage efficiencies. Xu et al. [155] displayed that the traditional impeller design through one-dimensional analysis cannot predict the internal flow, hence making it difficult to directly improve the design. As an alternative approach, a mean line design, component design, CFD simulation, and multidisciplinary optimization methodology was proposed. The method facilitated achieving a high pressure ratio and high efficiency by optimizing the geometric parameters of the compressor blade such as angle, thickness, and meridional channel.

In addition to the traditional simulation-optimization methods, the exploitation of genetic algorithms, artificial neural networks, and the design of experiments in centrifugal compressors optimization has become popular in recent years. In this regard, Table 6 presents some research works pertinent to centrifugal compressors of the same size adopted in MGTs through algorithms. The relevant objects, optimization methods, control points selection, and evaluation indexes are introduced and explained.

#### 5.1.4. Summary

This subsection is chiefly aimed to review the latest progress of MGT centrifugal compressors from three directions: stability, loss mechanism and optimization. The research on the stability expansion and efficiency enhancement has been extended from the impeller to the compressor system, emphasizing that the impact of the accessories on the stability cannot be ignored. The conducted studies on the loss correlation mainly contribute to an accurate evaluation of the efficiency. Recently, the algorithm employed for multi-objective optimization of centrifugal compressors has become attractive. We believe that efficient and accurate algorithms can assist the design of MGT centrifugal compressors in the near future.

## 5.2. Turbine

The turbine is a key component to convert the internal energy of gas into mechanical work. The efficiency and service life of a gas turbine chiefly depend on whether the

**Table 6** The optimization approaches employed for micro-size centrifugal compressors optimization methods.

Reference	Objects	Optimization methods	Control points	Results
Verstraete [156]	Small scale centrifugal compressor	Genetic algorithm, Artificial neural networks	Blade thickness, Blade leading edge inclination and height, Blade trailing edge height, Overall blade torsional curvature	A 370 MPa (relatively 49.4%) stress reduction was achieved at the cost of 2.3% (relatively 3%) efficiency loss.
Van den Braembussche [157]	Low solidity diffusers	Design of experiment, Artificial neural network, Genetic algorithms, Combined RANS&FEA	A total of 6 variables under low, medium and high flow states: Bezier blade with four control points, Scale factor of the thickness distribution, Number of blades	Stable operation at low mass flow and large pressure rise with little loss at high mass flow was achieved.
Moussavi [158]	Separate blades of impeller	Genetic algorithms	Position of the separation blade on the hub curve, Angle between the radial plane	The CFD results were verified by experiments. The optimized impeller achieved a 2.7% efficiency improvement while the separation was delayed, which improved the margin by up to 31%.
Cho [159]	Centrifugal compressor impeller	Evolutionary algorithm, Artificial neural networks based on the design of experiment and improved by genetic algorithms	8 control points in the Bezier curve	After 6 generations, the prediction result is close to the numerical simulation. The optimized centrifugal compressor improved the efficiency by 1.4% without pressure loss and obtained the Pareto optimality of the efficiency and pressure ratio after 21 generations.
Ha [160]	Centrifugal compressor system including compressor impeller, vaneless diffuser and volute	Surrogate management framework, Approximation model based on the Kriging method, Pattern search method, Design of Experiments	Impeller Outlet radius, Outlet blade angle, Mass flow coefficient	The difference between the prediction results of Kriging method and numerical simulation is small, which proves the feasibility of this optimization method.
Oka [161]	Centrifugal compressor impeller	A two-dimensional inverse blade design method based on a meridional viscous flow analysis, Non-dominated sorting genetic algorithm (NSGA-II)	Blade loads on a total of 27 control points, including 18 points on main blades and 9 points on separate blades.	The best impeller geometry and blade load distribution were obtained. Flow separation on the suction side of the blade was suppressed in the optimized impeller, and the compressor performance is improved. Numerical simulation and experimental results show that the pressure ratio and adiabatic efficiency under Pareto optimal design are improved.
Tüchler [162]	Centrifugal compressor of a turbocharger	Coupling of Steady-State Reynolds Average Solver and genetic algorithm	Shape of blades, Outline of meridian channel	While the compressor margin is unchanged, the efficiency of the operating point near surge is increased by about 2%. The author also points out that the flow loss at the operating point near surge mainly comes from the volute. The decrease of entropy production in the wake area is probably the reason for the significant improvement in compressor performance.

turbine can work efficiently and reliably [163]. According to the Brayton cycle, high TIT can remarkably enhance the efficiency of the MGT cycle [164]. Such a pattern has been also proved for existing MGTs. Therefore, increasing the turbine temperature tolerance and improving the turbine's aerodynamic efficiency have always been the focus of attention of turbine designers. Until now, some investigations to cover turbine materials, cooling structures and design/optimization methods have been conducted.

### 5.2.1. Turbine materials

At present, the research and development of high-temperature alloy materials for turbines are essentially oriented to the needs of large and heavy gas turbines. For instance, ReneN5, Rene80 and Rene125 are put to use in GE's LM2500 series gas turbines. Rolls-Royce's MT-50 uses the third-generation nickel-based single crystal superalloy CMSX-10 [165]. GE 9H-class heavy gas turbines have recently adopted GTD444 and GTD222 single crystal alloys. With the exploitation of thermal barrier coatings and cooling technology, the TIT could reach 2200 K [166]. In general, the turbine component of MGTs is difficult to be manufactured due to its small size, no matter in the form of radial or axial flow. The previous generation alloy materials, such as GTD111, PWA1483, and IN718/738 are commonly utilized [167].

Compared to superalloys developed for heavy gas turbines, ceramic materials may be a better choice for application in MGTs. Ceramics are considered as an effective medium for enhancing the temperature/performance of turbines with the characteristics of high heat resistance, high strength, small creep, good hardness and good corrosion resistance in the presence of high temperatures [168,169]. Additionally, with low density, a ceramics impeller can help to reduce the shaft load. However, ceramic materials suffer from several shortcomings such as, brittleness, difficulty in machining, and susceptibility to cracks under the action of pressure. Since the thermal expansion coefficient of ceramics is much smaller than that of metals, the connection of ceramic turbines to metal parts is also a challenging issue [170].

**Table 7** provides the currently reported test rigs and prototypes with ceramic-based turbines. As it is seen, the research on ceramic turbines has been continuously intensified since the 1960s. The corresponding allowable TIT is greater than 1150 °C, which is about 200 °C higher than the limit value of the superalloy impeller. With considerable isentropic efficiency, the overall performance of MGTs has been enhanced, reaching a global efficiency of 36.5% [171] or 42.1% [172].

In the connection between ceramics and metals, brazing is a feasible approach. To this end, the ceramic surface should be metal treated and then welded to the shaft through a thermally expanded intermediate layer [173]. The application of non-integrated connections has been also reported in the literature. In 2016, the US. Naval Research Laboratory [170] demonstrated a recuperative MGT with ceramic components, with a novel connection between the ceramic turbine and the metal shaft. The turbine had a tapered stub shaft with a cylindrical portion and a pin joint at the end. An insulating zirconia coupling, which was permanently joined to the shaft, was utilized to connect the rotor to the shaft, as shown in **Figure 17** [170]. This coupling had two specific advantages. Firstly, the thermal conductivity of zirconia is very low, which can be employed to isolate heat. Secondly, it can axially slide to accommodate various thermal expansion rates of steel, zirconia, and silicon nitride ceramics. An included taper angle of

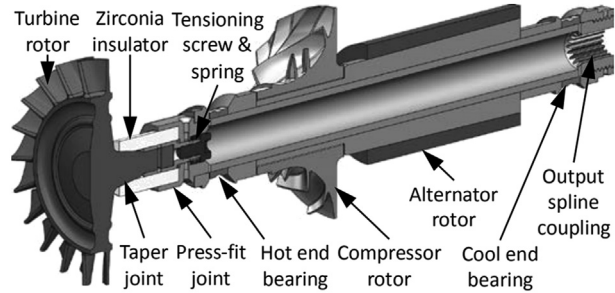


**Figure 17** Diagram of the MGT shaft with zirconia insulator [170].

**Table 7** Test rigs and prototypes using ceramic turbines.

Year/Reference	Model/Project	Materials	Modus	TIT (°C)	Rotating speed (rpm)	Turbine efficiency
1967/[174]	DARPA, Ford	—	—	1370	50,000	—
1970/[175]	AGT-100, Allison	SN22M/SN250 Hexoloy SA	Two stage radial flow	1204	86,500 68,500	80.2%/86.1%
1987/[176]	AGT-5, ATTAP	SiC-Si <sub>3</sub> N <sub>4</sub>	Two stage axial flow	1204	—	—
1999/[173,177]	AGATA	Si <sub>3</sub> N <sub>4</sub> -CSN101	Radial flow	1350	125,000	84%
1997/[171]	ACGTD <sub>P</sub>	C(f)/SiC-Si <sub>3</sub> N <sub>4</sub>	Radial flow	1350	110,000	85%
2002/[172]	CGT302, KHI	SN281/282	Axial flow	1350	64,000/48,000	87%
2005/[178,179]	J-850, AIST	Kyocera SN235	Radial flow	1280	140,000	—
2009/[169]	CF McDonald	—	Radial flow	1170	160,000	83%
2016/[170]	US. Naval Research Laboratory	SN282	Axial flow	1225	135,000	78%

19.46° is also selected, which can enhance the “self-releasing”, maintaining concentricity with the change of temperature.

The manufacturing technology is gradually maturing. Huang et al. [180] developed a technical route for alumina ceramic turbines using a tailored gelcasting process. Wen et al. [181] studied the fabrication processing and mechanical properties of  $\text{Si}_3\text{N}_4$  ceramic turbines. The obtained results revealed that although ceramic materials have excellent temperature tolerance, there are still problems in investment cost and service life span. As brittle products, ceramic turbines are commonly influenced by thermal stress and aerodynamic forces. The ceramic turbines can break if the rim speed exceeds 480 m/s [172], or confront resonance issues [171].

Ceramic-matrix composites (CMCs) have been developed to overcome the brittleness of the monolithic (pure ceramic) [182], which show greater competitiveness, and have been exploited in the latest military/civil aircraft engines. The study or applications of CMCs has been developed from low-stress components (i.e., nozzle, flame tube) to high-stress ones (i.e., turbine guide vanes and turbine rotor blades) [183]. Figure 18 [184] shows the relationship between the specific strength and the temperature of different materials. Carbon fiber reinforced SiC ceramic matrix composites (Cf/SiC) and SiC fiber reinforced SiC ceramic matrix composites (SiCf/SiC) have exhibited excellent high-temperature performance. The latter is more suitable for hot end components with long service life [184], which respond to the needs of MGTs.

For SiC CMCs reinforced by continuous fiber, the micro-hardness could reach as high as 2840–3320 kg/mm<sup>2</sup>. The machinability is extremely poor and the processes of subtractive manufacturing are still under exploration [185]. Conventional crafts like grinding and cutting [186], ultrasonic-assisted machining [187] or laser-assisted machining [188] commonly cause defects and damage, which cannot be compensated by the surface strengthening process. Therefore, for the radial impeller, the processing of complex surfaces will be the main factor restricting the exploitation of CMCs. In recent years, GE (America) and IHI Corporation (Japan) have introduced the

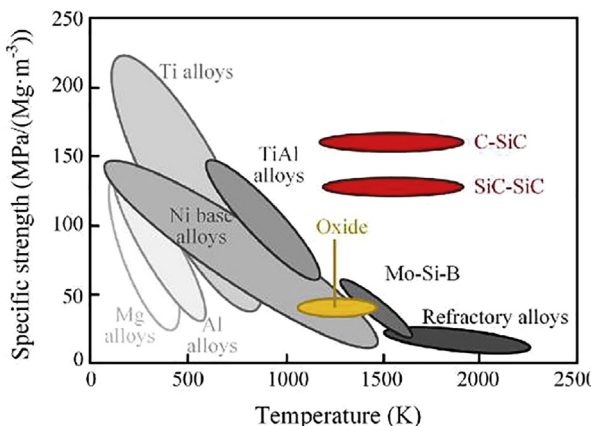


Figure 18 Specific strength as a function of the temperature for different materials [184].

application of CMCs on axial flow turbine rotors. However, for the radial turbine commonly used in MGTs, the relevant research and sample still remain in the early 21st century, and need further research.

### 5.2.2. Thermal protection technology

Thermal protection technology includes passive thermal protection and active cooling technology. Typical cooling methods, such as impingement cooling, convective cooling, rib spoiler cooling and film cooling, have been extensively employed in aero engines and large gas turbines [189–191], however, the application of cooling in MGTs confronts the following challenging issues.

- a. For the axial flow turbine, the size of its blades is limited by the small mass flow powered by MGTs, and this leads to increasing difficulty in processing typical cooling methods.
- b. For the radial flow turbine, it is difficult to arrange cooling channels due to the lack of related designs for the machining method of casting or cutting.
- c. The compact overall structure of the MGT possess challenges to the layout of the cooling air passage.

To enhance the design of axial flow turbines, efficient cooling approaches can be employed to reduce the complexity of the internal flow passage of blades. Zhu et al. [192] stated that pre-rotating cooling can effectively enhance the cooling effect of turbine blades without adopting complex cooling structures and facilitate the machining of small-sized turbine blades.

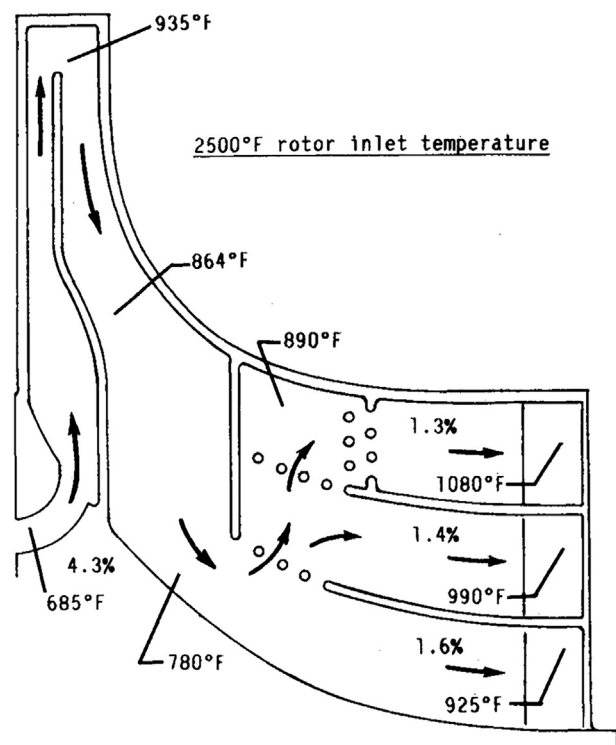
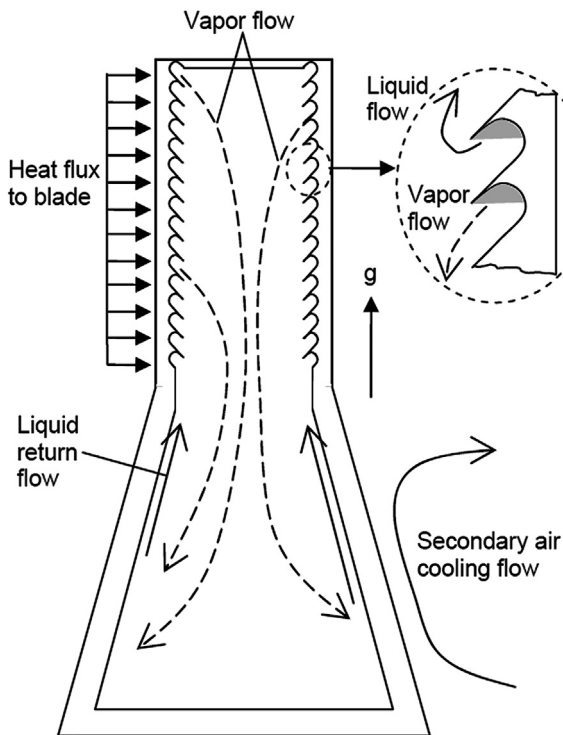


Figure 19 The internal air-cooling scheme for a radial flow turbine [194].

To resolve the problems associated with the radial flow turbine, extensive investigations have been conducted. Buchi et al. [193] proposed a film cooling methodology by spraying gas onto the inlet of the hub through the cavity at the back of the impeller. Snyder et al. [194] designed three air cooling schemes for the radial flow turbine. An optimal scheme was then selected through conducting experiments, as illustrated in Figure 19 [194]. In the design of internal cooling channels for the turbine, spoilers were utilized to provide resistance to overcome the rotating centrifugal force, thus achieving uniform distribution of the cooling flow. The blade and the hub were bonded using HIP technology. Jiang et al. [195] presented a cooling approach based on the research of Buchi and Snyder. The high-temperature region on the blade and hub was cooled by opening holes on the blade, hub and casing surface.

Except for gas cooling, evaporative cooling is exploited in the MGT due to the internal circulation of coolant. Townsend et al. [196] verified the application of potassium evaporative cooling in an axial flow turbine. For this purpose, potassium with a large latent heat of vaporization was utilized as the coolant. The conceptual structure of the blade has been illustrated in Figure 20 [196], applying the technique of return flow cascade. The coolant is retained by the cascade to prevent the coolant from accumulating on the top of the blade due to centrifugation. The experimental results revealed that the evaporative cooling systems could help to maintain a near uniform blade temperature as long as the speed was sufficient for the cascade to take effect. Kerrebrock et al. [197] provided an



**Figure 20** The conceptual structure of evaporative cooling in blades [196].

internal evaporative cooling structure for a radial turbine. The impeller was divided into two parts for an easier fabrication, the blades and hub would be connected by brazing. By punching through the top of the blade, cascades made of inner channels were also exploited in the blades to capture the return flow and overcome the centrifugation. The advantage of evaporative cooling is that it facilitates the arrangement of cooling air, since the condenser is mounted at the back of the turbine, and is separated from the hot gas flow path.

Limited by the complex structure, as mentioned, conventional processing approaches are difficult to achieve the cooling structure. A rare way to do so faces extra performance loss. The rapid development of additive manufacturing (AM) technology provides a new direction for the manufacturing of cold channels in small turbines. The internal cooling axial flow turbines were proposed in Ref. [198]. Although there exist few explorations on the additive manufacturing of inter-cooled centrifugal turbines, it undoubtedly provides potential possibilities.

Zhang et al. [199] developed a radial turbine with internal cooling channels and fabricated the turbine by selective laser melting additive manufacturing. The physical map of the turbine and the schematic diagram of the cooling channel are demonstrated in Figure 21 [199]. The cold air enters the hollow shaft from the inlet of the compressor, passes the cooling channel inside, and exits from the opening presented in Figure 21(b). An appropriate additive manufacturing alloy, namely CM247-LC, was chosen, which could withstand temperatures of about 1050 °C and was believed to work at TIT of 1200 °C with internal cooling. Nevertheless, a three-stage process including a hot isostatic pressing step was stated to be under further investigation. Thus, the tested prototypes were made of Inconel 625.

Although Zhang et al. stated that the technique requires substantial further work accounting for the durability, performance at higher temperatures and the efficiency detriment of cooling air interaction. The aforementioned work demonstrated the potential of AM techniques in radially cooled turbines. The additive manufacturing of superalloy, particularly of forming, curing, and strengthening techniques, deserves more attention.

Compared with active cooling, thermal barrier coating (TBC) as passive thermal protection may be a better choice for microturbines with the maturity of existing technology. A coating consisting of the ceramic topcoat (TC) layer, bond coat (BC) layer, and thermally grown oxide (TGO) layer provides thermal insulation to improve the temperature field and service life of metal impellers [200]. A coating with a thickness of 120–400 µm can reduce the temperature of the alloy by about 300 °C relative to the hot gas [201].

Some coating technologies, such as plasma spraying and physical vapor deposition, have been applied to thermal barrier coating on turbine blades of large gas turbines [202], but are rarely implemented in MGTs, which may be due to

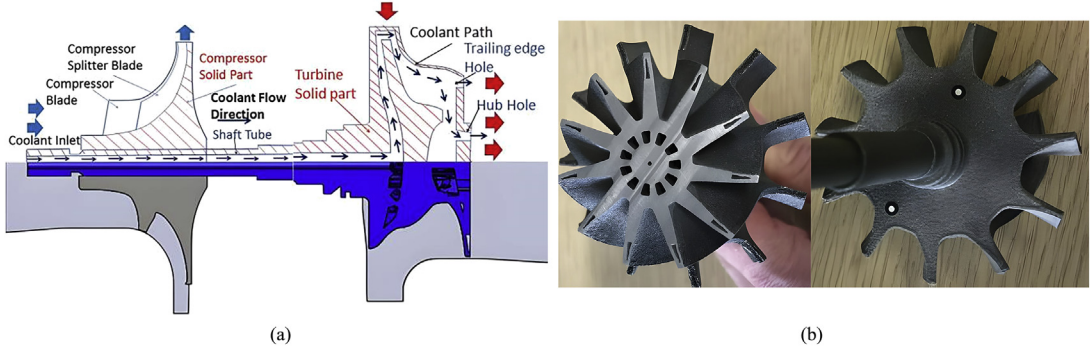


**Figure 21** Schematic representations of: (a) cooling channel and cooling flow strategy (b) as-built cooled turbine wheel [199].

the wide application of radial turbines in MGTs. The complex geometry restricts the application of coating techniques such as atmospheric plasma spraying. New techniques such as plasma spraying physical vapor deposition may improve the situation, but their applications in radial impellers is lacking.

The failure of thermal barrier coatings is a major challenge, particularly for applications in gas turbines, in which the coatings should work in high temperature environments for long durations. As for MGTs use, the flexible and variable working conditions will also bring alternating thermal and stress conditions to the coatings. Thermal fatigue can substantially influence the coating service life [203]. The study on the mechanism of delamination cracks will help to understand and optimize the service life of thermal barrier coatings in gas turbines. Notably, as the rotational speed of gas turbines increases with the decrease of the power level, the application of coatings on small-scale gas turbines can be a challenging issue. It should be noticed that the exerted load on micro-turbines may be comparable to or even greater than that of the larger gas turbine since the centrifugal load is proportional to the square of the rotational speed.



**Figure 22** In-situ deposited white layers on the hot gas components: (a) combustion chamber, (b) nozzles, (c) back side of turbine, (d) front side of turbine [204].

Kim et al. [204] established an in-situ deposition-based silica coating technology for MGTs. Unlike the prefabrication TBC, the in-situ deposition works by adding a precursor to the fuel and depositing it on the surface through which the gas passes after combustion. As illustrated in Figure 22 [204], the deposited layer covers the surface of hot end components well. The silica coating has higher porosity to achieve thermal conductivity as low as yttria stabilized zirconia. Their study revealed that the silica coating could not be deposited on the turbine blades for a long time, but it was possible to replenish the coating by periodically adding precursors under operating conditions.

In summary, the application of cooling technology to MGT-based turbines urgently requires signs of progress in processing technology. Whether the coating technology is suitable for MGTs requires further investigation and experiments before concluding. However, we believe the future is positive as long as the spraying process is developed and the service life problems are resolved.

### 5.2.3. *Turbine design and optimization*

Predecessors have formulated a mature systemic design method of radial turbines. Firstly, the aerodynamic design for the one-dimensional meridian is carried out, and then the three-dimensional modeling of the impeller is performed. Finally, the flow and solid characteristics of the impeller are analyzed and optimized by numerical simulations. A brief literature survey shows that a lot of research works have been conducted in this regard.

Rodgers et al. [205] summarized the existing methods for determining the minimum number of blades, and discussed the influence of parameters such as wheel diameter ratio and degree of reaction on the performance of radial turbines. Noughabi et al. [206] introduced the preliminary design method of radial turbines, including the design of the inlet and outlet speed triangles, the selection of the number of impeller blades and the basic thermal equations. Caldiño-Herrera et al. [207] employed higher-order Bezier curves to model the meridional shape and blade angle. The optimal scheme was chosen based on the numerical simulation and gained improvement in adiabatic efficiency.

In recent years, researchers have paid more attention to design and optimization methods specifically for MGT-

based turbines. Pakle et al. [208] reported a study on the design of double-curvature blades according to the characteristics of low mass flow rate and the high-pressure ratio of a 20 kW MGT. A traditional turbine was designed also based on the idea of Aungier [209] and Rahbar [210], and was optimized by the inverse method based on the meridional viscous flow analysis. Compared to the original design, the optimized turbine could output a maximum of more than 100 kW of mechanical power under low mass flow conditions, and provide an approximately 6% increase in total-to-static efficiency on average and a 6 kW increase in power output at high expansion ratios. Fu et al. [211] has proposed a design method different from the previously nonlinear iteration method [212]. They explained that the optimization process of turbines could be divided into three steps. The shape of the meridian was modified to change the hub diameter, then the main geometric control parameters of the blade were adjusted, and finally, the local optimization along the blade height was carried out. The flow passage capacity and efficiency were evaluated through experiments, and the total-static efficiency of the radial turbine reached up to 84.3% at the design speed. Barsi et al. [213] performed multi-disciplinary optimization on a radial turbine by implementing RANS and FEA to design and perform fluid-structure coupling analysis. To this end, scripts of Python/Fortran were employed to exchange data. The efficiency and aerodynamic performances of the designed turbine were in line with expectations.

#### 5.2.4. Summary

This subsection reviews the research on materials, cooling, and design optimization of turbines. Through the detailed review, it is proved that composite reinforced ceramics may be utilized as materials for turbines in the future. With the development of superalloy manufacturing technology, cooling methods can be considered as an effective means of increasing the TIT. By summarizing the existing methodologies, we believe that internal cooling has certain advantages in MGTs, but needs further investigation. The small mass flow and high-pressure ratio characteristics of turbines in MGTs will be the focus of further design and optimization.

### 5.3. Combustion chamber

Fuel is converted into energy in the combustion chamber. A high-quality burned gas contributes to more efficient work in the turbine, and the quality of combustion directly affects the emission level of MGTs.

Compared with traditional gas turbines, the combustion chamber of MGTs has some unique features given as follows [214].

- Single-stage centrifugal compressors are generally used in MGTs, resulting in a lower pressure in the combustion chamber.

- The air entering the combustion chamber is preheated by the recuperator, resulting in a higher inlet temperature. Since the TIT is limited, the equivalence ratio of air and fuel is relatively low.
- The mass flow of MGTs is low, leading to a lower volume flow despite a low inlet density.
- The combustion chamber should be considered in conjunction with other components for compactness

Current research on MGT combustors aims to lessen emissions, improve efficiency, and adapt to multiple fuels. The research results can be evaluated based on the temperature distribution and the level of emissions of the combustion chamber outlet.

#### 5.3.1. Combustion technology

Annular and cylindrical are two common structures utilized for the combustion chamber in MGTs. The structure of the combustion chamber is commonly determined by combustion technology. Currently, low-emission combustion technologies applied in gas turbines and aero engines essentially include diffusion combustion (DIFF) [215], lean-premix combustion (LP) [216,217], rich-quench-lean combustion (RQL) [218,219], flameless combustion [220], lean direct inject combustion (LDI) [221], and trapped vortex combustion [222]. The LDI and trapped vortex technology are rarely employed in MGTs because of the limitations of the size and sensitivity to losses.

A DIFF combustor has a suitable gas-oil ratio, while an LP combustor with a primary air excess during premix is considered to be advantageous over the DIFF combustor when burning natural gas [223] and hence is broadly utilized in current MGTs [224]. Axial staged combustion represents a kind of combustion organizing technology, which is proven to reduce NO<sub>x</sub> emissions by controlling the residence time of high-temperature gas, including fuel staged and air staged. An RQL combustor is characterized by a rich oil primary mixture, followed by the quenching air supply and the combustion under lean oil conditions [225], which belongs to axial air staged combustion and has been applied to aero-engines. Although the sudden temperature rise produces a surging NO formation when quenching air is supplied, due to the little residence time of the process, the RQL combustor still has advantages over the LP combustor in terms of overall NO emissions. Therefore, the RQL combustor is considered as a viable alternative to the LP combustor [214].

Laranci [226,227] designed a new RQL annular combustor based on the Elliott TA80R MGT. To this end, mixing holes instead of the original mixing tubes were used, and the original geometry with fairly low manufacturing cost is maintained. The CFD based simulations were also performed to verify the adaptability of various kinds of fuel.

The jet stabilization approach in combustion chamber has the features of the RQL combustion, as demonstrated in the streamlines of Figure 23(b) [228]. Oxidant rushes in at a

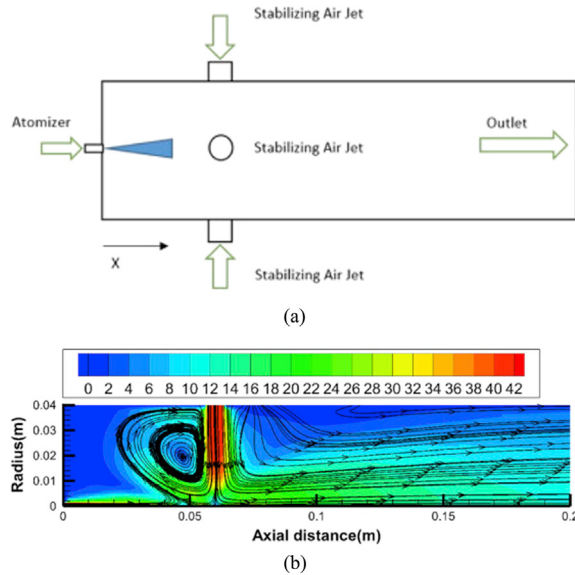


**Figure 23** (a) Schematic view of a jet-stabilized combustor, (b) velocity contours along with streamlines on the centerline plane [228].

certain axial position, forming vortex structures for stable combustion. Alemi et al. [228] examined the effect of jet characteristics on the combustion and NO emissions in a jet-stabilized combustor. Three-dimensional simulations were performed for various jet angles and Reynolds numbers, and the NO production was predicted by the thermal Zeldovich mechanism. The obtained results indicated that the lowest NO emissions can be obtained by spraying downstream at high jet Reynolds numbers. Yang et al. [229] developed a novel elliptical jet-stabilized combustor. Numerical investigations were conducted also on the combustion and emission characteristics by changing the ellipse's major/minor axis ratio. The gained results revealed that the elliptical combustor achieved a stronger mixing performance than the circular combustor, leading to a 50% reduction of NO under an appropriate major/minor axis ratio. Hasemann et al. [230] conducted an experimental study of a single-stage jet-stabilized combustor with various numbers of nozzles, diameters, and mixing zone lengths for MGTs. The investigators pointed out that the number of nozzles influences the length of the reaction area, and the change of nozzle diameter can affect the jet speed. The results also indicated that an increase in nozzles can lead to a decrease in emissions and the diameter of the nozzles impacts the pressure loss and emission of the combustor.

Flameless combustions, also known as flameless oxidation (FLOX), were firstly utilized in boilers [230]. There exists a recirculation region where fresh air is diluted to be thoroughly mixed with gas and heated above the flash point in the FLOX combustor. In contrast to the combustion within stabilized flames, temperature peaks can be avoided at flameless oxidation. Actually, the uniform temperature distribution leads to an ultra-low NO emission. Zanger et al. designed a two-stage combustion system based on the

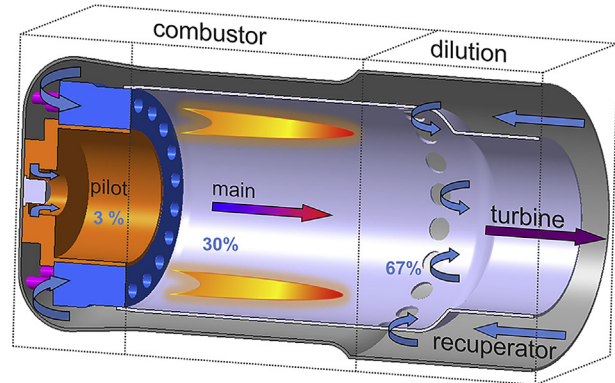


**Figure 24** Schematic view of a double stage FLOX combustor using jet-stabilized method [231].

FLOX concept, as presented in Figure 24 [231]. The combustion chamber had a vortex-stabilized pilot stage and the main combustion section was designed based on the principle of jet stabilization, which generated a large amount of flue gas backflow, thereby causing flameless oxidation. The designed system was then successfully tested on the Turbec T100 test rig. Schwärzle et al. [232] explored the above-mentioned two-stage combustion chamber. The scholars employed an ICCD camera to capture the OH signal and investigated the shape, length, and lift-off height of the flame. NO<sub>x</sub>, CO, and UHC emissions were also detected, while the pressure loss and gas residence time of the combustor still should be improved. Figure 25 illustrates the dependence of NO<sub>x</sub> and CO emissions on the equivalence ratio in a FLOX combustor (also known as the MILD concept) [233]. Low emissions were found at equivalence ratios between 0.35 and 0.5, which proved the outstanding performance of the FLOX combustor. However, Perpignan

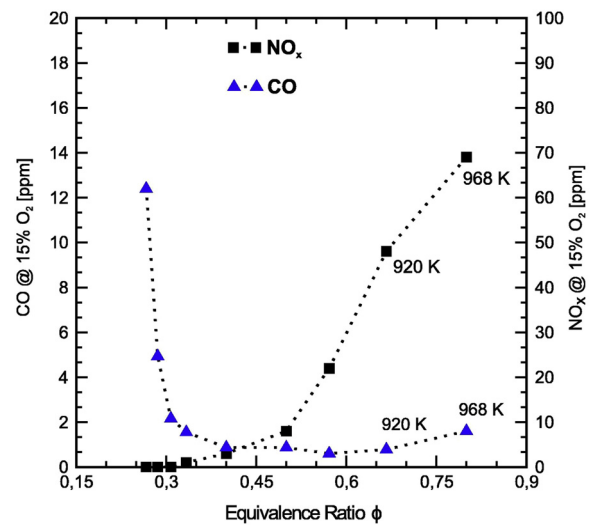


**Figure 25** NO<sub>x</sub> and CO emissions in terms of the equivalence ratio in a FLOX combustor [233].

et al. [234] displayed that the FLOX combustor requires a large volume, presenting challenges for integration into space-sensitive engines such as the MGTs. As jet entrainment and large recirculation zone are commonly implemented to strengthen the performance of the FLOX combustor, the problems of pressure loss, gas residence time, and working range should be rationally resolved. This fact requires earlier consideration of the integration design between the combustor and the whole engine.

The pressure gained combustion (i.e., constant volume combustion) that changes the cycle mode to obtain higher mean-effect heat addition temperature has high cycle theoretical efficiency. Nevertheless, the combination of pressure gained combustion with continuous fluid in gas turbines is a cumbersome task, and detonation can be a possible solution. Compared with pulse detonation, rotating detonation has more potential applications in gas turbine combustors due to its self-sustaining characteristics. The rotating detonation has strong adaptability to the mass rate of working fluid [235] and products fairly low emissions [236]. Sousa et al. [237] established a gas turbine model with a rotating detonation combustor. Compared with the deflagration combustor, the obtained results showed that the overall efficiency rises by about 5% under low-pressure ratio circumstances. A supersonic turbine fitting to the detonation combust was also declared to be redesigned. Apparently, the detonation combustors need further improvements to be applied in MGT systems where emissions and fuel adaptability are of great concern.

### 5.3.2. Fuel type

In recent years, in view of the requirements for the wide applicability of fuels, various types of fuels with various characteristics have been extensively exploited by MGTs. Commonly, these fuels and combustion techniques are first tested on existing MGT platforms before applying them to large gas turbines. The introduction of gaseous and liquid fuels will be separately organized.

The representative of gaseous fuels is natural gas, having been broadly used MGTs. The emission data of commercial MGTs is generally based on the burning natural gas conditions. Natural gas has the advantages of low ignition temperature, high calorific value, and appropriate combustion speed. The liquefied natural gas is also conducive to transport and storage. Sufficient research has been conducted on stable combustion based on natural gas. The current study research mainly focuses on its injection

methods. The influences of swirler or injector geometric on combustion and emission were also reported and discussed [238].

A series of low calorific fuels, mixed with hydrogen, carbon monoxide and methane or extracted from bio-processing, has attracted attention from researchers and engineers. Commercially available MGTs can only handle low calorific fuels in limited operating ranges [239], which means further explorations should be carried out to adapt these low calorific fuels. Swirl stabilization and jet stabilization are two common methods for low calorific fuels. Swirler could stabilize the flame, but leads to bad combustion in the later stage. Jet stabilization confronts flame stability issues [240]. Bower et al. [239] have constructed a combustor with the stabilized main stage and swirl stabilized pilot stage, which is similar to the FLOX combustor described previously [231]. The combustor was then tested on an atmospheric test rig and showed good NO<sub>x</sub> emissions in the fuel calorific value range of 7–49 MJ/kg. Khalil et al. [241] reported a colorless distributed combustion (similar to FLOX/MILD) combustor with vortex stabilization induced by a tangential jet. Methane diluted with nitrogen was set to simulate landfill gas with different compositions or low heating value fuels. This issue reveals the good adaptability of FLOX/CDC technology in low calorific value fuels.

On facing application in waste gas treatment, Cameretti et al. [242] examined the performance of gas fuels from biomass treatment, solid waste pyrolysis and anaerobic digestion processes in MGTs. The results revealed that the given low heat value fuel can alter the geometric properties of the combustion temperature zone, leaving the traditional LP combustor in atypical operating conditions. Schwärzle [243] sent the waste gas containing volatile organic compounds (VOC) into the combustor and co-fired with natural gas via chemiluminescence images and exhaust gas monitor to analyze the flames and combustion. The addition of VOC helped to reduce the emissions of CO and NO<sub>x</sub> in the presence of high combustion temperatures. At low temperatures, the air content in VOC had a positive correlation with CO and a negative correlation with NO<sub>x</sub>.

Hydrogen is recognized as a pure clean fuel that is without carbon emissions. There exist great differences in physical and chemical properties between hydrogen and hydrocarbon fuels. As illustrated in Table 8 [244,245], the volume energy density of hydrogen is only about 1/3 of that of methane, resulting in a three-times higher volume flow/velocity (in the case of using the same pipes) during

**Table 8** Physical and combustion characteristics of typical gaseous fuels [244,245].

Fuel	Density (kg/m <sup>3</sup> )	Volume calorific value (MJ/m <sup>3</sup> )	Ignition temperature (°C)	Laminar flame velocity (cm/s)
Methane	0.717	35.6	540	38
Hydrogen	0.089	12.6	571	351
Ammonia	0.771	14.4	651	7

Note: under standard state conditions (101.325 kPa, 15 °C).

providing the same amount of heat. This fact yields barriers to the flexible adaptation of combustion systems between hydrogen and hydrocarbon fuels [246]. The study of mixing hydrogen into natural gas has proved that the addition of hydrogen will weaken the swirl stability effect [247]. Therefore, new technology was developed to burn hydrogen-rich fuel or pure hydrogen in an MGT combustor. Beita et al. [248] reviewed the thermo-acoustic instability of hydrogen-rich fuel combustion and pointed out that the combustion of 100% hydrogen fuel faces great challenges. Hydrogen enrichment makes combustion in low equivalent ratio regions unstable, and flame morphology variations are often detectable. Karyeyen et al. [249] developed a distributed combustion combustor for hydrogen-rich gas, and simulated the fuel with a hydrogen volume fraction higher than 44% to predict the thermal field. The CO emission results were claimed to be nearly equal to zero, while the NO<sub>x</sub> emission was lower than 20 ppm under specific conditions. Reale et al. [250] simulated the combustion of diluted hydrogen under a maximum 30% volume fraction. For this purpose, wet cycle technology was utilized to realize the combustion of hydrogen-rich fuel in the none-modify combustor of T100. Hydrogen embrittlement and water corrosion failure caused by hydrogen were also reported. The coating and low hydrogen permeability materials are anticipated to resolve the raised issues.

Ammonia as another common gaseous fuel is considered as a potential hydrogen carrier that can achieve carbon-free power generation. Similar to hydrogen, ammonia combusts at different rates and mechanisms than conventional fuels. New combustion technology for ammonia application in MGTs has been established. The AIST first achieved successful NH<sub>3</sub>-kerosene-air gas turbine power generation in 2014, and then in 2017 extended the system to NH<sub>3</sub>-air combustion without the need for any additives or pre-cracking devices. Kurata et al. [215] released the research report on the NH<sub>3</sub>-air power generation system, which was modified from a 50 kW class MGT, TRC50 from Tokyo turbine INC., and had a wider operating range. Their obtained results showed that by using NH<sub>3</sub> fuel, combustion efficiency of 86%–96% is achievable. The experimentally obtained results also indicated that NO and NH<sub>3</sub> emissions are affected by the inlet temperature of the combustion chamber. The mechanism explorations revealed that the unburnt NH<sub>3</sub> was expected to react with NO generated in the lean fuel zone through selective non-catalytic reduction (SNCR). Therefore, bringing in excess NH<sub>3</sub> fuel to produce both rich and lean fuel mixtures in the primary zone was recommended to reduce emissions. The recent study by Okafor [251] demonstrated an ammonia combustion chamber technology with high efficiency. Swirler and nozzle structures were modified to improve the premixing effect and gas residence time to reduce NO<sub>x</sub> emission and achieve higher combustion efficiency. According to the obtained experimental results, NO<sub>x</sub> emission of 42 ppmv and ammonia combustion efficiency of 99.5% was achieved at 0.3 MPa

for fuel input power of 31.44 kW. The spray combustion of liquefied ammonia was expected to lessen the cost and size of MGTs. The flame control of spray combustion of liquefied ammonia was firstly explored by Ayaz et al. [252]. The performed research suggested that ammonia would not be suitable for premixed combustion because of high ignition energy, and co-combustion with methane exhibited better emission performance. A lifecycle-based scrutiny further revealed the operating cost and emission level of ammonia fuel. Ammonia, as an additive gas, could decrease carbon oxide emissions by nearly 50% [123].

Liquid fuels such as gasoline, kerosene and biomass oil have the advantages of good stability and easy storage, which makes them have extensive applications. Before entering the combustor, liquid fuels should be atomized for stabilizing combustion [253]. Therefore, research on spray and atomization is a crucial branch in the realm of research on liquid fuel.

Biomass fuels (i.e., vegetable oil, diesel oil, and bio-ethanol) are typical alternative fuels. Renewability and low emission potential have attracted attention for their application in MGTs. Specifically, straight vegetable oil (SVO) for MGT use has been encouraged in recent years since the SVO is not suitable for large-scale exploitation due to limitations in the cultivation of raw materials. Bio-oil can be pyrolyzed from an unlimited number of organic fuels and is also considered as a potential fuel for distributed MGT systems [254]. Figure 26 demonstrates the physical and chemical properties of several common biomass fuels currently used in gas turbines, as summarized by Chiong [255]. The viscosity values of SVO and bio-oil are times higher than that of diesel, which leads to negative effects and makes it difficult to atomize. Air-assisted pressure-swirl atomizers are believed to help atomize and burn high-viscosity fuels while preheating can reduce the viscosity to enhance the atomization performance with a marked increase in emission [256,257]. Additionally, the problem of coking and clogging caused by doping components in bio-fuels still should be methodically examined since durability is of the major concern.

Through investigation, some bio-fuels applied to MGTs have been also reported. Buffi et al. [258] scrutinized the application of fast pyrolysis bio-oil (FPBO) in MGTs. The gained results revealed that the viscosity of FPBO affects the volume of atomized droplets, leading to an increase in CO emission, and the water vapor produced by combustion positively incorporates into the overall efficiency of MGTs. Broumand et al. [259] discovered that the addition of ethanol can improve the volatility of FPBO to inhibit coking, and the new two-fluid nozzle is designed for atomization since 100% FPBO is hard to combust alone [260]. Another fuel that exploits ethanol to help combust is liquefied wood (LW) [261]. The LW-ethanol-based fuel can combust stably in MGTs, but exhibits a substantial gap in emissions compared to traditional fuel. The investigators pointed out that emissions can be reduced by increasing the proportion of the LW and the primary flame temperature,

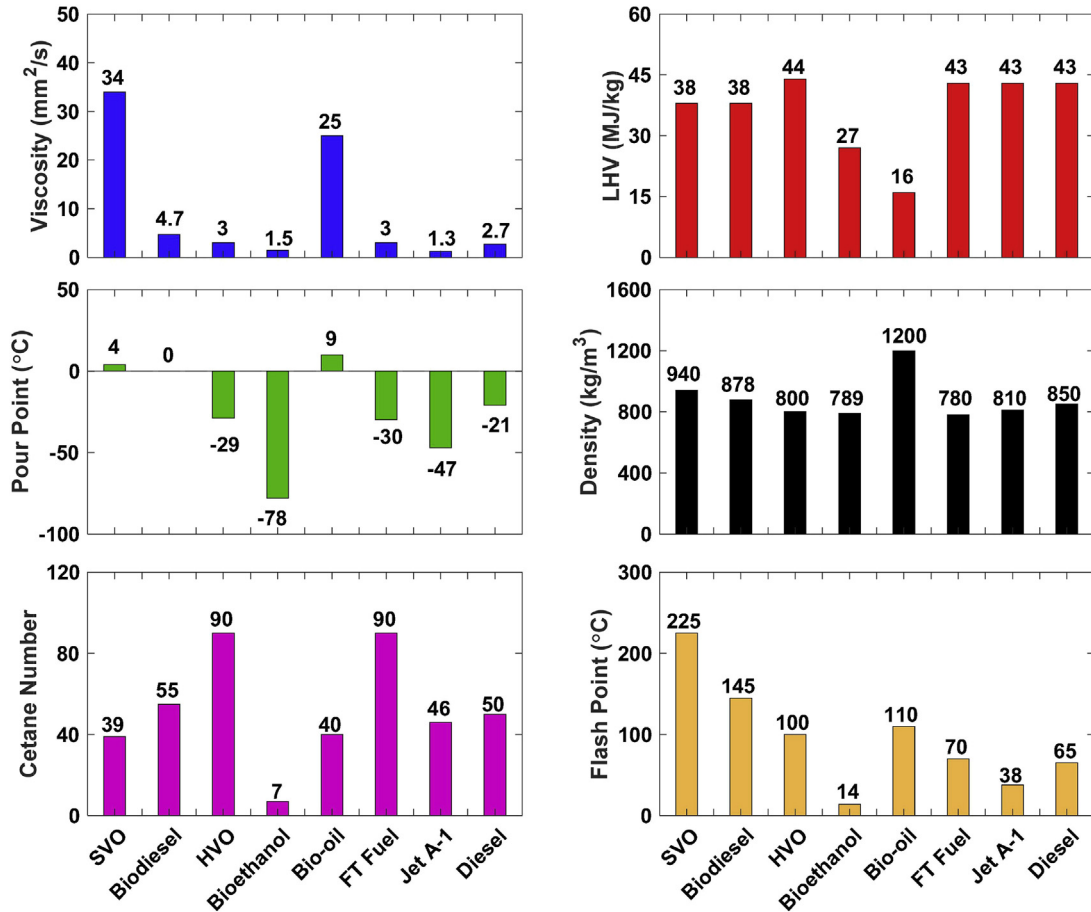


**Figure 26** The physical and chemical properties of biomass fuels and typical fossil fuels [255].

leading to enhance heat transfer and accelerate evaporation. Further, microalgae biofuel extracted by a chemical approach was compared with Jet-A fuel on a small turbojet engine. The addition of biofuel noticeably lessened CO, CO<sub>2</sub> and NO<sub>x</sub> emissions, but the proportion of biofuel should not be too high [262].

Hoxie et al. [263] investigated the feasibility of exploiting ultra-low-sulfur diesel (ULSD) combined with vegetable oil in MGTs and conducted that vegetable oil can replace ULSD to some extent. To this end, an optimal mixing ratio of vegetable oil at 75% was proposed. Furthermore, the specific gravity, viscosity, higher heating value, flash point, and other properties of this mixed fuel were measured, providing a basis for the improvement of atomization.

Figure 27 summarizes the combustion emissions of the fuels utilized in MGTs. It should be noticed that the most balanced or the lowest emission data under rated conditions of MGTs are selected and various emission control measures can be applied to these fuels. Natural gas still has absolute advantages in emissions, biofuels can be employed as a supplement to natural gas, and some blended fuels have exhibited excellent emissions performance.

The impact of fuel on the service life of MGTs is clearly a matter of concern. Alternative fuels, particularly biofuels, can affect the service life of MGTs due to the inadequate

content of cetane and other elements contained. Coking or corrosion would be the subject matter, however, there are few quantitative results due to rare studies on the effects of service life, which may be attributed to the immaturity of alternative fuels employed in MGTs.

### 5.3.3. Impacts of manufacture technology on combustion chamber

Due to the limitations of low power levels and small mass flow, the small-size MGTs combustors confront serious challenges in their design and manufacturing. The parasitic energy losses relative to net power output sharply increase as size decreases. Actually, the geometry and boundary conditions of the combustor also have a great impact on the performance and service life span of MGTs [264].

In a single-cylinder, cannular or annular combustion chamber, traditional manufacturing techniques are exploited more often. Fuel nozzle, swirler, and flame tube are manufactured by a machine tool or casting and then appropriately assembled. The conventional manufacturing methods undoubtedly limit the original design of the components, potentially resulting in greater losses or worse emission levels, compared with the ideal design without specific

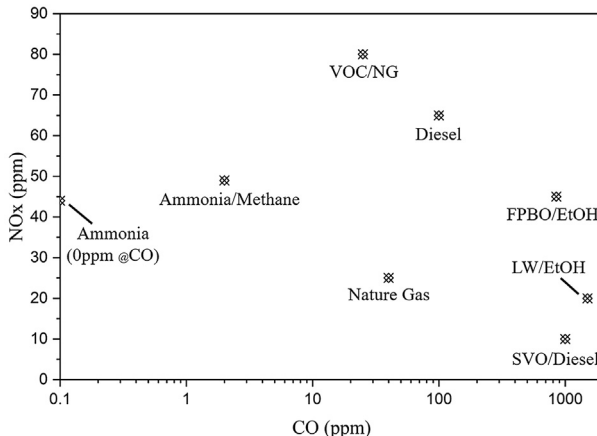


**Figure 27** The CO and NO<sub>x</sub> emissions from several fuels.

limitations. To achieve this goal, additive manufacturing may be a suitable solution since it can reduce the number of assembly processes, and realize the production of complex structures, providing higher accuracy in smaller dimensions.

Although there exists a certain discrepancy between the components produced by metal additive manufacturing and those of the traditional method in terms of surface roughness, it is sufficient for the exploitation of the combustion chamber [265]. In particular, additive manufacturing significantly increases the design freedom of the combustor. It overcomes the drawbacks of traditional manufacturing methods in small-size complex structural machining, and increases the variability of geometric shapes [266]. Additive manufacturing has shown great potential in a variety of combustion components, such as the LEAP fuel injector conducted by GE [267]. The additive technology is also adopted by Siemens to repair the combustion chamber tip of the SGT gas turbine to prolong its service life [268]. The five-axis directed energy deposition (DED) system produced by TWI Corporation has been employed to produce superalloy annular combustors for helicopter engines [269]. Although these applications or explorations have been carried out in large-scale combustion chambers, additive manufacture is undoubtedly suitable for MGTs since the combustion chambers do not have to withstand high-intensity creep at the pressure or temperature level of MGTs.

Adamou et al. [270] have proposed a concept for designing of MGTs based on additive manufacturing, which is unlike the idea of traditional manufacturing. The conical swirler, lattice structure mixer, upstream augmented cooling backside mixer, and flat swirler designed were all appropriately designed based on the concept of additive manufacturing. Through CFD simulations, the designed combustor demonstrated excellent temperature control and fuel-air mixing capability, with a 75% and 40% reduction in nitric oxide and carbon monoxide, respectively. The later experimental tests also revealed that the additively manufactured features improved the distribution and quality of

the air-fuel mixture and performed well in the whole airflow range, which was considered not possible with the baseline designs [271].

Additive manufacturing also has certain limitations. In order to avoid the additional support frame which is essential to beam structures, the design of components should be intentionally chosen to achieve self-supporting features. Another consideration is the size of the hole, the aperture should not be too small to avoid the blocking during printing, or the inaccuracy affected by the surface roughness. The limitation on the minimum aperture can be different for various additive manufacturing technologies. For instance, for metal additive manufacturing, selective laser melting (SLM) has the highest resolution accuracy. The minimum aperture allowed by the SLM depends on the size of the source beam, which may be around 0.27–0.35 mm for conventional devices [272], corresponding to a minimum aperture of about 0.8 mm. In the research work by Adamou [270], the minimum aperture of parts made by Inconel 625 was limited to 0.75 mm.

The additive manufacturing not only revolutionizes the way small components are processed, but also has a noticeable impact on the overall design concept of combustion chambers. Currently, studies on combustion chambers have been mostly conducted in traditional frameworks, and only a few investigations have been devoted to MGTs combustion chambers in the context of additive manufacturing. However, it is anticipated that such research works will rapidly grow. Additionally, the structure of multistage cyclones and oil-gas mixed cavities can be further examined.

### 5.3.4. Summary

This subsection is aimed to review the research on combustion technology and fuel adaptability of combustors in MGTs. Among several high-efficiency combustion technologies, the RQL combustion has certain advantages, which can limit NO<sub>x</sub> emissions to a fairly low level. Flameless oxidation with the characteristic of ideal emissions and wide calorific value adaptability has attracted the attention of many scholars and technology developers. In addition to traditional fuels, emerging bio-fuel, ammonia, exhaust gas, and various mixed fuels have been confirmed to be effective for MGTs. In order to achieve enhanced performance, specific designs or optimizations should be accomplished due to the various properties of the fuels used. Additive manufacturing has opened up possibility of beneficial changes on combustion chamber, deserving further researches and attempts.

### 5.4. Recuperator

The recuperator ensures the efficient operation of MGTs, but the extra cost and weight cannot be ignored. For use in MGTs, some small-sized, low-cost and high-effectiveness recuperators have been designed.

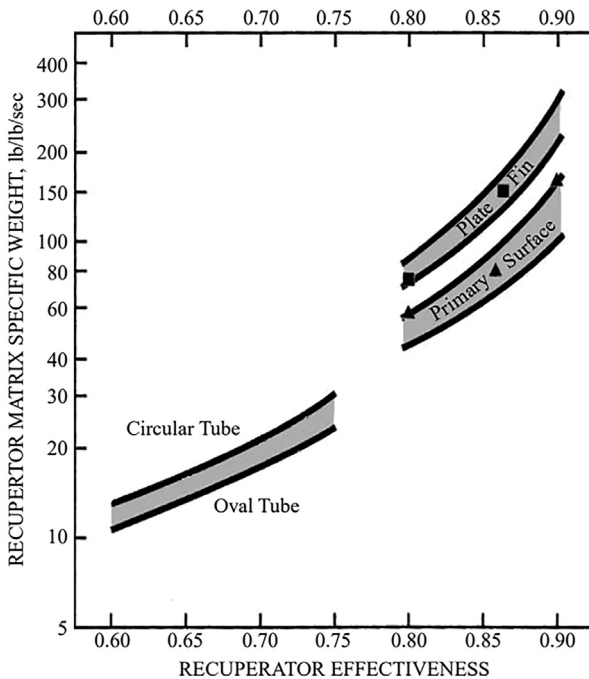


**Figure 28** The specific weight trends of the gas turbine recuperator matrix for various surface geometries [274].

#### 5.4.1. Structure and materials

The recuperator employed for MGTs has been reviewed in detail in Ref. [5]. According to the heat exchange surface

geometry, the recuperator is essentially divided into three types: plate-fin, primary surface and tube. Zhang et al. [273] compared the performances and costs of three types of recuperators. The authors believed that the plate-fin recuperator had favorable geometry and performance, but was bulky and not suitable for mobile devices. In contrast, the tube recuperator was more suitable for helicopters or other mobile vehicles equipped with recuperative gas turbines. The primary surface recuperators might be the development trend in the future, which was also approved by McDonald [274]. According to the accumulated performance demonstrated in Figure 28 [274], the tube recuperator was less efficient, but gained low overall weight. Both plate-fin and primary surface recuperators present suitable effectiveness regimes for power generations, while primary surface recuperators have the advantage of heat transfer density.

Figure 29 [275–278] illustrates some existing recuperators. Ingersoll-Rand developed a plate-fin recuperator with an operating temperature of 600–700 °C in 1994 [275]. RSAB developed a primary surface counter-current recuperator with a cross-corrugated (CC) structure [276]. The substrates stamped with corrugated surfaces were stacked together by laser welding to form the core while the intake and exhaust manifolds were welded at the opening aside. This specific recuperator was cost-effective and convenient for production. Solar Turbines designed an annular primary surface recuperator with a cross-wavy (CW) structure, which was later licensed for Capstone C30 [277]. The

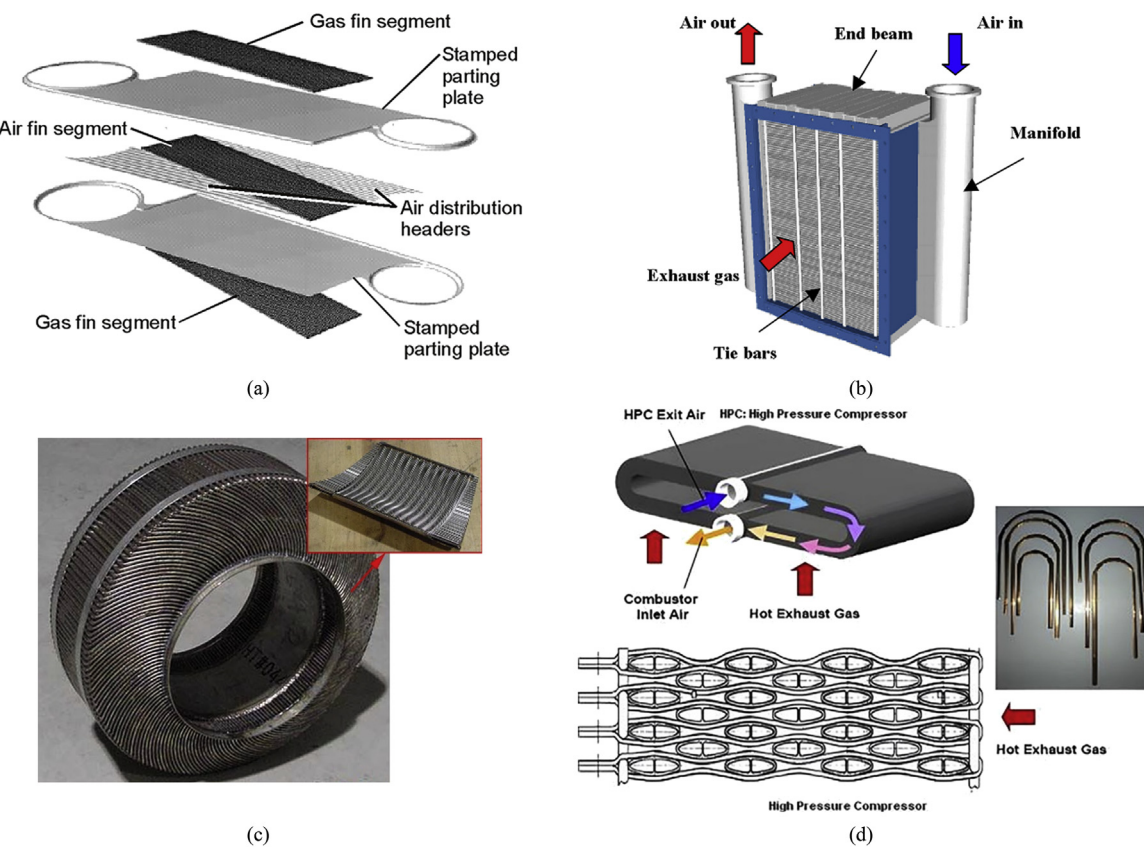


**Figure 29** Different recuperators: (a) Ingersoll-Rand [275], (b) RASB [276], (c) Solar Turbines [277], (d) MTU [278].

recuperator was made of stainless steel, the heat exchange substrate welded by laser had an involute design, and multiple substrates were rolled up to form the complete recuperator. MTU [278] developed an elliptical tubular recuperator consisting of two manifolds brazed with shaped tubes. The cold air flew in and out of the tube bundle through manifolds while heat exchange occurred as the gas flew through the space between the tubes. This tubular recuperator has been reported to be applied in aero engines [279].

In recent years, some new structures have been designed. Counterflow recuperators with larger heat transfer surfaces are favored because of higher average temperature differences and larger specific surface areas. A counterflow recuperator with wavy fins for submicron gas turbines was designed by Kim et al. [280]. Experimental research on pressure drop and heat transfer indicated that an increase in the inlet temperature of hot gas would result in an increase in the average specific volume and then led to a higher pressure drop in the presence of high temperatures. Do et al. [281] designed and manufactured a single-pass counterflow recuperator with offset strip fins. The recuperator consists of six units, which were annularly mounted outside of the combustor at equal intervals, as demonstrated in Figure 30(b). Each unit was stacked by substrates with offset strip fins, and vacuum furnace brazing was exploited to connect the substrates and the fins. The characteristics of pressure drop and effectiveness, which were similar to those of Kim et al. [280], were obtained through experimentation.

Micro power units developed at the US Naval Research Laboratory [170] had a ceramic-made plate-fin recuperator that could withstand an inlet temperature of 1040 °C. The recuperator units in a small volume had axial and radial stacking designs. A total of 1200 ceramic pieces formed a complete recuperator. The bumps on the substrate surfaces shown in Figure 30(c) were designed to resist gas pressure and thus reduce stresses, while on the other hand, the bumps could serve a crucial purpose during sintering.

At present, most of the preferred recuperators are heat exchangers whose integration with rotor systems is concerned since the MGTs are commonly designed as a

complete system. This results in a challenge for recuperators' design and processing. However, for some distinct applications such as CSP and FC, the MGT can be split and reintegrated into a complete system. In this case, the recuperators can be designed and manufactured based on the ordinary counter-flow/cross-flow gas-to-gas heat exchanger, reducing a certain cost.

As mentioned above, superalloys have already been exploited in additive manufacturing, and have shown good sealing performance and strength. Therefore, additive manufacturing can offer more efficient and economical solutions for the production of MGT recuperators.

Figure 31 shows the recuperator manufactured by HiETA [282] for the MGT-RE of Delta motorsport. The additively manufactured recuperator unit is 33% smaller in volume and 9.4% more effective against the conventional competition for the same specification. Zhang et al. [283] have designed an additively manufactured manifold-microchannel gas-gas heat exchanger using Inconel 718 superalloy. Compared with the conventional plate fin heat exchanger, the heat transfer density increased by 25% for the same heat transfer ratio to pressure drop. Since the material takes up a large proportion of the cost of recuperators, additive manufacturing can minimize the material waste and thus lessen the overall cost. AM technology has also shown advantages in the production cycle.

Similar to the design of combustor components, additive manufacturing also liberates some design ideas for heat transfer microstructures, which are commonly subjected to conventional processing techniques. For instance, the classical enhanced heat transfer approach, fins or ribs, can be vary in shape, including triangle, star-shape, and dimpled-sphere [284]. An additively manufactured vortex generator in the microchannel can be exploited to strengthen the laminar heat transfer [285]. These structures can make the recuperators manufactured by additive technology exhibit smaller volumes or higher effectiveness than recuperators produced by traditional manufacturing methodologies.

However, in terms of the overall performance of micro gas turbines, the enhancement of heat transfer needs to be viewed dialectically. Considering that the MGT system is sensitive to pressure loss between the compressor and

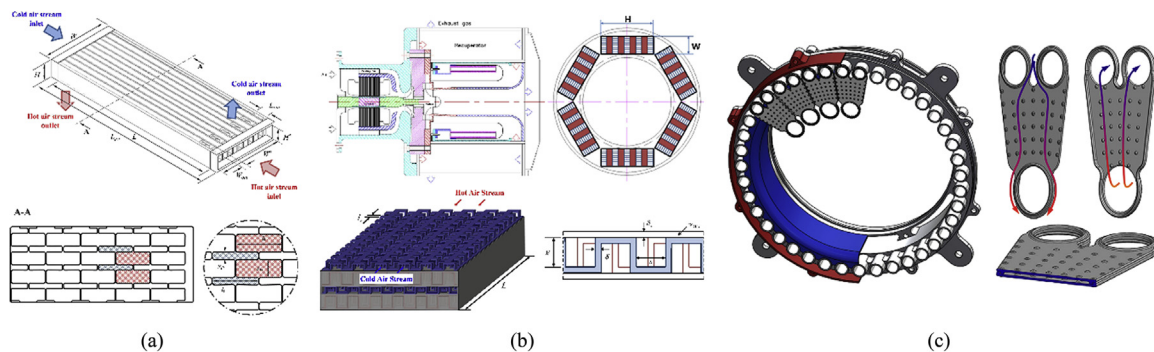


**Figure 30** Recuperators designed by (a) Kim [280], (b) Do [281] and (c) Michael Vick [170].



**Figure 31** Additively manufactured recuperator made by HiETA equipped in an MGT-RE [282].

turbine [286], the recuperator with balancing heat transfer efficiency and pressure loss is more recommended. The enhanced heat transfer structure may reduce the total area and thus reduce the friction loss, but the flow loss introduced by the structure alone may be larger. The roughness of the heat transfer surface should be taken into concern since it will increase the heat transfer but bring more pressure loss [287]. However, for additively manufactured heat exchangers, the control of surface roughness is one of the difficulties, but it is easy to solve by machining or other manufacturing approaches.

In addition, the heat exchangers processed by diffusion weldings such as PCHE and PFHE are recommended, because they have no solder residue and small deformation, and are suitable for both steel and non-metallic materials. Nevertheless, a current processing cost perspective reveals that brazing is less expensive and suitable for the temperature and pressure levels of MGTs.

It is foreseeable that material cost will still be the main component of recuperator processing. For the case where the inlet temperature of the recuperator is less than 675 °C, 347 stainless steel can meet the requirements. Inconel 625, costs five times of 347 steel, leading to an increase in the allowable inlet temperature of the recuperator by 800 °C based on McDonald [169]. The corresponding TIT is up to 1150 °C, which is hard to maintain under the state of art on turbines. In fact, based on the turbine material and their allowable TIT discussed above, the commonly used superalloy can meet the needs of the recuperator and maintain low cost. Additionally, facing the development of ceramic/CMCs turbines or centripetal turbines with cooling, the study of ceramic recuperators as technical reserves is highly necessary. The binder jetting method (additive manufacturing) [288] and diffusion welding have been employed in the processing of SiC ceramics, furthermore, some other ceramic plate-fin recuperators have been reported [289]. Xiao [5] believed that the development of reliable and low-cost recuperators of ceramic materials is still in progress. However, considering the influence of the inlet temperature of the

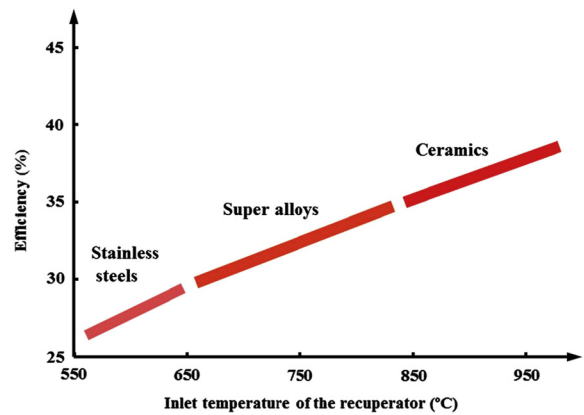


**Figure 32** Effect of recuperator-inlet temperatures [5].

recuperators on the overall efficiency of the MGT shown in Figure 32 [5], the deployment of superalloys and ceramics is still the first choice for more development of recuperators.

#### 5.4.2. Recuperator optimization

Stevens et al. [290] examined the optimization of MGT recuperators and pursued higher heat exchange effectiveness and low-pressure drop to achieve higher overall-cycle efficiency. The authors remarked that there was a correlation between the pressure drop of the cold side and that of the hot side of the recuperator, which depends on the pressure ratio of the compressor. A simplified procedure was the proposed and its good consistency with other multi-objective optimization results was presented.

Cai et al. [291] optimized a cross-wavy primary surface with the design of a circular involute. A calculation model of related heat transfer and pressure drop was then established, and the genetic algorithm was employed for multiple optimizations. The developed optimization was based on the recuperator of C30/C65, aiming to reduce the total pressure loss. The obtained results were successfully verified with the experimentally observed data, and a noticeable reduction in the pressure loss was achieved.

Zhang et al. [292] proposed an optimization approach for the primary surface recuperator on a turbo-shaft engine for helicopters. The interdependence between the recuperator weight and effectiveness was appropriately quantified under specific constraints relative to the selected heat transfer surface geometry. By employing multi-objective genetic algorithm optimization, the best balance point between the performance and the recuperator weight was obtained and discussed.

Giugno et al. [293] scrutinized the influence of design parameters on the cost and volume of recuperators by implementing the Monte Carlo method and response sensitivity analysis. The minimum volume, minimum cost, and compromise schemes were proposed with a minimum average volume of 2.52 dm<sup>3</sup> and a minimum average cost of 1652.6 euros.

Maghsoudi et al. [294] performed a thermal-economic analysis of plate-fin recuperators with different fins and flow forms. The performed study was mainly based on a 200 kW MGT recuperator model. Cross and counter-flow plate-fin recuperators employing rectangular, triangular, offset strip, and louver fins were then optimized for effectiveness and cost via NSGA-II. The data envelopment analysis (DEA) model was then utilized to evaluate the total cost, pressure drop, volume, and weight. The authors carried out a similar study in another work [295], which first optimized various forms of recuperators, and sorted the optimal solutions by using the normalization method and the concept of non-dominated sorting. The results obtained showed that offset strips and louvered fins provide high-pressure drop and the best heat transfer performance. Economic analysis and multi-objective optimization of offset fin heat exchangers were further examined [296]. The undertaken study took the geometry of the heat exchange fins as optimization variables, and cycle efficiency and discounted payback period as the main considerations. For a 200 kW MGT, the optimization results were reported to be 29.5% overall efficiency and a discounted payback period of about 1.4 years.

#### 5.4.3. Summary

In this subsection, recuperators of MGTs were briefly sorted out by introducing a few structures and optimization methodologies. An ideal recuperator for MGTs requires high recuperation, high effectiveness, and low pressure drop. In this regard, the primary surface recuperators have attracted special attention due to their outstanding compactness and low losses. The recuperator also should have good performances in anti-oxidation and creep resistance at high temperatures. In general, ceramics or superalloys perform better than stainless steel. Superalloys can meet the needs of current TIT conditions, and thereby, ceramics will be the future direction. The application of additive technologies can bring considerable benefits to the recuperators in terms of density and cost. However, some enhanced approaches unlocked by AM need to be estimated under the framework of overall performance of MGTs

before being employed. Similar to the impellers, the exploitation of optimization algorithms in the design of recuperators has recently attracted the attention of investigators.

### 5.5. Rotor and bearing

Rotor and bearing have a direct impact on the working state of MGTs. Therefore, the rotor systems and support schemes of MGTs should be methodically designed and verified. This subsection is aimed to analyze the relationship between the rotor systems and the support schemes based on the existing prototypes, and then introduces some mainstream bearing technologies.

#### 5.5.1. Rotor system and support

As a high-speed machine, the design of the rotor system of MGTs is of great importance. Generally, the connection between the turbine shaft and the generator shaft can affect the support scheme. Some models employ the gearbox transmission [27,32], and only the gas turbine part's support requires consideration. Some models have independent support for both shafts [31] and the shafts are connected by a coupling. The shafts can be considered as a single equivalent shaft, whose stiffness equals the superposition of the stiffness of the turbine shaft and generator shaft. The concept of the integrated shaft is mostly employed in existing MGTs, designed with the impeller arranged back-to-back [18,19,23,26,30]. The support is usually placed in front of the compressor and separated on both sides of the motor.

Since the compressor and turbine have divided the shaft into three parts, the supporting scheme can be expressed as x-x-x according to the number of bearings in each part. For example, the supporting scheme with two bearings in front of the compressor is stated by 2-0-0. Table 9 presents the shaft connection, support schemes and bearing types of current commercial MGTs.

Some experimental works on MGTs exhibited unique support schemes, as shown in Table 10. The 100 kW-MGT developed by KIMM [297] was supported by air bearings.

**Table 9** Support and rotor characteristics of commercial MGTs.

Model/Reference	Shaft	Connection	Support scheme	Bearing	Rotating speed (rpm)
Capstone/[18]	1	Integrated	2-0-0	Air bearing	96,000
AlliedSignal/[19]	1	Integrated	2-0-0	Air bearing	72,000
Elliott/[23]	1	Integrated	2-0-0	Liquid(oil) bearing	116,000
Turbec/[26]	1	Integrated	2-0-0	Liquid(oil) bearing	70,000
ET Group/[30]	1	Integrated	2-0-0	—	60,000
ENN/[31]	1	Coupling	(2+2)-0-0	Liquid(oil) bearing	51,000
Flex/[27]	2	Gearbox & Coupling	2-0-0	Liquid(oil) bearing	—
PowerWorks/[4]	2	Gearbox & Coupling	—	Liquid(oil) bearing	60,000
Wisdom/[32]	2	Gearbox & Coupling	Gas: 1-0-1 Power: 0-3-1	—	54,000/44,000

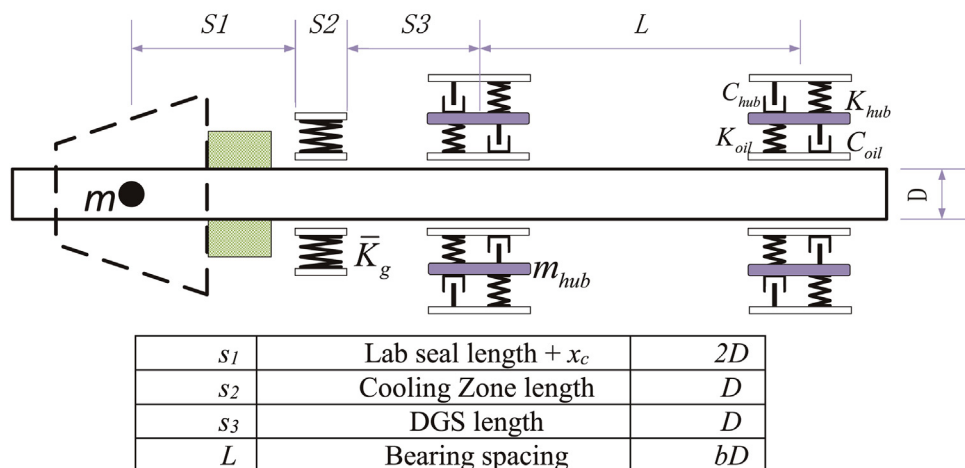
**Table 10** The characteristics of the support and rotor of tested MGTs.

Work/Reference	Shaft	Connection	Support scheme	Bearing	Rotating speed (rpm)
Maia/[298]	1	Integrated	0-2-0	Float ring	70,000
Ji/[57]	1	Coupling	0-3-0	Float ring	100,000
Arroyo/[299]	1	Integrated	2-0-0	Ceramic ball bearing	100,000
Lim/[297]	1	Coupling	2-1-0	Air bearing	47,500
Vick/[170]	1	Coupling	1-1-0	Liquid(oil) bearing	135,000
Sim/[71]	2	Gearbox & Coupling	Gas: 0-2-0 Power: 0-0-2	Ceramic ball bearing	170,000

The radial bearings and thrust bearings in order were arranged at both sides of the generator rotor and the back of the compressor, forming a 2-1-0 support scheme. The motor shaft and the gas turbine shaft were connected by an elastic coupling. Micro power units developed by the US Naval Research Laboratory [170] utilized liquid-lubricated bearings and couplings. The compressor arranged in reverse was capable of the reduction of the axial force, and the two radial bearings were organized in a 1-1-0 form. The dual-shaft MGT designed by Sim et al. [71] had four supports. The gas shaft was supported by two ceramic ball bearings set between the compressor and the turbine, and the power shaft was supported at the back of the turbine. The obtained results revealed that the ceramic ball bearings could reach a speed of up to 170,000 rpm. Maia et al. [298] designed the rotor system of the turbocharger. The topology of an integral shaft with compressor, generator, and turbine arranged was selected after the experiment, indicating that the application of 0-2-0 support leads to the best vibration scenario.

For the rotor systems and supports, rotor dynamics analysis should be also performed, from which the modality can be obtained to evaluate the critical speed. The aggressive control methods on rotated speed are utilized to cross the critical speed as soon as possible during verifying the working conditions since the deformation at the transcritical speed may lead to the impeller collision. The 2-0-0 support

mainly possesses the characteristic of a cantilever. It is easily understood that the cantilever length and shaft end load have substantial influences on the deformation of the cantilever shaft. Therefore, for the 2-0-0 support scheme, the second bearing is placed closer to the compressor and even integrated into the compressor hub. The support scheme with bearing all between compressor and turbine is similar to that of a common turbocharger and has better modal characteristics in theory [300,301]. But in this way, the support and lubrication of the generator shaft require additional consideration. The method of establishing parametric models and optimizing objective functions by algorithms has been adopted in the optimization of the rotor system. Figure 33 illustrates the topology of the rotor system in Ref. [302], and the parameters shown in the figure were regarded as input objects. The bearing spacing was stated as the product of the axle diameter and the objective optimization coefficient. By considering the optimization effect, a model was established to evaluate the maximum peak of the unbalance response, the absolute value of the difference between the operating speed and the nearest critical speed and the derivative of the amplitude of the unbalance response at the working speed point to the frequency. Further, the structural parameters were obtained by particle swarm optimization, and hence the unbalanced response was lessened. A similar method can also be implemented for the shafting setting of MGTs.

**Figure 33** Topology of the rotor system in an ORC system [302].

### 5.5.2. Bearings

A brief literature survey based on the above statistics reveals that liquid-lubricated bearings with oil as the lubricant are mostly employed. Oil-lubricated bearings can withstand large loads and possess a specific damping effect, but may suffer from frictional losses at a high speed [303,304]. A relevant oil supply system is also required. Floating ring and semi-floating ring bearings, as special oil-lubricated bearings, have good rotational and damping characteristics and thereby are commonly adopted in turbochargers. The relevant technologies have been also implemented in MGT presently [305,306]. The air bearings have a relatively higher speed and a smaller loss, but with poor rotational stability [307]. Thus, the air bearings for MGTs do not yet exhibit a substantial difference in rotating speed with respect to the case of using the oil-lubricated bearing. In addition, water-lubricated bearings have been reported used in MGTs under humidified circulation to reduce the type of working medium [308]. For lubricated bearings, the influence of frictional heat cannot be ignored [300]. The thermal expansion and the distribution of temperature and viscosity inside the oil film can affect the support effect. Furthermore, the heat transfer between the hot-end components and the bearings cannot be overlooked. In this view, placing bearings before the compressor has particular advantages.

As a third type of bearings, magnetic bearings possess the characteristics of non-contact, non-lubrication, long life, and controllability [309], which have attracted the interest of researchers [310–312]. NREC developed ORC energy recovery machinery using active magnetic bearings, emphasizing that the exploitation of active magnetic bearings results in significant cost reductions in weight, space, and system complexity [313]. The active magnetic bearings can also serve as displacement sensors. The magnetic bearings are rarely utilized in MGTs since the coupling effect with the magnetic field of the generator is the essential obstacle. Shenyang Liming of AECC reported their developed WD095 MGT on the basis of magnetic bearings, which are now available for commercial purchases.

### 5.5.3. Summary

Influenced by the back-to-back layout of the impeller, the support scheme of 2-0-0 is widely used in MGTs presently. Concentrated mass distribution at the cantilever's end has brought special challenges to the design of the shaft. The liquid lubricated bearing is widely used because of its high maturity. The air bearing has the advantage of lower loss under high rotating speed conditions, but the speed limit is not much different from that of the oil bearing in MGTs. The magnetic bearings have performance advantages, but their application in MGTs still needs further research and development.

## 6. Conclusions and prospective

In the present paper, we have made a comprehensive review of MGTs, covering the developments of commercial

MGTs, applications, performances and the latest attractive research on MGT components. According to the performed investigations, the MGT itself has become a relatively mature industrial product, and commercial products have also been applied in a certain field. Generally, the configuration of MGTs tends to be similar. Technologies such as full radial flow structure, lubricated bearings, and high-efficiency heat exchangers have been broadly employed in commercial MGTs and have brought considerable benefits to the system.

MGTs have exhibited excellent performance and have broad application prospects. The low power generation costs and good comprehensive energy utilization are well demonstrated in the field of distributed energy systems. The potential of low-vibration and low-emission has made MGTs particularly competitive in the market of ranger extenders, as high investment costs and insufficient response speed make them drag the leg. The combination of MGTs with concentrated solar power or fuel cell systems greatly expands the flexibility and stability of the original systems. This co-generation also enables the MGT cycle to break through to higher thermal efficiency, which offers an appropriate replacement for distributed energy and mobile power generation. The influence of component parameters on the performance of MGTs is briefly introduced in Section 4. The hot-end components have a considerable impact on the performance of the steady-state, transient, and thermal economy, which means that research on turbines or recuperators should have a higher priority.

In order to further enhance the performance of MGTs and expand their applications in the energy industry, MGTs still confront serious challenges in subsequent development. The future development of MGTs will mainly depend on the research progress in the following aspects.

### 1. Prototyping technology of hot end components and auxiliary thermal protection technology

The ultimate goal is to increase TIT, which is critical to overall efficiency. The conceivable technical routes include advances in material technology and applications of thermal protection technologies. For the development of materials, given that superalloys have been exploited in combustion chambers, guide vanes, and turbine impellers, ceramics or ceramic matrix composites with high thermal resistance manufactured for the hot-end components will be of decisive value progress. Achieving higher TITs and then reducing maintenance costs result in prolonging the service life of components. Similar to the early use of superalloys, the processing quality restricts the application of ceramic matrix composites or other advanced high temperature materials. New processes to reduce the surface damage and residual stress caused by machining should be concerned. Additive manufacturing is a potential digital forming technology, but the mechanical and geometric accuracy of CMCs components produced by the AM is poor. A variety of AM technologies (including direct ink writing, binder

jetting, selective laser sintering, laminated object manufacturing and stereolithography) have not yet demonstrated the characteristics applicable to turbines with requirements of high precision and high bearing capacity. The AM technology that is suitable for manufacturing continuous fiber toughened ceramic composites with better mechanical properties will be an important direction.

Meanwhile, with AM technology, the digital manufacturing of nickel-based superalloys provides the possibility of active thermal protection in MGTs, as the processing of complex geometries, including cooling channels or room for heat pipes is implemented. By allowing the single-phase or two-phase cooling technologies to be applied to the centrifugal impeller, the flow temperature increases on the basis of the existing material performance. The coating technology will also be a pivotal part of MGT thermal protection. Although the present literature suffers from the lack of application of centrifugal impellers, the attempts in MGT turbines based on existing coating technologies should be highly encouraged.

The next-generation MGT turbine form is expected to be a ceramic impeller equipped with anti-corrosion coating and internal cooling channels, which is a combination of passive protection and active cooling technology.

## 2. Adaptive combustion technology

Adaptive combustion technology should be examined to reduce emissions and further expand the application of eco-friendly and sustainable fuels. New layouts or designs based on advanced manufacturing technology is to be expected. Among the existing technologies, the flameless combustion has better emission performance and is suitable for a wide range of fuel calorific. The further research and applications in MGTs are of high interest. A generic combustion structure/technology to lessen the hardware cost of MGT switching between various fuels will be another intriguing direction. In the future, the decentralization of constant volume combustion/detonation technology will be a revolutionary development in MGTs.

## 3. High-precision simulation and intelligent optimization

CFD methods have already been employed for the geometric design and verification of MGT components, which greatly reduces the experimental cost and shortens the design cycle. With great progress in computational ability, the use of high-precision numerical simulation to capture aerodynamic and heat transfer phenomena will be more accurate. Thereby, the caused mechanism can be rationally explained and interpreted, and a suitable basis for the design of components can be given. Artificial intelligence methodologies such as genetic algorithms and artificial neural networks are vitally beneficial in design and optimization.

Given that most of the current research works are focused on independent components, the interactions between different components are rarely involved. Digital twin

technology is the development process of future simulation technology. MGT-based digital modeling can provide online information exchange, which greatly contributes to the study of dynamic work and coupled effects between components. Data collection and mining based on the digital twin model are means to achieve health monitoring and service life prediction, which is important for commercial MGTs, and will be a focused process.

## 4. High-efficiency and low-cost heat exchange technology

Heat exchangers play important roles in MGTs as well as in their corresponding coupling systems. In the case that material costs exist objectively, efficient heat exchange technology significantly lessens investment costs and flow losses. The primary surface heat exchangers and microchannel heat exchangers have specific potentials. The additive approaches are believed to reduce costs, and the bionic technologies are also expected to lessen the additional losses during growing the heat transfer capacity. The materials with high-temperature resistance, high thermal conductivity, and low heat capacity will help to increase the working range and reduce the thermal inertia of the heat exchanger.

## 5. Efficient waste heat recovery cycles

The current co-production technology mainly realizes waste heat recovery by direct heating or absorption cooling. The waste heat is individually utilized, and thereby the efficiency is low. Among various approaches, the Stirling engine and ORC cycle are more efficient ways of heat utilization, which are expected to be applied to the waste heat recovery of MGTs. The cooperative performance of MGTs and heat recovery cycle should be further scrutinized to attain high overall thermal efficiency.

## 6. Intelligent control technology

The regulation of complex cycles, including MGTs, is undoubtedly complicated, and this necessitates establishing a global regulation model as well as a control method for each specific system. However, for applications such as range extenders, MGTs are only implemented as highly integrated power generation devices, and such applications have raised higher responsiveness requirements for MGTs. It is noteworthy to develop intelligent control systems to reduce the response delay and overshoot in dynamical conditions. Some advanced PID-based control schemes have been proposed, and the regulations with intelligent prediction through artificial neural networks, genetic algorithms, and machine learning are now under further exploration. Furthermore, given that the existing control system in MGTs is usually with a single object strategy on the fuel valve, the development of active control on high-speed generators is a good complement. This issue becomes more highlighted for commercial MGTs with features of the integrated shaft and the capability to start up and generate electricity with the same alternator.

## Acknowledgments

The authors appreciate the financial support provided by the National Science and Technology Major Project (Grant No. 2017-III-0003-0027).

## References

- [1] T. Ackermann, G. Andersson, L. Söder, Distributed generation: a definition, *Elec. Power Syst. Res.* 57 (3) (2001) 195–204.
- [2] J.L.D. Monaco, The Role of Distributed Generation in the Critical Electric Power Infrastructure, 2001 IEEE Power Engineering Society Winter Meeting, Conference Proceedings (Cat. No. 01CH37194), IEEE, Columbus, USA, 2001, pp. 144–145.
- [3] I.A. Waitz, G. Gauba, Y.S. Tzeng, Combustors for micro-gas turbine engines, *J. Fluid Eng.* 120 (1) (1998) 109–117.
- [4] M. Nascimento, L. Rodrigues, E. Santos, E. Gomes, F. Dias, E. Velásques, R. Carrillo, Micro Gas Turbine Engine: a Review, *Progress in Gas Turbine Performance*, InTech, 2013, pp. 107–141.
- [5] G. Xiao, T.F. Yang, H.L. Liu, D. Ni, M.L. Ferrari, M.C. Li, Z.Y. Luo, K. Cen, M.J. Ni, Recuperators for micro gas turbines: a review, *Appl. Energy* 197 (2017) 83–99.
- [6] M. Mehlkopf, Capstone Microturbine, Berlin, September, 2009. URL: [https://asue.de/sites/default/files/asue/termine\\_veranstaltungen/2009/fachveranstaltung2009/vortraege/capstone-microturbine.pdf](https://asue.de/sites/default/files/asue/termine_veranstaltungen/2009/fachveranstaltung2009/vortraege/capstone-microturbine.pdf).
- [7] C. Soares, Microturbines: Applications for Distributed Energy Systems, Elsevier, 2011.
- [8] F. Reale, R. Sannino, Numerical modeling of energy systems based on micro gas turbine: a review, *Energies* 15 (3) (2022) 900.
- [9] K.A. Al-attab, Z.A. Zainal, Externally fired gas turbine technology: a review, *Appl. Energy* 138 (2015) 474–487.
- [10] D.P. Ward, M.M. Carrero, S. Bram, A. Parente, F. Contino, Towards higher micro gas turbine efficiency and flexibility: humidified mGTs — a review, turbo expo: power for land, sea, and air, Charlotte, USA, 2017, V003T06A030.
- [11] M.A. Hashim, A. Khalid, H. Salleh, N.M. Sunar, Effects of fuel and nozzle characteristics on micro gas turbine system: a review, *IOP Conf. Ser.: Mater. Sci. Eng.* 226 (2017) 012006.
- [12] R.M. Lin, G.H. Jin, Gas Turbine Power Generation Device and its Application, China Electric Power Press, 2004.
- [13] H.J. Braun, The Chrysler automotive gas turbine engine, 1950–80, *Soc. Stud. Sci.* 22 (2) (1992) 339–351.
- [14] V.D. Biasi, Low Cost and High Efficiency Make 30 to 80 kW Microturbines Attractive, *Gas Turbine World*, 1998.
- [15] W.G. Scott, Micro-turbine generators for distribution systems, *IEEE Ind. Appl. Mag.* 4 (3) (1998) 57–62.
- [16] W.E. Liss, Natural gas power systems for the distributed generation market, *Proc. Power-Gen Int. Conf. GRI-99/0198* (1999).
- [17] S.H. Zhao, The development of new concepts of micro gas turbines, *Gas Turbine Technol.* 14 (2) (2001) 8–13, <https://doi.org/10.3969/j.issn.1009-2889.2001.02.003>.
- [18] Capstone Turbine Corporation, URL: <https://www.capstoneturbine.com> [cited 22 November 2020].
- [19] R.J. Yinger, Behavior of Capstone and Honeywell Microturbine Generators during Load Changes, Lawrence Berkeley National Laboratory, 2001.
- [20] Y.M. Zhang, W.J. Zhang, D.Y. Liu, L.G. Sun, X.H. Liu, J. Wang, Solar thermal power Series 17 Research and development of 70 kW tower solar thermal power generation system, *Sol. Energy* 11 (2007) 43–46, <https://doi.org/10.3969/j.issn.1003-0417.2007.11.008>.
- [21] J.B. Campbell, T.J. King, B. Ozpineci, D.T. Rizy, L.M. Tolbert, Y. Xu, X. Yu, Ancillary Services provided from DER, Oak Ridge National Lab (ORNL), Oak Ridge, USA, 2005.
- [22] I. Zamora, J.I.S. Martin, A.J. Mazón, J.J.S. Martín, V. Aperribay, Emergent technologies in electrical microgeneration, *Int. J. Emerg. Elec. Power Syst.* 3 (2) (2005).
- [23] R. Capata, E. Sciubba, The concept of the gas turbine-based hybrid vehicle: system, design and configuration issues, *Int. J. Energy Res.* 30 (9) (2006) 671–684.
- [24] Ansaldo, AE-T100, URL: <https://www.ansaldoenergia.com> [cited 22 November 2020].
- [25] European Turbine Network (ETN), Micro Gas Turbine Technology Summary: Research and Development for European Collaboration, 2017. URL: <https://etn.global/wp-content/uploads/2018/02/MGT-Technology-Summary-final-for-the-website.pdf>.
- [26] P.A. Pilavachi, Mini- and micro-gas turbines for combined heat and power, *Appl. Therm. Eng.* 22 (18) (2002) 2003–2014.
- [27] Flexturbine, URL: <https://www.flexenergy.com/turbine-innovations> [cited 22 November 2020].
- [28] Dresser-Rand KG2-3E, URL: [https://dalkos.ru/upload/documents/Dresser-Rand\\_KG2-3E.pdf](https://dalkos.ru/upload/documents/Dresser-Rand_KG2-3E.pdf) [cited 22 November 2020].
- [29] Bladon, URL: <https://www.bladonmt.com> [cited 22 November 2020].
- [30] ETGROUP, Micro-Gas Turbine, URL: <https://www.etgroup.nl/en/micro-gas-turbine> [cited 22 November 2020].
- [31] ENN, URL: <http://www.ennturbine.cn/productIntro.html> [cited 01 November 2020].
- [32] Wisdomturbine, URL: <http://www.wisdomturbine.com> [cited 01 November 2020].
- [33] Product introduction of AVIC Dong'an micro gas turbine, URL: <https://max.book118.com/html/2019/1023/5101343221002142.shtml> [cited 22 November 2020].
- [34] L. Goldstein, B. Hedman, D. Knowles, S.I. Freedman, T. Schweizer, Gas-Fired Distributed Energy Resource Technology Characterizations, 2003. NREL/TP-620-34783.
- [35] A. Datta, R. Ganguly, L. Sarkar, Energy and exergy analyses of an externally fired gas turbine (EFGT) cycle integrated with biomass gasifier for distributed power generation, *Energy* 35 (1) (2010) 341–350.
- [36] G. Pepermans, J. Driesen, D. Haeseldonckx, R. Belmans, W. D'Haeseleer, Distributed generation: definition, benefits and issues, *Energy Pol.* 33 (6) (2005) 787–798.
- [37] S. Jain, S. Roy, A. Aggarwal, D. Gupta, N. Kumar, Study on the parameters influencing efficiency of micro-gas turbines: a review, in: *Proceedings of the ASME 2015 Power Conference*, San Diego, USA, 2015. Paper No. V001T09A006.
- [38] E.S. Barbieri, P.R. Spina, M. Venturini, Analysis of innovative micro-CHP systems to meet household energy demands, *Appl. Energy* 97 (2012) 723–733.
- [39] P.A. Pilavachi, Power generation with gas turbine systems and combined heat and power, *Appl. Therm. Eng.* 20 (15–16) (2000) 1421–1429.
- [40] S. Murugan, B. Horák, A review of micro combined heat and power systems for residential applications, *Renew. Sustain. Energy Rev.* 64 (2016) 144–162.
- [41] F. Caresana, L. Pelagalli, G. Comodi, M. Renzi, Microturbogas cogeneration systems for distributed generation: effects of ambient temperature on global performance and components' behavior, *Appl. Energy* 124 (2014) 17–27.
- [42] A. Gimelli, M. Muccillo, Optimization criteria for cogeneration systems: multi-objective approach and application in an hospital facility, *Appl. Energy* 104 (2013) 910–923.
- [43] H.W. Zhang, Y. Long, S.Y. Huang, Scheme selection and performance analysis of distributed energy systems, *Heat. Vent. Air Cond.* 34 (5) (2004) 47–51, <https://doi.org/10.3969/j.issn.1002-8501.2004.05.010>.
- [44] I.G. Rice, Thermodynamic evaluation of gas turbine cogeneration cycles: Part I – heat balance method analysis, *J. Eng. Gas Turbines Power* 109 (1) (1987) 1–7.
- [45] K. Thu, B.B. Saha, K.J. Chua, T.D. Bui, Thermodynamic analysis on the part-load performance of a microturbine system for micro/minichp applications, *Appl. Energy* 178 (2016) 600–608.
- [46] F.F. Huang, Performance evaluation of selected combustion gas turbine cogeneration systems based on first and second-law analysis, *J. Eng. Gas Turbines Power* 112 (1) (1990) 117–121.

- [47] O. Balli, H. Aras, Energetic and exergetic performance evaluation of a combined heat and power system with the micro gas turbine (MGTCHP), *Int. J. Energy Res.* 31 (14) (2010) 1425–1440.
- [48] Z.B. Feng, H.G. Jin, Part-load performance of CCHP with gas turbine and storage system, *Proc. CSEE* 26 (4) (2006) 25–30, <https://doi.org/10.3321/j.issn:0258-8013.2006.04.006>.
- [49] P. Stathopoulos, C.O. Paschereit, Retrofitting micro gas turbines for wet operation. A way to increase operational flexibility in distributed CHP plants, *Appl. Energy* 154 (2015) 438–446.
- [50] J.J. Lee, R.S. Jeon, R.S. Kim, The influence of water and steam injection on the performance of a recuperated cycle microturbine for combined heat and power application, *Appl. Energy* 87 (4) (2010) 1307–1316.
- [51] E. Tate, M.O. Harpster, P.J. Savagian, The electrification of the automobile: from conventional hybrid, to plug-in hybrids, to extended-range electric vehicles, *SAE Int. J. Passenger Cars Electron. Electr. Syst.* 1 (1) (2008) 156–166.
- [52] A.M. Andwari, A. Pesyridis, S. Rajoo, R. Martinez-Botas, V. Esfahanian, A review of battery electric vehicle technology and readiness levels, *Renew. Sustain. Energy Rev.* 78 (2017) 414–430.
- [53] F.R. Kalhammer, B.M. Kopf, D.H. Swan, V.P. Roan, M.P. Walsh, Status and prospects for zero emissions vehicle technology, *Rep. ARB Independ. Expert Panel* 1 (1) (2007) 12–36.
- [54] R. Virsik, A. Heron, Free piston linear generator in comparison to other range-extender technologies, *World Electr. Vehicle J.* 6 (2) (2013) 426–432.
- [55] A. Heron, F. Rinderknecht, Comparison of range extender technologies for battery electric vehicles, in: 2013 Eighth International Conference and Exhibition on Ecological Vehicles and Renewable Energies (EVER), IEEE, Monte Carlo, Monaco, 2013, pp. 1–6.
- [56] B.L. Arav, R. Shulman, V.A. Kozminykh, Refinement of hybrid motor-transmission set using micro turbine generator, *Procedia Eng.* 129 (2015) 166–170.
- [57] F.Z. Ji, X.B. Zhang, F.R. Du, S.T. Ding, Y.H. Zhao, Z. Xu, Y. Wang, Y. Zhou, Experimental and numerical investigation on micro gas turbine as a range extender for electric vehicle, *Appl. Therm. Eng.* 173 (2020) 115236.
- [58] A. Olsson, B. Jönsson, L. Sundin, The Volvo Heavy Truck Gas Turbine VT300, 2005. *SAE Technical Paper* 2005-01-3504.
- [59] Jeff Salton, Capstone CMT-380 electric hybrid supercar with microturbines, URL: <https://newatlas.com/capstone-cmt-380-an-electric-hybrid-featuring-wind-turbines/13517> [cited 22 November 2020].
- [60] Bladon Jets, Jaguar cx75 concept case study, URL: <http://www.bladonjets.com/applications/automotive/jaguar-c-x75-concept-case-study> [cited 22 November 2020].
- [61] K. Sangani, A jet for every home, *Eng. Technol.* 6 (2) (2011) 42–45.
- [62] TXR-S, URL: <http://www.txr-s.com/?technology/id/7.html> [cited 22 November 2020].
- [63] Techrules, URL: <http://www.techrules.cn> [cited 22 November 2020].
- [64] R. Golan, The turbine-electric Mitsubishi Mi-Tech reminds us what's great about concepts, URL: <https://www.digitrends.com/cars/2019-mitsubishi-mi-tech-turbine-electric-convertible-suv-concept-unveiled> [cited 22 November 2020].
- [65] Hybrid Kinetic, URL: <http://www.hkmotors.com/Industrial/car.aspx> [cited 22 November 2020].
- [66] Delta Motorsport, URL: <https://www.delta-motorsport.com> [cited 22 November 2020].
- [67] I. Wright, Wrightspeed Powertrains, ACT Expo 2015, Dallas, USA, May 4-7, 2015. URL: <https://cdn.actexpo.com/pdfs/ACTE2015-presentations/5-1EDTA2/1MediumHeavyEVTech/1Wrightspeed.pdf>.
- [68] A. Karvountzis-Kontakiotis, A.M. Andwari, A. Pesyridis, S. Russo, R. Tuccillo, V. Esfahanian, Application of micro gas turbine in range-extended electric vehicles, *Energy* 147 (2018) 351–361.
- [69] F.X. Tan, M.S. Chiong, S. Rajoo, A. Romagnoli, T. Palenschat, R.F. Martinez-Botas, Analytical and experimental study of micro gas turbine as range extender for electric vehicles in asian cities, *Energy Proc.* 143 (2017) 53–60.
- [70] M.A. Arefin, R. Islam, Investigation of different validation parameters of micro gas turbine for range extender electric truck, *Int. J. Eng.* 31 (10) (2018) 1782–1788.
- [71] K. Sim, B. Koo, H.K. Chang, T.H. Kim, Development and performance measurement of micro-power pack using micro-gas turbine driven automotive alternators, *Appl. Energy* 102 (2013) 309–319.
- [72] M.K. Tran, A. Bhatti, R. Vrolyk, D. Wong, R. Fraser, A review of range extenders in battery electric vehicles: current progress and future perspectives, *World Electr. Vehicle J.* 12 (2) (2021) 54.
- [73] A. Javed, H.A. Khalid, S. Arif, M. Imran, Z.A. Khan, Micro gas turbine small-scale effects in range extended electric vehicles, *J. Energy Resour. Technol.* 143 (12) (2021) 120906.
- [74] R.M.R.A. Shah, A. McGordon, M.M. Rahman, M. Amor-Segán, P. Jennings, Characterisation of micro turbine generator as a range extender using an automotive drive cycle for series hybrid electric vehicle application, *Appl. Therm. Eng.* 184 (2020) 116302.
- [75] H.L. Liu, D. Chen, T.F. Yang, G. Xiao, X. Zhou, J.L. Chen, Z.H. Luo, M.J. Ni, K.F. Cen, Solar gas turbine power generation technology: a review, *Therm. Power Gener.* 47 (2) (2018) 6–15, <https://doi.org/10.19666/j.rlfd.201710111>, 62.
- [76] J.B. Schroeder, Closed Brayton cycle advanced central receiver solar-electric power system, in: Volume 1: Executive Summary, Final Report, Boeing Engineering and Construction Co., Seattle, USA, November, 1978.
- [77] S.C. Kuo, Large Gas-Turbine Modifications for Solar-Fossil Hybrid Operation, Final Report, United Technologies Research Center, East Hartford, USA, 1983.
- [78] P. Schwarzbzl, R. Buck, C. Sugarmen, A. Ring, J. Enrile, Solar gas turbine systems: design, cost and perspectives, *Sol. Energy* 80 (10) (2006) 1231–1240.
- [79] R. Korzynietz, J.A. Brios, A. del Rio, M. Quero, M. Gallas, R. Uhlig, M. Ebert, R. Buck, D. Teraji, Solugas-comprehensive analysis of the solar hybrid Brayton plant, *Sol. Energy* 135 (2016) 579–589.
- [80] S. Alshahrani, A. Engeda, Performance analysis of a solar-biogas hybrid micro gas turbine for power generation, *J. Sol. Energy Eng.* 143 (2) (2020) 1–40.
- [81] W. Roux, A. Sciacovelli, Recuperated solar-dish Brayton cycle using turbocharger and short-term thermal storage, *Sol. Energy* 194 (2019) 569–580.
- [82] A. Jayachandran, A.Y. Tkachenko, H. Omar, A. Krishnakumar, Modeling and parametric optimization for a solar-powered closed-cycle micro gas turbine for space applications, *J. Phys. Conf.* 1745 (2021) 012099.
- [83] European Commission, Directorate-General for Research and Innovation, SOLGATE: Solar Hybrid Gas Turbine Electric Power System, Final Report, Publications Office, 2005. URL: <https://op.europa.eu/en/publication-detail/-/publication/e4f88dd1-74ac-4416-aba-03868cc8ea5ca>.
- [84] P. Heller, M. Pfaender, T. Denk, F. Tellez, A. Valverde, J. Fernandez, A. Ring, Test and evaluation of a solar powered gas turbine system, *Sol. Energy* 80 (10) (2006) 1225–1230.
- [85] L. Amsbeck, R. Buck, P. Heller, J. Jedamski, R. Uhlig, Development of a tube receiver for a solar-hybrid microturbine system, in: Proceedings of 14th Biennial CSP Solarpaces Symposium, Las Vegas, USA, 2008.
- [86] L. Amsbeck, T. Denk, M. Ebert, C. Gertig, P. Heller, P. Herrman, J. Jedamski, J. John, P. Tobias, J. Rehn, Test of a solar-hybrid microturbine system and evaluation of storage deployment, in: Proceedings of Solar PACES, DLR, Perpignan, France, 2010.
- [87] A. Giostri, M. Binotti, C. Sterpos, G. Lozza, Small scale solar tower coupled with micro gas turbine, *Renew. Energy* 147 (2020) 570–583.
- [88] Z. Rosenzweig, U. Collaboration, Where renewable energy and higher education converge, *Renew. Energy Focus* 17 (4) (2016) 145–146.
- [89] South West Solar. URL: <http://www.swsolartech.com> [cited 22 November 2020].

- [90] W. Schiel, T. Keck, Parabolic Dish Concentrating Solar Power (CSP) Systems: Concentrating Solar Power Technology, Woodhead Publishing, 2012, pp. 248–322.
- [91] M. Lanchi, M. Montecchi, T. Crescenzi, D. Mele, A. Miliozzi, V. Russo, D. Mazzei, M. Misceo, M. Falchetta, R. Mancini, Investigation into the coupling of micro gas turbines with CSP technology: OMSOp project, *Energy Proc.* 69 (2015) 1317–1326.
- [92] G. Gavagnin, D. Sánchez, G.S. Martínez, J.M. Rodríguez, A. Muñoz, Cost analysis of solar thermal power generators based on parabolic dish and micro gas turbine: manufacturing, transportation and installation, *Appl. Energy* 194 (2017) 108–122.
- [93] A. Giostri, Preliminary analysis of solarized micro gas turbine application to CSP parabolic dish plants, *Energy Proc.* 142 (2017) 768–773.
- [94] P. Poživil, N. Ettlin, F. Stucker, A. Steinfeld, Modular design and experimental testing of a 50 kWth pressurized-air solar receiver for gas turbines, *J. Sol. Energy Eng.* 137 (3) (2015) 031002.
- [95] G. Ragnolo, L. Aichmayer, W. Wang, T. Strand, B. Laumert, Technoeconomic design of a micro gas-turbine for a solar dish system, *Energy Proc.* 69 (2015) 1133–1142.
- [96] M.C. Cameretti, Modelling of a hybrid solar micro-gas turbine fuelled by biomass from agriculture product, *Energy Rep.* 6 (3) (2020) 105–116.
- [97] D. Coppitters, F. Contino, A. El-Baz, P. Breuhaus, W.D. Paepe, Techno-economic feasibility study of a solar-powered distributed cogeneration system producing power and distillate water: sensitivity and exergy analysis, *Renew. Energy* 150 (2020) 1089–1097.
- [98] M. Babaelahi, H. Jafari, Analytical design and optimization of a new hybrid solar-driven micro gas turbine/stirling engine, based on exergo-enviro-economic concept, *Sustain. Energy Technol. Assessments* 42 (2020) 100845.
- [99] M. Bustamante, A. Engeda, W. Liao, Small-scale solar–bio-hybrid power generation using Brayton and Rankine cycles, *Energies* 14 (2) (2021) 472.
- [100] J.M. Yang, G. Xiao, M. Ghavami, J. Al-Zaili, T.F. Yang, A. Sayma, D. Ni, Thermodynamic modelling and real-time control strategies of solar micro gas turbine system with thermochemical energy storage, *J. Clean. Prod.* 304 (1) (2021) 127010.
- [101] C.F. McDonald, A.F. Massardo, T. Korakianitis, Microturbine/fuel-cell coupling for high-efficiency electrical-power generation, *J. Eng. Gas Turbines Power* 124 (1) (2002) 110–116.
- [102] R.P. Qiao, Q.C. Liang, J.N. He, F. Yang, Performance analysis of solid oxide fuel cell and micro gas turbine top-level cycle, *E3S Web Conf.* 261 (2021) 02015.
- [103] P. Costamagna, L. Magistri, A.F. Massardo, Design and part-load performance of a hybrid system based on a solid oxide fuel cell reactor and a micro gas turbine, *J. Power Sources* 96 (2) (2001) 352–368.
- [104] A. Layne, S. Samuels, M. Williams, P. Hoffman, Hybrid heat engines: the power generation systems of the future, in: ASME Turbo Expo 2000: Power for Land, Sea, and Air, Munich, Germany, 2000. Paper No. 2000-GT-0549 V002T02A063.
- [105] P. Lunghi, S. Ubertini, U. Desideri, Highly efficient electricity generation through a hybrid molten carbonate fuel cell-closed loop gas turbine plant, *Energy Convers. Manag.* 42 (14) (2001) 1657–1672.
- [106] Y. Komatsu, S. Kimijima, J.S. Szmyd, Performance analysis for the part-load operation of a solid oxide fuel cell–micro gas turbine hybrid system, *Energy* 35 (2) (2010) 982–988.
- [107] J.X. Jia, L.Y. Shu, G.Y. Zang, L.J. Xu, A. Abudula, K. Ge, Energy analysis and techno-economic assessment of a co-gasification of woody biomass and animal manure, solid oxide fuel cells and micro gas turbine hybrid system, *Energy* 149 (2018) 750–761.
- [108] M. Ebrahimi, I. Moradpoor, Combined solid oxide fuel cell, micro-gas turbine and organic Rankine cycle for power generation (SOFC–MGT–ORC), *Energy Convers. Manag.* 116 (2016) 120–133.
- [109] M.H. Karimi, N. Chitgar, M.A. Emadi, P. Ahmadi, M.A. Rosen, Performance assessment and optimization of a biomass-based solid oxide fuel cell and micro gas turbine system integrated with an organic Rankine cycle, *Int. J. Hydrogen Energy* 45 (11) (2020) 6262–6277.
- [110] A.G. Liu, Y.W. Weng, Performance analysis of a pressurized molten carbonate fuel cell/micro-gas turbine hybrid system, *J. Power Sources* 195 (1) (2010) 204–213.
- [111] J.H. Ahn, T.S. Kim, Performance evaluation of a molten carbonate fuel cell/micro gas turbine hybrid system with oxy-combustion carbon capture, *J. Eng. Gas Turbines Power* 140 (4) (2018) 041502.
- [112] J.H. Ahn, J.H. Jeong, T.S. Kim, Performance enhancement of a molten carbonate fuel cell/micro gas turbine hybrid system with carbon capture by off-gas recirculation, *J. Eng. Gas Turbines Power* 141 (4) (2019) 041036.
- [113] MHPS wins first order for integrated SOFC/gas turbine hybrid unit, *Fuel Cells Bull.* 2018 (2) (2018) 6.
- [114] T. Onishi, S. Burguburu, O. Dessornes, Y. Ribaud, Numerical design and study of a MEMS-based micro turbine, in: ASME Turbo Expo 2005: Power for Land, Sea, and Air, Reno, USA, 2005, pp. 847–855. Paper No: GT2005-68168.
- [115] O. Dessornes, S. Landais, R. Valle, A. Fourmaux, S. Burguburu, C. Zwyssig, Z. Kozanecki, Advances in the development of a micro-turbine engine at ONERA, *J. Eng. Gas Turbines Power* 136 (7) (2013) 071201.
- [116] L. Fu, Z.P. Feng, G.J. Li, Experimental investigation on overall performance of a millimeter-scale radial turbine for micro gas turbine, *Energy* 134 (2017) 1–9.
- [117] A. Javed, H.A. Khalid, S.U.B. Arif, M. Imran, A. Rezk, Z.A. Khan, Micro gas turbine small-scale effects in range extended electric vehicles, *J. Energy Resour. Technol.* 143 (12) (2021) 120906.
- [118] S. Safari, A.H. Ghasedi, H.A. Ozgoli, Integration of solar dryer with a hybrid system of gasifier-solid oxide fuel cell/micro gas turbine: energy, economy, and environmental analysis, *Environ. Prog. Sustain. Energy* 40 (3) (2021) e13569.
- [119] Y.A. Cengel, M.A. Boles, M. Kanoglu, Thermodynamics: An Engineering Approach, eighth ed., McGraw-Hill, New York, 2011.
- [120] P.P. Walsh, P. Fletcher, Gas Turbine Performance, second ed., Blackwell Publishing, 2004.
- [121] M. Henke, T. Monz, M. Aigner, Introduction of a new numerical simulation tool to analyze micro gas turbine cycle dynamics, *J. Eng. Gas Turbines Power* 139 (4) (2016) 042601.
- [122] L. Galanti, A.F. Massardo, Micro gas turbine thermodynamic and economic analysis up to 500 kWe size, *Appl. Energy* 88 (12) (2011) 4795–4802.
- [123] S.K. Ayaz, O. Altuntas, H. Caliskan, Enhanced life cycle modelling of a micro gas turbine fuelled with various fuels for sustainable electricity production, *Renew. Sustain. Energy Rev.* 149 (2021) 111323.
- [124] N. Zhang, R.X. Cai, Explicit Analyze Part-load performance solution of constant speed single shaft gas turbine and its cogeneration, *J. Eng. Thermophys.* 19 (2) (1998) 141–144. URL: <https://kns.cnki.net/KCMS/detail/detail.aspx?dbcode=CJFD&filename=GCRB199802002>.
- [125] C. Bo, C. Yuan, X. Zhao, L. Yuan, S.Y. Liao, Circulation analyze of externally fired micro gas turbine, *Chin. J. Power Eng.* 28 (6) (2008) 880–885, <https://doi.org/10.3321/j.issn:1000-6761.2008.06.012>.
- [126] Y.Y. Li, G.Q. Zhang, Z.W. Bai, X.W. Song, L.G. Wang, Y.P. Yang, Backpressure adjustable gas turbine combined cycle: a method to improve part-load efficiency, *Energy Convers. Manag.* 174 (2018) 739–754.
- [127] A. Rosini, A. Palmieri, D. Lanzarotto, R. Procopio, A. Bonfiglio, A model predictive control design for power generation heavy-duty gas turbines, *Energies* 12 (11) (2019) 2182.
- [128] R. Yang, Y.B. Liu, Y.H. Yu, X. He, H.S. Li, Hybrid improved particle swarm optimization-cuckoo search optimized fuzzy PID controller for micro gas turbine, *Energy Rep.* 7 (2021) 5446–5454.
- [129] W.L. Zeng, X.S. Wang, X.J. Lv, Y.W. Weng, Research on control performance of micro gas turbine generator set based on fuzzy PID,

- J. Eng. Therm. Energy Power 36 (10) (2021) 212–221, <https://doi.org/10.16146/j.cnki.rndlge.2021.10.028>.
- [130] A.F. Massardo, M. Scialo, Thermo-economic Analysis of gas turbine based cycles, *J. Eng. Gas Turbines Power* 122 (4) (2000) 664–671.
- [131] G.B.D. Campos, C. Bringhenti, A. Travsero, J.T. Tomita, Thermo-economic optimization of organic Rankine bottoming cycles for micro gas turbines, *Appl. Therm. Eng.* 164 (2020) 114477.
- [132] C.F. McDonald, Recuperator considerations for future higher efficiency microturbines, *Appl. Therm. Eng.* 23 (12) (2003) 1463–1487.
- [133] C.H. Wu, A General Theory of Three-Dimensional Flow in Subsonic and Supersonic Turbomachines of Axial-, Radial-, and Mixed-Flow Types, National Aeronautics and Space Administration, Washington DC, 1952.
- [134] Y.F. Zhang, X.G. Lu, W.L. Chu, J.Q. Zhu, Numerical investigation of the unsteady tip leakage flow and rotating stall inception in a transonic compressor, *J. Therm. Sci.* 19 (4) (2010) 310–317.
- [135] J.T. Xiang, J. Schluter, F. Duan, Numerical study of the tip clearance flow in miniature gas turbine compressors, *Aero. Sci. Technol.* 93 (2019) 105352.
- [136] J. Tiainen, A. Grönman, A. Jaatinen-Väri, J. Backman, Flow control methods and their applicability in low-Reynolds-number centrifugal compressors – a review, *Int. J. Turbomach. Propuls. Power* 3 (1) (2018) 2.
- [137] P.F. Xue, Z.X. Liu, X.J. Li, M. Zhao, Multi-component coupling optimization for stability improvement of transonic centrifugal compressor, *J. Aerosp. Power* (2022) 1–12, <https://doi.org/10.13224/j.cnki.jasp.20210427>.
- [138] F. Hellstrom, E. Gutmark, L. Fuchs, Large eddy simulation of the unsteady flow in a radial compressor operating near surge, *J. Turbomach.* 134 (5) (2010) 051006.
- [139] M. Olivero, A. Javed, J.P.V. Buijtenen, Aerodynamic analysis of a micro turbine centrifugal compressor, in: ASME Turbo Expo 2010: Power for Land, Sea, and Air, Glasgow, UK, 2010, pp. 2043–2052.
- [140] Q.C. Yang, L.S. Li, Y.Y. Zhao, J. Xiao, Y. Shu, Q. Zhang, Experimental investigation of an active control casing treatment of centrifugal compressors, *Exp. Therm. Fluid Sci.* 83 (2016) 107–117.
- [141] Z.Z. Sun, X.Q. Zheng, T. Kawakubo, Experimental investigation of instability induction and mechanism of centrifugal compressors with vane diffuser, *Appl. Therm. Eng.* 133 (2018) 464–471.
- [142] Z.Z. Sun, X.Q. Zheng, H. Tamaki, Y. Kaneko, Flow instability suppression and deep surge delay by non-axisymmetric vane diffuser in a centrifugal compressor, *Aerosp. Sci. Technol.* 95 (2019) 105494.
- [143] H.Z. Zhang, C. Yang, C.M. Yang, H. Zhang, L.L. Wang, J. Chen, Inlet bent torsional pipe effect on the performance and stability of a centrifugal compressor with volute, *Aerosp. Sci. Technol.* 93 (2019) 105322.
- [144] R. Kabral, M. Åbom, Investigation of turbocharger compressor surge inception by means of an acoustic two-port model, *J. Sound Vib.* 412 (2018) 270–286.
- [145] M. Åbom, Measurement of the scattering-matrix of acoustical two-ports, *Mech. Syst. Signal Process.* 5 (2) (1991) 89–104.
- [146] C.W. Zhang, X.Z. Dong, X.Y. Liu, Z.G. Sun, S.X. Wu, Q. Gao, C.Q. Tan, A method to select loss correlations for centrifugal compressor performance prediction, *Aerosp. Sci. Technol.* 93 (2019) 105335.
- [147] P.Y. Li, C.W. Gu, Y. Song, A new optimization method for centrifugal compressors based on 1D calculations and Analyses, *Energies* 8 (5) (2015) 4317–4334.
- [148] J. Tiainen, A. Jaatinen-Väri, A. Grönman, T. Fischer, J. Backman, Loss development analysis of a micro-scale centrifugal compressor, *Energy Convers. Manag.* 166 (2018) 297–307.
- [149] M.V. Casey, The effects of Reynolds number on the efficiency of centrifugal compressor stages, *J. Eng. Gas Turbines Power* 107 (2) (1985) 541–548.
- [150] F. Dietmann, M.V. Casey, The effects of Reynolds number and roughness on compressor performance, in: 10th European Conference on Turbomachinery Fluid dynamics & Thermodynamics, Lappeenranta, Finland, 2013. Paper ID. ETC2013-052.
- [151] X.Q. Zheng, Y. Lin, B.L. Gan, W.L. Zhuge, Y.J. Zhang, Effects of Reynolds number on the performance of a high pressure-ratio turbocharger compressor, *Sci. China Technol. Sci.* 56 (2013) 1361–1369.
- [152] J. Tiainen, A. Jaatinen-Väri, A. Grönman, T. Turunen-Saaretti, J. Backman, Effect of freestream velocity definition on boundary layer thickness and losses in centrifugal compressors, *J. Turbomach.* 140 (5) (2018) 051003.
- [153] A. Meroni, B. Zühlendorf, B. Elmegaard, F. Haglind, Design of centrifugal compressors for heat pump systems, *Appl. Energy* 232 (2018) 139–156.
- [154] S. Pakle, K. Jiang, Design of a high-performance centrifugal compressor with new surge margin improvement technique for high speed turbomachinery, *Propuls. Power Res.* 7 (1) (2018) 19–29.
- [155] C. Xu, R.S. Amano, Centrifugal compressor design impacts: lean and meridional shape, in: ASME Turbo Expo 2013: Turbine Technical Conference and Exposition, San Antonio, Texas, USA, 2013. Paper No. GT2013-94111 V05BT24A005.
- [156] T. Verstraete, Z. Alsalihi, R.A.V.D. Braembussche, Multidisciplinary optimization of a radial compressor for microgas turbine applications, *J. Turbomach.* 132 (3) (2010) 1291–1299.
- [157] R.A.V.D. Braembussche, Numerical Optimization for Advanced Turbomachinery Design. Optimization and Computational Fluid Dynamics, Springer, Berlin, Heidelberg, 2008, pp. 147–189.
- [158] S.A. Moussavi, A.H. Benisi, M. Durali, Effect of splitter leading edge location on performance of an automotive turbocharger compressor, *Energy* 123 (2017) 511–520.
- [159] S.Y. Cho, K.Y. Ahn, Y.D. Lee, Y.C. Kim, Optimal design of a centrifugal compressor impeller using evolutionary algorithms, *Math. Probl. Eng.* 2012 (2012) 1094–1099.
- [160] K.K. Ha, S.H. Kang, An optimization method for centrifugal compressor design using the surrogate management framework, in: Proceedings of the ASME-JSME-KSME 2011 Joint Fluids Engineering Conference, Hamamatsu, Japan, 2011, pp. 679–684.
- [161] N. Oka, M. Furukawa, K. Yamada, S. Itou, S. Ibaraki, K. Iwakiri, Y. Hayashi, Optimum aerodynamic design of centrifugal compressor impeller using an inverse method based on meridional viscous flow analysis, in: ASME Turbo Expo 2017: Turbomachinery Technical Conference and Exposition, Charlotte, USA, 2017. Paper No. GT2017-63539 V02CT44A013.
- [162] S. Tüchler, Z.H. Chen, C.D. Copeland, Multipoint shape optimisation of an automotive radial compressor using a coupled computational fluid dynamics and genetic algorithm approach, *Energy* 165 (Part A) (2018) 543–561.
- [163] J.S. Li, Cooling efficiency of turbine guide vane with vortex interlaced rib for gas turbine, *Aeroengine* 36 (4) (2010) 12–16, <https://doi.org/10.3969/j.issn.1672-3147.2010.04.004>.
- [164] P. Dong, Q. Wang, Z.Y. Guo, H.Y. Huang, G.T. Feng, Conjugate calculation of gas turbine vanes cooled with leading edge films, *Chin. J. Aeronaut.* 22 (2) (2009) 145–152.
- [165] N.S. Cheruvu, K.S. Chan, R. Viswanathan, Evaluation, degradation and life assessment of coatings for land based combustion turbines, *Energy Mater.* 1 (1) (2013) 33–47.
- [166] S. Hada, M. Yuri, J. Masada, E. Ito, K. Tsukagoshi, Evolution and Future Trend of Large Frame Gas Turbines: a New 1600 Degree C, J Class Gas Turbine, in: ASME Turbo Expo 2012: Turbine Technical Conference and Exposition, Copenhagen, Denmark, 2012, pp. 599–606. Paper No. GT2012-68574.
- [167] S.M. Spearing, K.S. Chen, Micro-gas turbine engine materials and structures, vol. 18, in: Proceedings of the 21st Annual Conference on Composites, Advanced Ceramics, Materials, and Structures—B: Ceramic Engineering and Science Proceedings, John Wiley & Sons, 1997, pp. 11–18.
- [168] F.W. Zok, Ceramic-matrix composites enable revolutionary gains in turbine engine efficiency, *Am. Ceram. Soc. Bull.* 95 (5) (2016) 22–28.

- [169] C.F. McDonald, C. Rodgers, Small recuperated ceramic microturbine demonstrator concept, *Appl. Therm. Eng.* 28 (1) (2008) 60–74.
- [170] M. Vick, T. Young, M. Kelly, S. Tuttle, K. Hinnant, A simple recuperated ceramic microturbine: design concept, cycle analysis, and recuperator component prototype tests, in: ASME Turbo Expo 2016: Turbomachinery Technical Conference and Exposition, Seoul, South Korea, 2016. Paper No. GT2016-57780 V008T23A030.
- [171] N. Nakazawa, M. Sasaki, T. Nishiyama, M. Iwai, H. Katagiri, N. Handa, Status of the automotive ceramic gas turbine development program — seven years' progress, in: ASME 1997 International Gas Turbine and Aeroengine Congress and Exhibition, Orlando, USA, 1997. Paper No. 97-GT-383 V001T04A008.
- [172] I. Takehara, T. Tatsumi, Y. Ichikawa, Summary of CGT302 ceramic gas turbine research and development program, *J. Eng. Gas Turbines Power* 124 (3) (2000) 627–635.
- [173] R. Lundberg, M. Ferrato, Ceramic component development for AGATA, in: ASME 1999 International Gas Turbine and Aeroengine Congress and Exhibition, Indianapolis, USA, 1999. Paper No. 99-GT-392 V001T04A005.
- [174] A.F. Mclean, E.A. Fisher, Brittle Materials Design, High Temperature Gas Turbine. Interior Report No. 11, Ford Motor Co., USA, 1977.
- [175] H.E. Helms, AGT 100 Project Summary, ASME 1988 International Gas Turbine and Aeroengine Congress and Exposition, Amsterdam, The Netherlands, 1988. Paper No. 88-GT-223 V002T04A009.
- [176] AlliedSignal Engines, Advanced Turbine Technology Applications Project (ATTAP) 1993 Annual Report, Phoenix, 1994, <https://www.osti.gov/servlets/purl/10195711>.
- [177] R. Lundberg, M.P. Moret, L. Garguet-Duport, HIPed Silicon Nitride Components for AGATA — Properties and Evaluation, ASME 1998 International Gas Turbine and Aeroengine Congress and Exhibition, Stockholm, Sweden, 1998. Paper No. 98-GT-566 V002T04A014.
- [178] H. Yoshida, T. Matsunuma, N. Iki, Y. Akimune, H. Hoya, Micro gas turbine with ceramic rotor, in: ASME Turbo Expo 2004: Power for Land, Sea, and Air. Vienna, Austria, 2004, pp. 45–49. Paper No. GT2004-53493.
- [179] T. Matsunuma, H. Yoshida, N. Iki, T. Ebara, S. Sodeoka, T. Inoue, M. Suzuki, Micro gas turbine with ceramic nozzle and rotor, in: ASME Turbo Expo 2005: Power for Land, Sea, and Air, Reno, Nevada, USA, 2005, pp. 973–979. Paper No. GT2005-68711.
- [180] M.Y. Huang, P.G. He, J.L. Yang, F. Duan, S.C. Lim, M.S. Yip, Fabrication and characterization of mini alumina ceramic turbine rotor using a tailored gelcasting process, *Ceram. Int.* 40 (6) (2014) 7711–7722.
- [181] D.S. Wen, S.R. Wang, G.Q. Wang, P.Q. Guo, L.Y. Yang, X.F. Yang, Fabrication processing and mechanical properties of  $\text{Si}_3\text{N}_4$  ceramic turbocharger wheel, *Ceram. Int.* 44 (9) (2018) 10596–10603.
- [182] H. Kaya, The application of ceramic-matrix composites to the automotive ceramic gas turbine, *Compos. Sci. Technol.* 59 (6) (1999) 861–872.
- [183] X.L. Wang, X.D. Gao, Z.H. Zhang, L.S. Cheng, H.P. Ma, W.M. Yang, Advances in modifications and high-temperature applications of silicon carbide ceramic matrix composites in aerospace: a focused review, *J. Eur. Ceram. Soc.* 41 (9) (2021) 4671–4688.
- [184] Q.L. An, J. Chen, W.W. Ming, M. Chen, Machining of  $\text{SiC}$  ceramic matrix composites: a review, *Chin. J. Aeronaut.* 34 (4) (2020) 540–567.
- [185] P.R. Wang, F.Q. Liu, H. Wang, H. Li, Y.Z. Gou, A review of third generation  $\text{SiC}$  fibers and  $\text{SiCf/SiC}$  composites, *J. Mater. Sci. Technol.* 35 (12) (2019) 2743–2750.
- [186] J. Chen, Q.L. An, M. Chen, Transformation of fracture mechanism and damage behavior of ceramic-matrix composites during nano-scratching, *Compos. Appl. Sci. Manuf.* 130 (3) (2019) 105756.
- [187] D.Z. Jia, C.H. Li, Y.B. Zhang, M. Yang, X.P. Zhang, R.Z. Li, H.J. Ji, Experimental evaluation of surface topographies of NMQL grinding  $\text{ZrO}_2$  ceramics combining multiangle ultrasonic vibration, *Int. J. Adv. Manuf. Technol.* 100 (2019) 457–473.
- [188] J.C. Rozzi, M.D. Barton, The laser-assisted edge milling of ceramic matrix composites, in: Proceedings of the ASME 2009 International Manufacturing Science and Engineering Conference, West Lafayette, USA, 2009, pp. 845–852.
- [189] J.C. Han, S. Dutta, S. Ekkad, *Gas Turbine Heat Transfer and Cooling Technology*, second ed., CRC Press, 2000.
- [190] J.C. Han, Recent studies in turbine blade cooling, *Int. J. Rotating Mach.* 10 (6) (2004) 443–457.
- [191] H.C. Cheng, H. Wu, Y.L. Li, S.T. Ding, Effect of rotation on a downstream sister holes film cooling performance in a flat plate model, *Exp. Therm. Fluid Sci.* 85 (2017) 154–166.
- [192] Q.H. Zhu, H.H. Ji, B. Zhang, G.Z. Cao, Y.B. Chen, S.R. Guan, Numerical study on the pre-swirl flow and heat transfer characteristics of a small gas turbine blade, *J. Propuls. Technol.* 33 (3) (2012) 455–462, <https://doi.org/10.13675/j.cnki.tjs.2012.03.024>.
- [193] A. Buchi, Winterthur, Switzerland, U.S. Patent Cooling device for radial gas turbines, Docket No. 2577179, 1945.
- [194] P.H. Snyder, R.J. Roelke, Design of an air-cooled metallic high-temperature radial turbine, *J. Propul. Power* 6 (3) (1990) 283–288.
- [195] L. Jiang, Numerical Study on Flow Field and the Rotor's Film Cooling of Radial Inflow Turbine in CCHP System, Master Dissertation, Harbin Institute of Technology, Harbin, P.R. China, 2015, <https://doi.org/10.7666/d.D753343>.
- [196] J. Townsend, J. Kerrebrock, D. Stickler, Experimental evaluation of a turbine blade with potassium evaporative cooling, *J. Propul. Power* 24 (3) (2008) 410–415.
- [197] J.L. Kerrebrock, Lincoln, USA, U.S. Patent Radial flow turbine with internal evaporative blade cooling, Docket No: 6192670B1, 1999.
- [198] I. Kaur, Y. Aider, K. Nithyanandam, P. Singh, Thermal-hydraulic performance of additively manufactured lattices for gas turbine blade trailing edge cooling, *Appl. Therm. Eng.* 211 (2022) 118461.
- [199] Y. Zhang, T. Duda, J.A. Scoble, C.M. Sangan, C.D. Copeland, A. Redwood, Design of an air-cooled radial turbine, part 2: experimental measurements of heat transfer, in: ASME Turbo Expo 2018: Turbomachinery Technical Conference and Exposition, Oslo, Norway, 2018. Paper No. GT2018-76384 V008T26A014.
- [200] O.T. Pirin, E.R. Jardón, J.C. García, Y. Mariac, Y.S. Hernández, R. Ñeco, O. Dávalos, Effect of thermal barrier coating on the thermal stress of gas microturbine blades and nozzles, *J. Mech. Eng.* 66 (10) (2020) 581–590.
- [201] P.G. Lashmi, P.V. Ananthapadmanabhan, G. Unnikrishnan, S.T. Aruna, Present status and future prospects of plasma sprayed multilayered thermal barrier coating systems, *J. Eur. Ceram. Soc.* 40 (8) (2020) 2731–2745.
- [202] S.H. Liu, J.P. Trelles, A.B. Murphy, W.T. He, J. Shi, S. Li, C.J. Li, C.X. Li, H.B. Guo, Low-pressure plasma-induced physical vapor deposition of advanced thermal barrier coatings: microstructures, modelling and mechanisms, *Mater. Today Phys.* 21 (2021) 100481.
- [203] I.H. Shin, J.M. Koo, C.S. Seok, S.H. Yang, T.W. Lee, B.S. Kim, Estimation of spallation life of thermal barrier coating of gas turbine blade by thermal fatigue test, *Surf. Coatings. Technol.* 205 (Sup2) (2011) S157–S160.
- [204] M.T. Kim, S.W. Lee, Application of in situ oxidation-resistant coating technology to a home-made 100 kW class gas turbine and its performance analysis, *Appl. Therm. Eng.* 40 (2012) 304–310.
- [205] C. Rodgers, Radial turbines - blade number and reaction effects, in: ASME Turbo Expo 2000: Power for Land, Sea, and Air, Munich, Germany, 2000. Paper No. 2000-GT-0456 V001T03A030.
- [206] A.K. Noughabi, S. Sammak, Detailed design and aerodynamic performance analysis of a radial-inflow turbine, *Appl. Sci.* 8 (11) (2018) 2207.
- [207] U. Caldiño-Herrera, J. García, F. Sierra-Espinosa, J.O. Dávalos, M.A. Lira, Radial inflow turbine geometry generation method using third order Bezier curves for blade design, in: ASME Turbo Expo 2019: Turbomachinery Technical Conference and Exposition, Phoenix, USA, 2019. Paper No. GT2019-90163 V008T26A002.
- [208] S. Pakle, J. Kyle, Design of double curvature radial turbine blades for a micro gas turbine, *Appl. Math. Model.* 67 (2019) 529–548.
- [209] R.H. Aungier, *Turbine Aerodynamics: Axial-Flow and Radial-Inflow Turbine Design and Analysis*, ASME Press, New York, 2005.
- [210] K. Rahbar, S. Mahmoud, R.K. Al-Dadah, Mean-line modeling and CFD analysis of a miniature radial turbine for distributed power generation systems, *Int. J. Low Carbon Technol.* 11 (2) (2014) 157–168.

- [211] L. Fu, Z.P. Feng, G.J. Li, Q.H. Deng, Y. Shi, T.Y. Gao, Experimental validation of an integrated optimization design of a radial turbine for micro gas turbines, *J. Zhejiang Univ. - Sci.* 16 (2015) 241–249.
- [212] L. Fu, Y. Shi, Q.H. Deng, H.Z. Li, Z.P. Feng, Integrated optimization design for a radial turbine wheel of a 100 kW-class microturbine, *J. Eng. Gas Turbines Power* 134 (1) (2012) 881–889.
- [213] D. Barsi, A. Perrone, L. Ratto, D. Simoni, P. Zunino, Radial inflow turbine design through multi-disciplinary optimisation technique, in: ASME Turbo Expo 2015: Turbine Technical Conference and Exposition, Montreal, Canada, 2015. Paper No. GT2015-42702 V008T23A009.
- [214] R. Tuccillo, M.C. Cameretti, Combustion and Combustors for MGT Applications, Educational Notes RTO-EN-AVT-13, 2005, pp. 1–56.
- [215] O. Kurata, N. Iki, T. Matsunuma, T. Inoue, T. Tsujimura, H. Furutani, H. Kobayashi, A. Hayakawa, Performances and emission characteristics of NH<sub>3</sub>-air and NH<sub>3</sub>CH<sub>4</sub>-air combustion gas-turbine power generations, *Proc. Combust. Inst.* 36 (3) (2016) 3351–3359.
- [216] M. Choi, Y. Sung, M. Won, Y. Park, M. Kim, G. Choi, D. Kim, Effect of fuel distribution on turbulence and combustion characteristics of a micro gas turbine combustor, *J. Ind. Eng. Chem.* 48 (2016) 24–35.
- [217] A. Valera-Medina, D.G. Pugh, P. Marsh, G. Bulat, P. Bowen, Preliminary study on lean premixed combustion of ammonia-hydrogen for swirling gas turbine combustors, *Int. J. Hydrogen Energy* 42 (38) (2017) 24495–24503.
- [218] G.J. Micklow, S. Roychoudhury, H.L. Nguyen, M.C. Cline, Emissions reduction by varying the swirler airflow split in advanced gas turbine combustors, in: ASME 1992 International Gas Turbine and Aeroengine Congress and Exposition, Cologne, Germany, 1992. Paper No. 92-GT-110 V003T06A007.
- [219] N. Zarzalis, F. Joos, B. Glaeser, T. Ripplinger, NO(x)-reduction by rich-lean combustion, in: 28th Joint Propulsion Conference and Exhibit, Nashville, USA, 1992. Paper No. AIAA-92-3339.
- [220] J.A. Wünnig, J.G. Wünnig, Flameless oxidation to reduce thermal no-formation, *Prog. Energy Combust. Sci.* 23 (1) (1997) 81–94.
- [221] J.W. Meadows, A.K. Agrawal, Porous inserts for passive control of noise and thermo-acoustic instabilities in LDI combustion, *Combust. Sci. Technol.* 187 (7) (2015) 1021–1035.
- [222] C. Bruno, M. Losurdo, The Trapped Vortex Combustor: an Advanced Combustion Technology for Aerospace and Gas Turbine Applications, Springer, Dordrecht, 2007, pp. 365–384.
- [223] X. Lu, Investigation of Flameless Combustion Technology for Hydrogen-Rich Fuels in Micro Gas Turbine, Ph.D. Dissertation, Institute of Engineering Thermophysics, Chinese Academy of Sciences, Beijing, P.R. China, 2010, <https://kns.cnki.net/KCMS/detail/detail.aspx?dbname=CDFD0911&filename=2010088115.nh>.
- [224] Y. Ohkubo, Low-NO<sub>x</sub> combustion technology, in: R&D Review of Toyota CRDL, 2006, p. 41.
- [225] S. Meziane, A. Bentebache, Numerical study of blended fuel natural gas-hydrogen combustion in rich/quench/lean combustor of a micro gas turbine, *Int. J. Hydrogen Energy* 44 (29) (2019) 15610–15621.
- [226] P. Laranci, G. Bidini, B. D'Alessandro, M. Zampilli, F. Forcella, F. Fantozzi, Improving lifetime and manufacturability of an RQL Combustor for microturbines: design and numerical validation, in: ASME Turbo Expo 2015: Turbine Technical Conference and Exposition, Montreal, Canada, 2015. Paper No. GT2015-43543 V003T03A009.
- [227] P. Laranci, M. Zampilli, M. D'Amico, P. Bartocci, G. Bidini, F. Fantozzi, Geometry optimization of a commercial annular RQL combustor of a micro gas turbine for use with natural gas and vegetal oils, *Energy Proc.* 126 (2017) 875–882.
- [228] E. Alemi, M.R. Zargarabadi, Effects of jet characteristics on NO formation in a jet-stabilized combustor, *Int. J. Therm. Sci.* 112 (2017) 55–67.
- [229] X. Yang, Z.H. He, P.H. Qiu, S.K. Dong, H.P. Tan, Numerical investigations on combustion and emission characteristics of a novel elliptical jet-stabilized model combustor, *Energy* 170 (2019) 1082–1097.
- [230] S. Hasemann, H. Seliger, P. Kutne, M. Aigner, Experimental and numerical design study for a small scale jet-stabilized micro gas turbine combustor, in: ASME Turbo Expo 2018: Turbomachinery Technical Conference and Exposition, Oslo, Norway, 2018. Paper No. GT2018-75050 V04AT04A002.
- [231] J. Zanger, T. Monz, M. Aigner, Experimental investigation of the combustion characteristics of a double-staged FLOX-based combustor on an atmospheric and a micro gas turbine test rig, in: ASME Turbo Expo 2015: Turbine Technical Conference and Exposition, Montreal, Canada, 2015. Paper No. GT2015-42313 V04AT04A027.
- [232] A. Schwärzle, T.O. Monz, M. Aigner, Detailed examination of two-staged micro gas turbine combustor, in: ASME Turbo Expo 2016: Turbomachinery Technical Conference and Exposition, Seoul, South Korea, 2016. Paper No. GT2016-57730 V04BT04A039.
- [233] S. Kruse, B. Kerschgens, L. Berger, E. Varea, H. Pitsch, Experimental and numerical study of MILD combustion for gas turbine applications, *Appl. Energy* 148 (2015) 456–465.
- [234] A.A.V. Perpignan, A.G. Rao, D.J.E.M. Roekaertsm, Flameless combustion and its potential towards gas turbines, *Prog. Energy Combust. Sci.* 69 (2018) 28–62.
- [235] Z. Rui, W. Dan, J.P. Wang, Progress of continuously rotating detonation engines, *Chin. J. Aeronaut.* 29 (1) (2016) 15–29.
- [236] V. Anand, E. Gutmark, A review of pollutants emissions in various pressure gain combustors, *Int. J. Spray Combust. Dyn.* 11 (2019) 1–18.
- [237] J. Sousa, G. Paniagua, E.C. Morata, Thermodynamic analysis of a gas turbine engine with a rotating detonation combustor, *Appl. Energy* 19 (2017) 247–256.
- [238] M. Nozari, S. Tabejamaat, H. Sadeghizade, M. Aghayari, Experimental investigation of the effect of gaseous fuel injector geometry on the pollutant formation and thermal characteristics of a micro gas turbine combustor, *Energy* 235 (2021) 121372.
- [239] H.E. Bower, A. Schwärzle, F. Grimm, T. Zornek, P. Kutne, Experimental analysis of a micro gas turbine combustor optimized for flexible operation with various gaseous fuel compositions, *J. Eng. Gas Turbines Power* 142 (3) (2020) 031015.
- [240] X.W. Guo, J. Zhang, Z.X. Zhang, H. Bai, J.J. Fan, J. Yu, D.G. Bi, Z.X. Zhu, P.P. Gao, Research status and development of low-nitrogen burner for low calorific value gas fuel, *IOP Conf. Ser. Earth Environ. Sci.* 252 (4) (2019) 042048.
- [241] A.E.E. Khalil, V.K. Arghode, A.K. Gupta, S.C. Lee, Low calorific value fuelled distributed combustion with swirl for gas turbine applications, *Appl. Energy* 98 (2012) 69–78.
- [242] M.C. Cameretti, R. Tuccillo, Combustion features of a bio-fuelled micro-gas turbine, *Appl. Therm. Eng.* 89 (2015) 280–290.
- [243] A. Schwärzle, T.O. Monz, M. Aigner, Thermal incineration of VOCs in a jet-stabilized micro gas turbine combustor, in: ASME Turbo Expo 2015: Turbine Technical Conference and Exposition, Montreal, Canada, 2015. Paper No. GT2015-43139 V04BT04A006.
- [244] W.M. Haynes, D.R. Lide, T.J. Bruno, CRC Handbook of Chemistry and Physics, 97th ed., CRC Press, Boca Raton, 2016.
- [245] C. Zamfirescu, I. Dincea, Ammonia as a green fuel and hydrogen source for vehicular applications, *Fuel Process. Technol.* 90 (5) (2009) 729–737.
- [246] K.K.J.R. Dinesh, X. Jiang, M.P. Kirkpatrick, W. Malalasekera, Combustion characteristics of H<sub>2</sub>/N<sub>2</sub> and H<sub>2</sub>/CO syngas non-premixed flames, *Int. J. Hydrogen Energy* 37 (21) (2012) 16186–16200.
- [247] S.R. Zhu, S. Acharya, Effects of hydrogen addition on swirl-stabilized flame properties, in: ASME Turbo Expo 2010: Power for Land, Sea, and Air, Glasgow, UK, 2010, pp. 1277–1287. Paper No. GT2010-23686.
- [248] J. Beita, M. Talibi, S. Sadasivuni, R. Balachandran, Thermoacoustic instability considerations for high hydrogen combustion in lean premixed gas turbine combustors: a review, *Hydro* 2 (1) (2021) 33–57.
- [249] S. Karyeyen, M. Ilbas, Application of distributed combustion technique to hydrogen-rich coal gases: a numerical investigation, *Int. J. Hydrogen Energy* 45 (5) (2020) 3641–3650.
- [250] F. Reale, R. Sannino, Water and steam injection in micro gas turbine supplied by hydrogen enriched fuels: numerical investigation and

- performance analysis, *Int. J. Hydrogen Energy* 46 (40) (2021) 24366–24381.
- [251] E.C. Okafor, K.D.K.A. Somaratne, A. Hayakawa, T. Kudo, O. Kurata, N. Iki, H. Kobayashi, Towards the development of an efficient low- $\text{NO}_x$  ammonia combustor for a micro gas turbine, *Proc. Combust. Inst.* 37 (4) (2018) 4597–4606.
- [252] S.K. Ayaz, O. Altuntas, H. Caliskan, Thermoecologic assessment and life cycle-based environmental pollution cost analysis of microgas turbine, *J. Environ. Eng.* 146 (1) (2020) 04019096.
- [253] A.H. Lefebvre, V.G. McDonell, *Atomization and Sprays*, second ed., CRC Press, Boca Raton, 2017.
- [254] H. Panchasara, N. Ashwath, Effects of pyrolysis bio-oils on fuel atomisation — a review, *Energies* 14 (4) (2021) 794.
- [255] M.C. Chiong, C.T. Chong, J.H. Ng, S.S. Lam, M.V. Tran, W.W.F. Chong, M.N.M. Jaafar, A.V. Medina, Liquid biofuels production and emissions performance in gas turbines: a review, *Energy Convers. Manag.* 173 (2018) 640–658.
- [256] J.L.H.P. Salleveldt, J.E.P. Gudde, A.K. Pozarlik, G. Brem, The impact of spray quality on the combustion of a viscous biofuel in a micro gas turbine, *Appl. Energy* 132 (2014) 575–585.
- [257] M. Prussi, D. Chiaramonti, G. Riccio, F. Martelli, L. Pari, Straight vegetable oil use in micro-gas turbines: system adaptation and testing, *Appl. Energy* 89 (1) (2012) 287–295.
- [258] M. Buffi, A. Cappelletti, A.M. Rizzo, F. Martelli, D. Chiaramonti, Combustion of fast pyrolysis bio-oil and blends in a micro gas turbine, *Biomass Bioenergy* 115 (2018) 174–185.
- [259] M. Broumand, M.S. Khan, S. Yun, Z. Hong, M.J. Thomson, Feasibility of running a micro gas turbine on wood-derived fast pyrolysis bio-oils: effect of the fuel spray formation and preparation, *Renew. Energy* 178 (2021) 775–784.
- [260] M. Broumand, M.S. Khan, S. Yun, Z. Hong, M.J. Thomson, The effect of thermo-catalytic reforming of a pyrolysis bio-oil on its performance in a micro-gas turbine burner, *Appl. Energy Combust. Sci.* 5 (2021) 100017.
- [261] M. Buffi, A. Cappelletti, T. Seljak, T. Katrašnik, A. Valera-Medina, D. Chiaramonti, Emissions and combustion performance of a micro gas turbine powered with liquefied wood and its blends, *Energy Proc.* 142 (2017) 297–302.
- [262] P. Boomadevi, V. Paulson, S. Samlal, M. Varatharajan, M. Sekar, M. Alsehli, A. Elfasakhany, S. Tola, Impact of microalgae biofuel on micro gas turbine aviation engine: a combustion and emission study, *Fuel* 302 (2021) 121155.
- [263] A. Hoxie, M. Anderson, Evaluating high volume blends of vegetable oil in micro-gas turbine engines, *Renew. Energy* 101 (2017) 886–893.
- [264] F. Montomoli, M. Massini, Uncertainty quantification applied to gas turbine components, in: F. Montomoli (Ed.), *Uncertainty Quantification in Computational Fluid Dynamics and Aircraft Engines*, Springer, Cham, 2019, pp. 157–193.
- [265] B. Blakey-Milner, P. Gradl, G. Snedden, M. Brooks, J. Pitot, E. Lopez, M. Leary, F. Berto, A.D. Plessis, Metal additive manufacturing in aerospace: a review, *Mater. Des.* 209 (2021) 110008.
- [266] N. Mahto, S.R. Chakravarthy, Response surface methodology for design of gas turbine combustor, *Appl. Therm. Eng.* 211 (2022) 118449.
- [267] GE Aviation Blog, Manufacturing milestone: 30,000 additive fuel nozzles, URL: <https://blog.geaerospace.com/manufacturing/manufacturing-milestone-30000-additive-fuel-nozzles> [cited 15 August 2022].
- [268] Siemens, Additive Manufacturing: Siemens uses innovative technology to produce gas turbines, URL: <https://press.siemens.com/global/en/feature/additive-manufacturing-siemens-uses-innovative-technology-produce-gas-turbines> [cited 15 August 2022].
- [269] TWI, Case study: laser powder metal deposition manufacturing of complex real parts, URL: <https://docplayer.net/48458850-Case-study-laser-powder-metal-deposition-manufacturing-of-complex-real-parts.html> [cited 15 August 2022].
- [270] A. Adamou, J. Turner, A. Costall, A. Jones, C. Copeland, Design, simulation, and validation of additively manufactured high-temperature combustion chambers for micro gas turbines, *Energy Convers. Manag.* 248 (2021) 114805.
- [271] A. Adamou, A. Costall, J.W.G. Turner, A. Jones, C. Copeland, Experimental performance and emissions of additively manufactured high-temperature combustion chambers for micro-gas turbines, *Int. J. Engine Res.* (2022) 1–17.
- [272] M. Galati, A. Snis, L. Iuliano, Experimental validation of a numerical thermal model of the EBM process for Ti6Al4V, *Comput. Math. Appl.* 78 (7) (2019) 2417–2427.
- [273] C.Y. Zhang, V. Güümmer, High temperature heat exchangers for recuperated rotorcraft powerplants, *Appl. Therm. Eng.* 154 (2019) 548–561.
- [274] C.F. McDonald, A.F. Massardo, C. Rodgers, A. Stone, Recuperated gas turbine aeroengines, part II: engine design studies following early development testing, *Aircraft Eng. Aero. Technol.* 80 (3) (2008) 280–294.
- [275] J. Kesseli, T. Wolf, J. Nash, S. Freedman, Micro, industrial, and advanced gas turbines employing recuperators, in: ASME Turbo Expo 2003, Collocated with the 2003 International Joint Power Generation Conference, Atlanta, USA, 2003, pp. 789–794. Paper No. GT2003-38938.
- [276] G. Lagerström, M. Xie, High performance and cost effective recuperator for micro-gas turbines, in: ASME Turbo Expo 2002: Power for Land, Sea, and Air, Amsterdam, The Netherlands, 2002, pp. 1003–1007. Paper No. GT2002-30402.
- [277] B. Treece, P. Vessa, R. McKeirnan, Microturbine recuperator manufacturing and operating experience, in: ASME Turbo Expo 2002: Power for Land, Sea, and Air, Amsterdam, The Netherlands, 2002, pp. 1017–1023. Paper No. GT2002-30404.
- [278] C. Albanakis, K. Yakinthos, K. Kritikos, D. Missirlis, A. Goulas, P. Storm, The effect of heat transfer on the pressure drop through a heat exchanger for aero engine applications, *Appl. Therm. Eng.* 29 (4) (2009) 634–644.
- [279] G. Wilfert, B. Kriegel, H. Scheugenpflug, J. Bernard, X. Ruiz, S. Eury, Clean — validation of a high efficient low  $\text{NO}_x$  core, a GTF high speed turbine and an integration of a recuperator in an environmental friendly engine concept, in: 41st AIAA/ASME- SAE/ASEE Joint Propulsion Conference & Exhibit, Tucson, USA, 2005. Paper No. AIAA-2005-4195.
- [280] T. Kim, B.I. Choi, Y.S. Han, K.H. Do, Experimental and analytical investigation of a wavy fin recuperator for a micro gas turbine, *Int. J. Heat Mass Tran.* 148 (2019) 118998.
- [281] K.H. Do, B.I. Choi, Y.S. Han, T. Kim, Experimental investigation on the pressure drop and heat transfer characteristics of a recuperator with offset strip fins for a micro gas turbine, *Int. J. Heat Mass Tran.* 103 (2016) 457–467.
- [282] A. Hussein, Additive Manufacturing of Compact Heat Exchangers, in: 34th Heat Exchanger Action Group Meeting, 2017. URL: [http://hexag.org/news/34/ahmed\\_hussein.pdf](http://hexag.org/news/34/ahmed_hussein.pdf).
- [283] X. Zhang, R. Tiwari, A.H. Shooshtari, M.M. Ohadi, An additively manufactured metallic manifold-microchannel heat exchanger for high temperature applications, *Appl. Therm. Eng.* 143 (2018) 899–908.
- [284] K.K. Ferster, K.L. Kirsch, K.A. Thole, Effects of geometry, spacing, and number of pin fins in additively manufactured microchannel pin fin arrays, *J. Turbomach.* 140 (1) (2018) 011007.
- [285] H. Rastan, A. Abdi, B. Hamawandi, M. Ignatowicz, J.P. Meyer, B. Palm, Heat transfer study of enhanced additively manufactured minichannel heat exchangers, *Int. J. Heat Mass Tran.* 161 (2020) 120271.
- [286] J. Zanger, A. Widenhorn, M. Aigner, Experimental investigations of pressure losses on the performance of a micro gas turbine system, *J. Eng. Gas Turbines Power* 133 (8) (2011) 082302.
- [287] I. Kaur, P. Singh, State-of-the-art in heat exchanger additive manufacturing, *Int. J. Heat Mass Tran.* 178 (2021) 121600.
- [288] D. Singh, W.H. Yu, D.M. France, T.P. Allred, I.H. Liu, W.C. Du, B. Barua, M.C. Messner, One piece ceramic heat exchanger for concentrating solar power electric plants, *Renew. Energy* 160 (2020) 1308–1315.
- [289] B.G. Carman, J.S. Kapat, L.C. Chow, L. An, Impact of a ceramic microchannel heat exchanger on a micro turbine, in: ASME Turbo

- Expo 2002: Power for Land, Sea, and Air, Amsterdam, The Netherlands, 2002, pp. 1053–1060. Paper No. GT2002-30544.
- [290] T. Stevens, M. Baelmans, Optimal pressure drop ratio for micro recuperators in small sized gas turbines, *Appl. Therm. Eng.* 28 (17–18) (2008) 2353–2359.
- [291] J. Cai, X.L. Huai, W.X. Xi, An optimal design approach for the annular involute-profile cross wavy primary surface recuperator in microturbine and an application case study, *Energy* 153 (2018) 80–89.
- [292] C.Y. Zhang, V. Gümmer, Multi-objective optimization and system evaluation of recuperated helicopter turboshaft engines, *Energy* 191 (2019) 116477.
- [293] A. Giugno, A. Cuneo, A. Traverso, Analysis of uncertainties in compact plate-fin recuperators for microturbines, *Appl. Therm. Eng.* 150 (2019) 1243–1251.
- [294] P. Maghsoudi, S. Sadeghi, H. Khanjarpanah, H.H. Gorgani, A comprehensive thermo-economic analysis, optimization and ranking of different microturbine plate-fin recuperators designs employing similar and dissimilar fins on hot and cold sides with NSGA-II algorithm and DEA model, *Appl. Therm. Eng.* 130 (2018) 1090–1104.
- [295] P. Maghsoudi, S. Sadeghi, H.H. Gorgani, Comparative study and multi-objective optimization of plate-fin recuperators applied in 200kW microturbines based on non-dominated sorting and normalization method considering recuperator effectiveness, exergy efficiency and total cost, *Int. J. Therm. Sci.* 124 (2018) 50–67.
- [296] P. Maghsoudi, S. Sadeghi, A novel economic analysis and multi-objective optimization of a 200-kW recuperated micro gas turbine considering cycle thermal efficiency and discounted payback period, *Appl. Therm. Eng.* 166 (2020) 114644.
- [297] H.S. Lim, J.S. Bang, B.S. Choi, M.R. Park, J.Y. Park, J. Seo, S.C. Hwang, J.K. Sohn, B.O. Kim, Secondary flow stabilization of 100 kW-class micro gas turbine, *J. Mech. Sci. Technol.* 31 (4) (2017) 1753–1761.
- [298] T.A.C. Maia, O.A. Faria, J.E.M. Barros, M.P. Porto, B.J.C. Filho, Test and simulation of an electric generator driven by a micro-turbine, *Elec. Power Syst. Res.* 147 (2017) 224–232.
- [299] A. Arroyo, M. McLorn, M. Fabian, M. White, A.I. Sayma, Rotor-dynamics of different shaft configurations for a 6 kW micro gas turbine for concentrated solar power, in: ASME Turbo Expo 2016: Turbomachinery Technical Conference and Exposition, Seoul, South Korea, 2016. Paper No. GT2016-56479 V008T23A009.
- [300] Y.J. Li, F. Liang, Y. Zhou, S.T. Ding, F.R. Du, M. Zhou, J.G. Bi, Y. Cai, Numerical and experimental investigation on thermohydrodynamic performance of turbocharger rotor-bearing system, *Appl. Therm. Eng.* 121 (2017) 27–38.
- [301] P. Koutsovasilis, Automotive turbocharger rotordynamics: interaction of thrust and radial bearings in shaft motion simulation, *J. Sound Vib.* 455 (2019) 413–429.
- [302] J. Li, H. Gurgenci, J.S. Li, L. Li, Z.Q. Guan, F. Yang, Optimal design to control rotor shaft vibrations and thermal management on a supercritical CO<sub>2</sub> microturbine, *Mech. Ind.* 22 (2021) 22.
- [303] J.W. Lund, K.K. Thomsen, A calculation method and data for the dynamic coefficients of oil-lubricated journal bearings, in: Topics in Fluid Film Bearing and Rotor Bearing System Design and Optimization, 1978, 10000118.
- [304] J.W. Lund, Spring and damping coefficients for the tilting-pad journal bearing, *ASLE Trans.* 7 (1964) 342–352.
- [305] X.H. Wang, H.G. Li, G. Meng, Rotordynamic coefficients of a controllable magnetorheological fluid lubricated floating ring bearing, *Tribol. Int.* 114 (2017) 1–14.
- [306] L. Tian, W.J. Wang, Z.J. Peng, Nonlinear effects of unbalance in the rotor-floating ring bearing system of turbochargers, *Mech. Syst. Signal Process.* 34 (1–2) (2013) 298–320.
- [307] D. Kim, Parametric studies on static and dynamic performance of air foil bearings with different top foil geometries and bump stiffness distributions, *J. Tribol.* 129 (2) (2007) 354–364.
- [308] S. Nakano, T. Kishibe, H. Araki, M. Yagi, K. Tsubouchi, M. Ichinose, Y. Hayasaka, M. Sasaki, T. Inoue, K. Yamaguchi, H. Shiraiwa, Development of a 150 kW microturbine system which applies the humid air turbine cycle, in: ASME Turbo Expo 2007: Power for Land, Sea, and Air, Montreal, Canada, 2007, pp. 1041–1048. Paper No. GT2007-28192.
- [309] G. Schweitzer, Active magnetic bearings – chances and limitations, in: 6th International Conference on Rotor Dynamics, 2002, pp. 1–14.
- [310] X. Zhang, B.C. Han, X. Liu, Y.L. Chen, L.X. Zhai, Prediction and experiment of DC- bias iron loss in radial magnetic bearing for a small scale turbomolecular pump, *Vacuum* 163 (2019) 224–235.
- [311] X.N. Liu, Y. Zhou, X.S. Yan, J.J. Zhao, Z.G. Shi, J.Q. Chen, Y.L. Zhao, G.J. Yang, Experimental study on the novel rolling-sliding integrated auxiliary bearing in active magnetic bearing during rotor drop, *Ann. Nucl. Energy* 136 (2020) 107044.
- [312] S. Zheng, B.C. Han, R. Feng, Y.X. Jiang, Vibration suppression control for AMB supported motor driveline system using synchronous rotating frame transformation, *IEEE Trans. Ind. Electron.* 62 (9) (2015) 5700–5708.
- [313] Concepts Nrec, URL: <https://www.conceptsnrec.com/solutions/manufacturing/products/turbine-generators> [cited 22 November 2020].